University of Bergen

Department of Physics and Technology

Masters Thesis

Measurements of GABA and GSH with Magnetic Resonance Spectroscopy using HERMES and MEGA-PRESS

Author: Gunnhild Ager-Wick

Supervisor: Assoc. Prof. Eli Renate Grüner

June 3, 2019

Abstract

Magnetic resonance spectroscopy with the use of spectral editing, provides direct measurements of metabolites with low-concentrations, like GABA+ and GSH, in vivo in the human brain. The most common sequences used in spectral editing are HERMES and MEGA-PRESS, which are typically implemented as work-in-progress sequences at research sites and thus not standardized across vendors. Postdoctoral Fellow Muhammad Saleh and colleagues at the Johns Hopkins University School of Medicine, Baltimore, USA, therefore recently developed a universal editing sequence with common RF pulse shapes and timings for major MR vendors. As part of the collaboration with the group in Baltimore, GE and Siemens 3 Tesla systems at the Department of Radiology, Haukeland University Hospital, are used to test the universal HERMES and MEGA-PRESS sequences and compare to vendor provided (vendor-native) work-in-progress versions of HERMES and MEGA-PRESS respectively. This thesis aims to test the reproducibility of GABA+ and GSH using these editing techniques, to see if the values from HERMES and MEGA-PRESS correlate on either system, and investigate if the universal implementation is superior to the vendor specific implementations for measurements across vendors. As such, this thesis provides a summary of the current use of the vendor-native and universal-sequences and for the first time compares, vendor specific implementations with universal sequences in the field of GABA+ and GSH edited MRS. Areas were further optimization and standardization is needed are discussed. This project is part of the ongoing research in the Bergen fMRI group, University of Bergen/ Haukeland University Hospital.

Acknowledgements

I want to thank everyone who has helped me during my work for this thesis. Having the support of such a strong research group and the support of so many people made working on this project a pleasure to be a part of.

First, I would like to thank my brilliant supervisor, Assoc. Prof. Renate Grüner for introducing me to this project and to wonders of MR-spectroscopy. Her encouraging words, guidance and continued positivity throughout this thesis were so encouraging. I am also grateful she introduced me to so many wonderful people in the MMIV department like Frank Riemer and Hauke Bartsch who supported me and made me feel very welcome.

I also want to thank my co-supervisor Lars Ersland for his assistance with spectral analysis and spending many hours with me at the GE and Siemens scanners at Haukeland University Hospital and answering all my questions. This thesis would have been very difficult had it not been for his guidance.

Thanks also to the radiographers from Haukeland University Hospital Department of Radiology for their work at the MRI scanner, and to all the volunteers that made this thesis possible.

I also want to thank my family and friends for always supporting me, and Odin Asbjørnsen for all the love, cooking and encouragement.

Table of Content

List of Tables

List of Figures

Abbreviations

^1H	$^1Hydrogen$
CHESS	CHEmical Shift-Selective
Cr	Creatine
Coefficient of variations	CV
df	Degree of freedom
FID	Free-Induction-Decay
FOV	Field of view
FWHM	Full Width Half Maximum
GABA	γ-aminobutyric acid
Glu	Glutamate
Gradient Echo sequence	GRE
GSH	Glutathione (reduced)
GSSG	Glutathione (oxidized)
HERMES	Hadamard Encoding and Reconstruction of MEGA-Edited Spectroscopy
Hz	Hertz
i.u	Institutional units
M	Molar
MHz	Megahertz
MEGA-PRESS	MEscher-GArwood Point RESolved
min	Minutes
MR	Magnetic Resonans
MRI	Magnetic Resonans Imaging
MRS	Magnetic Resonans Spectroscopy
msec	Milliseconds
NMR	Nuclear Magnetic Resonans
Outer volume suppression	OVS
ppm	parts per million
PRESS	Point REsolved Spectroscopy Sequence
Proton Brain Exam	PROBE-P

RF	Radio Frequency
sec	seconds
SNR	Signal-to-Noise Ratio
Spin Echo sequence	SE
Spoiled Gradient Recalled Acquisition in Steady State	SPGR
Stimulated excitation method	STEAM
T	Tesla (SI unit of magnetic flux density)
TMS	Tetramethylsilane
T1	Longitudinal relaxation time
T2	Transverse relaxation time
TE	Echo Time
TR	Repetition Time
Variable power and optimized relaxation delays	VAPOR
VOI	Volume of Interest
VF	Voxel fraction

1 Introduction

When one needs information about the inside of an object, a picture may not always suffice. Images can be useful for identifying what an object geometrically looks like, while spectroscopy may provide an understanding of the biochemistry whitin the object. Spectroscopy is by definition the study of how electromagnetic radiation interacts with matter [1]. It was first used to study visible light from prisms and later to look at absorption lines from gasses. In the 1950s one could, by using a strong magnet, coils and radio waves, detect changes in resonance frequency of atomic nuclei due to their chemical bonds [2]. This technology led to Magnetic Resonance Spectroscopy, MRS, which is the MR-technique that presents information about biochemical compounds in an object. The clinical scanners used in hospitals today typically have a magnetic field strength of 1.5-3 tesla (T), where 3T is preferred for brain imaging due to the higher spectral resolution and the increased signal to noise ratio (SNR) [3].

MRS provides a non-invasive analysis and can therefore complement Magnetic Resonance Imaging, MRI. Where MRI can give excellent structural information about the object, mostly from water and fat, MRS suppresses the water and fat signals to receive signals from molecules with a much lower concentration in the millimolar (mM) range as opposed to the molar range. Concentration of biochemical compounds can correlate with diseases affecting the metabolic changes in the brain and has because of this become the clinical assessment of conditions such as epilepsy, multiple sclerosis and cancer due to its non-invasive procedure [4].

The reason why one would want to know the concentration of GABA and GSH is that it can help understand diseases or disorders of the human central nervous system. GABA is the most important inhibitory neurotransmitter in the central nervous system in the brain, and its concentration has a connection to several mood disorders like schizophrenia [20]. GSH, on the other hand, is an important antioxidant. Oxidative stress appears to be connected with diseases like Alzheimer's- and Parkinson's disease [36], and it can therefore be essential to find good editing technics for molecules like GABA and GSH to get a diagnosis of a disease correctly.

Chemical compounds like GABA and GSH are difficult to detect due to their low concentration and frequency overlap with other signals in the brain. Advanced editing techniques are therefore required to be able to find the concentration of these molecules. HERMES (HERMES & Hadamard Encoding and Reconstruction of MEGA-Edited Spectroscopy) and MEGA-PRESS (MEscher-GArwood Point RESolved) are two editing techniques that will be used in this assignment to find the concentration of both GABA and GSH in healthy participants. These editing techniques often vary

depending on the vendor, so a new universal HERMES and MEGA-PRESS technique that potentionally improves similarity in measurements across scanners is developed together with International collaborators and is also evaluated in the current thesis.

The purpose of this study is to evaluate how well MRS techniques can measure small biochemical concentrations of GABA and GSH. These techniques will be evaluated experimentally using healthy participants by comparing the different editing techniques, testing their reproducibility and between-vendor differences.

2 Theory

2.1 Basic Principles of Magnetic Resonance Spectroscopy

2.1.1 Nuclear Magnetic Resonance

Nuclear Magnetic Resonance (NMR) is the phenomenon where a nucleus that possesses non-zero spin can absorb electromagnetic radiation with a specific frequency when influenced by a strong magnetic field [5]. The nucleus can be considered to rotate about an axis at constant velocity and rate. The net spin depends on its composition, so a nucleus spin is determined by the number of protons and neutrons in the nucleus. The spin of the nucleus is quantised to three different values [6]:

- Zero – When the number of protons and the number of neutrons are both odd
- Half-integer values – When the number of protons are odd and neutrons even, or vice versa
- Integer values – When the number of protons and the number of neutrons are both even.

A nucleus with zero spin cannot be studied with an MR-scanner as the nucleus does not interact with an external magnetic field. The nucleus that interacts the strongest with an external field is half-integer spins such as ^{1}H [6]. ^{1}H exists naturally in large amounts which is why ^{1}H NMR is the most commonly used technique in clinical practice and research.

When an object with a charge, mass and spin interacts with an external magnetic field, a vector μ, often called the magnetic dipole moment, is used to describe the tendency of the object's interactions

with this field. The relation of μ and the nuclear spin is given in the equation below.

$$\mu = \gamma J \tag{1}$$

Here, J is the total angular momentum, and γ is the gyromagnetic ratio measured in MHzT^{-1}, which is a unique constant different for each nuclear isotope possessing spin. The gyromagnetic ratio of ^1H is one of the highest of all elements and has a value of 42.6 MHzT^{-1} [6].

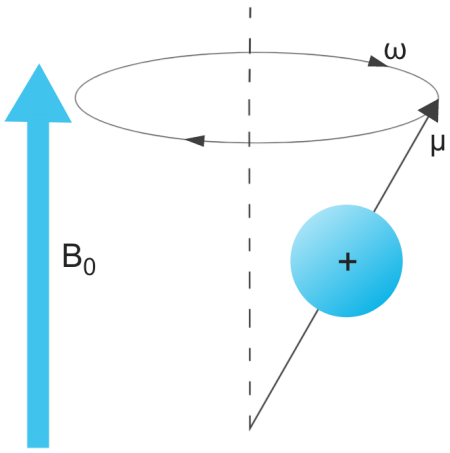

Figure 1: Precession of a particle about an applied magnetic field. B_0 is the external magnetic field, μ is the magnetic dipole moment and ω is the angular frequency. The image is made online with Sketchpad 5.1 (Sketch.IO, Inc).

The small magnetic moment is randomly oriented unless exposed to an external magnetic field B_0, as illustrated in figure 1. For spin $^1/_2$ systems, two energy levels are possible. If μ align parallel to B_0, the magnetic moment would be in its lowest energy state. If it were to align in the opposite direction, it would be in its highest energy state, because additional energy would be needed to move it in the other direction and to hold it there. When the particle is not perfectly parallel or antiparallel, like the wiggling particles in a magnetic field, it will experience a torque $\tau = \mu B_0$ and the energy of the magnetic dipole moment is given by the dot product of μ and the magnetic field:

$$E = \mu B_0 \tag{2}$$

The energy difference between these two states is then given by equation 3 (using $J_z = \pm\frac{1}{2}\hbar$ for the z-direction).

$$\Delta E = \gamma \hbar B_0 \tag{3}$$

Since the magnetic moment does not align the magnetic field perfectly, it starts rotating around the magnetic field lines with a unique frequency for each proton. This frequency is called the Larmor frequency and is given equation 4 (using $E = h\upsilon$):

$$\omega = \gamma B_0 \tag{4}$$

where ω is the angular frequency required to excite the particle from a lower energy level to the higher energy level [6]. In other words, it gives the proton enough energy to flip away from the external magnetic field lines before it again loses its energy and start wobbling around the external field line like before. When a voxel containing several particles with the same Larmor frequency is excited, it will affect the direction of the magnetic field in the voxel. This change of the magnetic field in the voxel is what gives the measurable signal in NMR imaging and spectroscopy [8].

2.1.2 The NMR Signal

When an external magnet is present, and the sample is at equilibrium, there is a slight net alignment of the dipole moments in the direction of the magnetic field. The current from a single proton is so small that it will not be noticed in an MR-scanner. μ therefore has almost zero dimension and is not a measurable unit by itself. The sum of the individual magnetic moments in a macroscopic sample, on the other hand, is measurable [7]. The sum of all the magnetic moments is referred to as the macroscopic magnetisation of the sample, $\mathbf{M} = \Sigma\mu$. The z-contribution to $\mathbf{M}$ is given in equation 5, known as Curie's Law [7].

$$M_z = \frac{N_0 \gamma^2 \hbar^2 I(I+1)}{3k_B T} B_0 \tag{5}$$

Curie's law shows that M_z is directly proportional to the external magnetic field, B_0, and the gyromagnetic ratio squared, γ^2. This relationship indicates that high magnetic field strength and gyromagnetic ratio results in a stronger macroscopic magnetisation.

As mentioned in section 2.1.1, spins can be distributed in two states: aligned with the external magnetic field or against it. The ratio of spins in a higher energy state and a lower energy state is

described by the Boltzmann distribution in equation 6 [7].

$$\frac{N_+}{N_-} = e^{\frac{-\Delta E}{kT}} \tag{6}$$

Here, N_+ is the number of spins with high energy, N_- is the number of spins with low energy, k is the Boltzmann constant, and T is the absolute temperature as measured in Kelvin. From equation 6 one could find that only 1 out of 10^5 protons would contribute to the macroscopic magnetisation (using $\Delta E = \gamma \hbar B$) when the temperature is 311 K, the magnetic field strength is 3 T and that γ for protons is $2.68 * 10^8$. The equation therefore illustrates how important it is to have a reasonably sized voxel, as well as high magnetic field strength and gyromagnetic ratio to be able to get a detectable signal from the volume of interest (VOI).

In addition to the external magnetic field, three orthogonal gradient coils are added to manipulate the field strength so that it varies linearly in the MR-scanner.

$$G_x = \frac{\partial B_z}{\partial x}, G_y = \frac{\partial B_z}{\partial y}, G_z = \frac{\partial B_z}{\partial z} \tag{7}$$

Here, G_z is referred to as the longitudinal gradient, and G_x and G_y are referred to as the transverse gradients. These gradients change the magnetic field in the x-, y- and z-direction. The gradient strength used in medical imaging is usually around 0.04 T, which means that if the external magnetic field is 1 T, it will change 0,04 T per meter. By adding these gradients to the machine, the resonance frequency of **M** change throughout the object. In that way, one can find information about a specific area of interest by sending radio frequency (RF) pulses with the resonance frequency this volume possesses.

The degree of rotation of **M**, also called the flip angle (α), is not only dependent on the Larmore frequency from the RF-pulse but also on how long the RF-pulse is applied to the desired slice [11]. One can thereby control the rotation of M by regulating the duration of the pulse.

A flip angle of 90° is often used to excite **M** to the transverse plane. The time it takes for **M** to lose its additional energy from the excitation pulse and return to its initial state is called relaxation time. When the RF-pulse is removed, **M** experiences two relaxation processes as it recovers toward the longitudinal direction [7]:

- T1-relaxation: Describes how long it takes for 63% of the original **M** to be restored in the z-plane

- T2-relaxation: Describes how long it takes before there is only 37% of the flipped **M** in the xy-plane

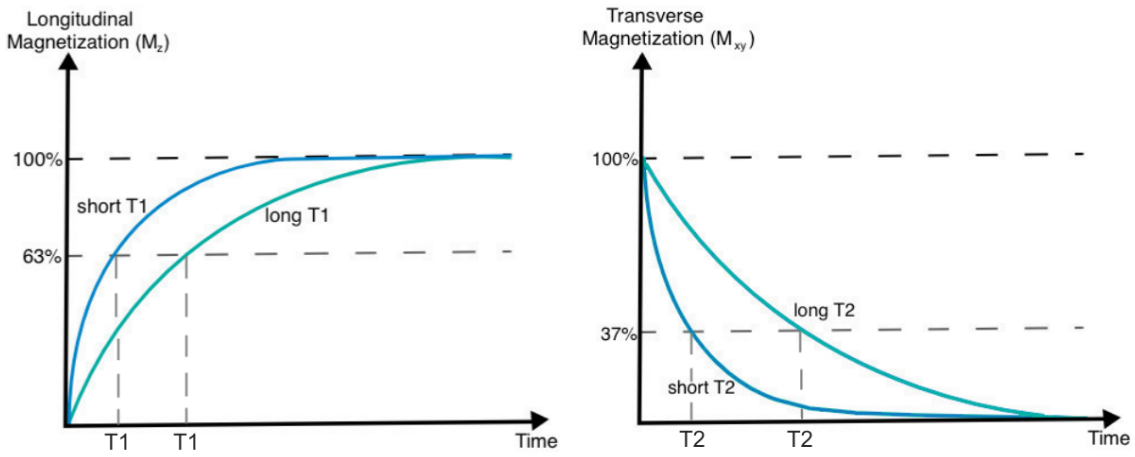

(a) T1-relaxation

(b) T2-relaxation

Figure 2: T1- and T2-relaxation. (a) The tissue represented by the blue line has a short T1 while the tissue represented by the green line has a long T1. (b) The green line has a longer relaxation time and higher signal at longer amount of time than the blue line. Images are made online with Sketchpad 5.1 (Sketch.IO, Inc).

Different tissues have different relaxation times, and it is therefore possible to see different types of tissue in *T1-weighted* or *T2-weighted* image. T1-weighted images present tissues with long T1-relaxation, such as water as a black, or dark grey colour, since very little of **M** from water has started to return to its initial state, compared to tissues with short relaxation time, like fat. Tissue with short relaxation time loses more energy faster, moving from the xy-plane to z-axis, and appears bright. The opposite is true for T2-weighted images, where the signal generated from tissue with short T2-relaxation time, like fat, is weaker than the signal generated from long T2-relaxation time, like water. T2-weighted images therefore show water with white or light grey and fat as a dark grey or black.

The RF-pulse that excited **M** to a higher energy is transformed to heat when the signal recovers towards its initial state, so the signal generated in the MR-scanner is, as briefly mentioned in section 2.1.1, the result of a change in the magnetic field **M**. Faraday's law states that if a change in the

magnetic flux occurs in a loop of wire, a current is created [12]. Coils in the MR-scanner do therefore not only change the magnetic field or send RF-pulses; they also work as antennas. When a change in the magnetic field from a voxel accrues, a current in the coil generates a signal [12].

The signal one would detect after sending in one RF-pulse with a flip angle of 90° is a damped sine wave called Free-Induction-Decay (FID) signal. It starts big and gradually declines in size due to excited protons losing their energy to their surroundings and the change in magnetisation stops [6]. This signal declines too fast for the machine to have time to spatially encode the signal, and the signal is very much affected by local magnetic field inhomogeneity [9]. The FID signal must therefore be manipulated either by sending a 180° pulse after the first 90° pulse to create an echo signal at a later time, called a spin echo sequence (SE), or by using magnetic gradient reversal to create an echo, called gradient echo sequences (GRE). This will be discussed further in section 2.1.4.

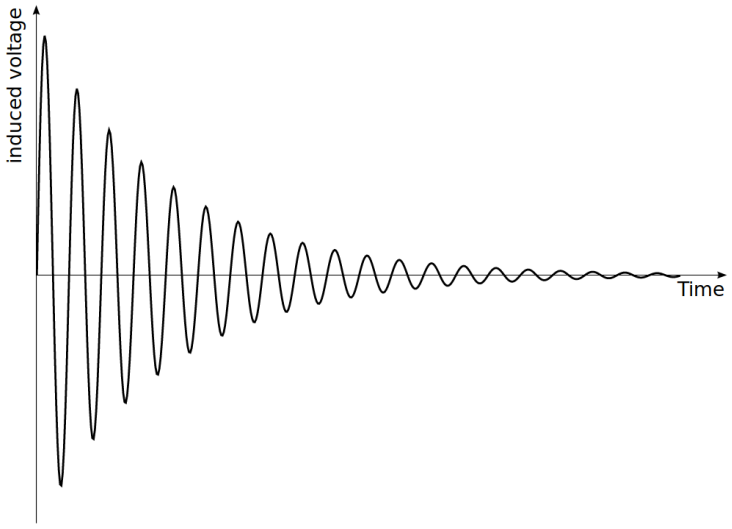

Figure 3: Free Induction Decay (FID) nuclear magnetic resonance signal [50].

2.1.3 Chemical Shift and J-Coupling

All molecules are surrounded by different electron clouds with magnetic dipoles pointing in random directions. The precessing electrons can be compared to small rotating currents, where under the influence of a magnetic field the small currents create an induced magnetic field, B_{in}, that opposes the external magnetic field, B_0, as seen in figure 4.

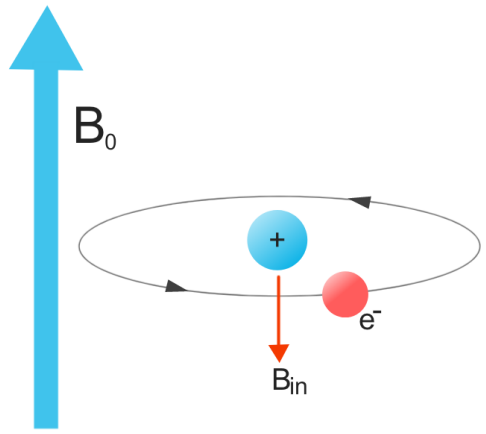

Figure 4: Electron creates an induced magnetic field in the opposite direction to the external field by Lenz's law. The image is made online with Sketchpad 5.1 (Sketch.IO, Inc).

The magnetic field felt by the proton is called the effective magnetic field, $B_{0,eff}$, expressed in equation 8.

$$B_{0,eff} = B_0 - B_{in} \tag{8}$$

$B_{0,eff}$ for a proton determines the energy difference in the spin states due to $\Delta E = \gamma \hbar B_{0,eff}$. Considering that the frequency is proportional to the energy and therefore also to $B_{0,eff}$, the frequency of this proton can be expressed as equation 9 (using $E = h\upsilon$).

$$\upsilon = \frac{\gamma B_{0,eff}}{2\pi} \tag{9}$$

The effect where the electron cloud determines the resonance frequency is known as chemical shift, δ [10]. The environment of protons altering the resonance frequency makes it possible to analyse the molecular structure of a sample. Protons from hydrogen atoms in water molecules are for instance less shielded than some other molecules since oxygen draws the electrons from the protons, making the magnetic field felt by the protons stronger than for a proton surrounded by electrons. The molecule tetramethylsilane (TMS) is more shielded than almost any other molecule and is therefore used as the reference frequency for other molecules. In MRS, molecules are presented

in a spectrum with TMS on the far left side of a spectrum. Any other molecule would be on the right side, and one would say that they have a higher frequency or a higher chemical shift [13].

Chemical shift is measured in parts per million (ppm) with TMS defined to be 0 ppm. The chemical shift can be measured using equation 10.

$$\delta = \frac{(\upsilon - \upsilon_{ref}) * 10^6}{\upsilon_{ref}} \tag{10}$$

Here, υ_{ref} is the reference frequency and υ the resonance frequency to the protons in question. Since TMS does not occur naturally in the body, another internal reference frequency must be used. Creatin (Cr) and water, which has a chemical shift at $\delta_{Cr} = 2.02$ ppm and $\delta_{H2O} = 4.8$ ppm, are stable values in humans and are therefore often used as a reference in clinical use. From equation 10 it is now possible to separate substances from each other and make a spectrum were each top on the x-axis represents a molecule, and the area under the graph is proportional to the concentration of the molecule.

It is, however, not always the case that one molecule emits one signal. The composition of a molecule determines the number of signals received from it. Methane, for instance, has four protons in the same environment, and would therefore produce one signal as seen in figure 5. The propane signal, on the other hand, has two hydrogen atoms in the same environment and six other hydrogen atoms in the same environment. Propane would then have two signals from the two different environments, as seen in figure 6.

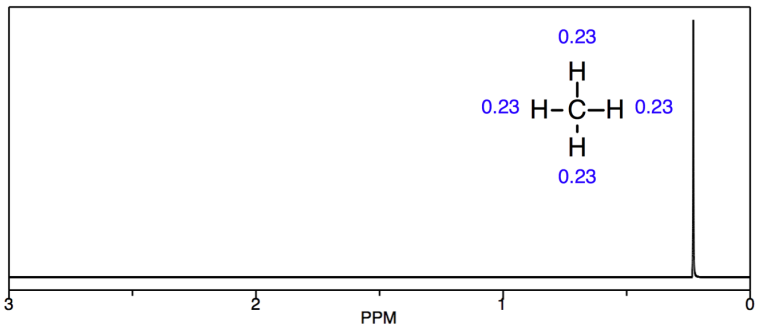

Figure 5: This figure illustrates a H^1 NMR prediction of what a signal from Methane would look like. The spectre is made with ChemDraw 18 (PerkinElmer, USA).

An additional feature one can observe from MRS is the spitting of resonance frequencies in the spectre. This phenomenon is called J coupling, or spin-spin coupling, and originates from the fact

that nuclei can affect each other through the magnetic moment of their electron bonds [14]. As mentioned before, electrons can be considered a current, with a magnetic field on the inside of the current and a magnetic field on the outside pointing in the opposite direction. The magnetic field on the inside can affect the B_{eff} of the proton on the inside, creating a chemical shift, while the magnetic field on the outside of the electrons current affect the neighbouring protons, creating the J-coupling phenomena. The magnetic field created by the electron can induce or reduce the strength of the neighbouring proton making the B_{eff} felt by this proton bigger or smaller, which results in a frequency shift upwards or downwards, respectively [15][16]. This means that one signal can be split into two or more signals. Figure 6 shows J coupling for propane made in ChemDraw (PerkinElmer, USA) [76].

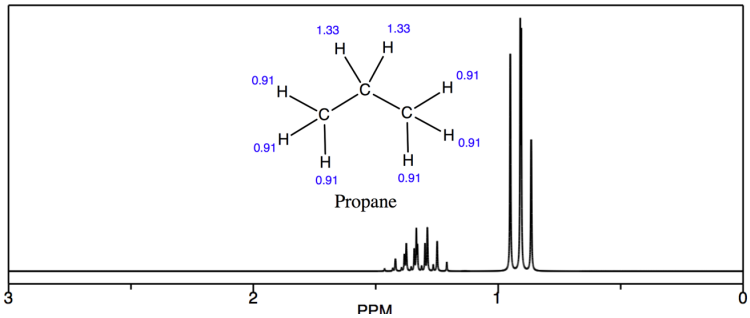

Figure 6: H^1 NMR prediction of propane. The spectre has two peaks with a chemical shift of 0.91 ppm split into three peaks and 1.33 ppm split into 7 peaks due to J-coupling. The spectre is made with ChemDraw 18 (PerkinElmer, USA).

The molecules that will be looked at in this thesis, GABA and GSH, both have protons in different environments, and will therefore have several peaks in the spectra. This will be discussed further in section 2.3.

2.1.4 Pulse Sequences

The purpose of a pulse sequence is to construct an output that is readable. This is done by manipulating the FID signal into generating an *echo* singal. Creating an echo signal can be done in different ways, but the most basic sequences are the GRE sequence and the SE sequence. The GRE sequence uses one 90 degree pulse to flip the net magnetisation to the transverse plane. Since the protons do not all precess with the same frequency, they become out of phase. A dephasing gradient

is added to the sequence to accelerate this dephasing and then a rephasing gradient is added to put them in phase again.

A basic GRE sequence is shown in figure 7. Here, one can see the three different gradients; G_z is the slice gradient, G_y the phase gradient and G_x the frequency encoding gradient. The frequency encoding gradient is the one used to dephase and re-phase the local magnetic fields in a given slice decided by G_z. When the magnetic fields in a slice are aligning, an echo is created.

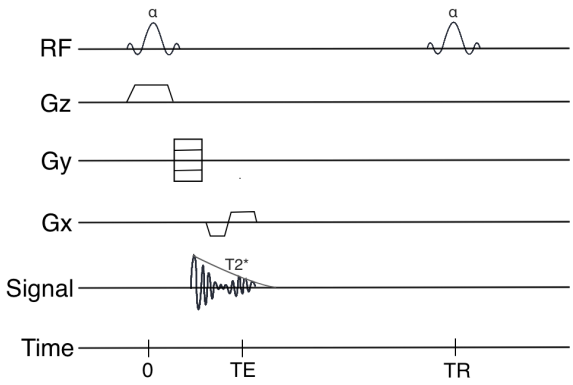

Figure 7: Simple GRE-sequence with one pulse flipping the signal and the frequency encoding gradient creating the echo signal. A new sequence starts at the second pulse sequence. The image is made online with Sketchpad 5.1 (Sketch.IO, Inc).

To be able to get an MR-image, one needs to send several RF-signals to the voxel of interest. The time it takes between every RF-pulse is called the *repetition time*, TR, and the time it takes for the RF-pulse to the peak of signal readout is called *echo time*, TE. These parameters are illustrated in figure 7.

The echo for a GRE sequence decays at the same paste as the FID signal, exponentially with a constant called T2* as illustrated in figure 8. T2* is a time constant that reflects T2 while also considering that the magnetic field is inhomogeneous and other contributing molecular mechanisms [9]. T2* is therefore shorter than T2 due to protons dephasing faster.

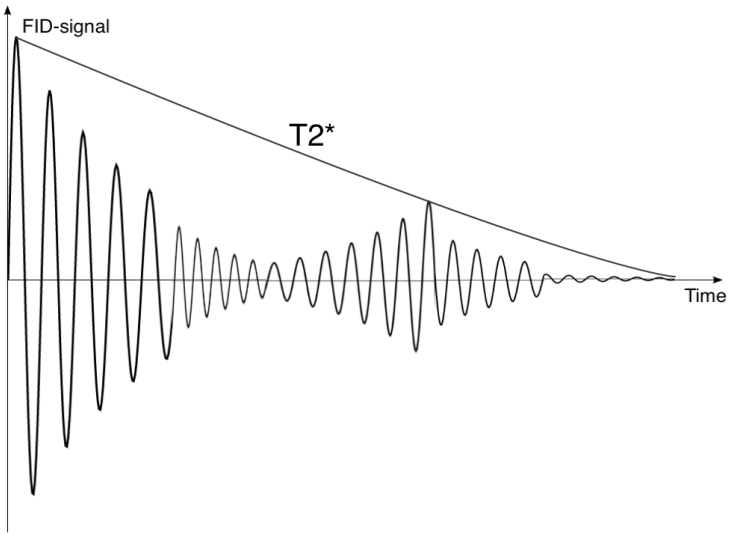

Figure 8: The FID- and echo signal decaying exponentally with T2*. The image is made online with Sketchpad 5.1 (Sketch.IO, Inc).

An SE sequence also uses a 90 degree pulse to flip the net magnetisation, and then a 180 degree pulse to flip the spins 180 degrees into phase with each other, making the magnetic poles in the sample align. The echo signal will decay exponentially with the time constant T2, while the echo generated from the GRE sequence decays with the time constant T2*. The image will therefore have a higher resolution in an SE sequence, but the TE will be longer.

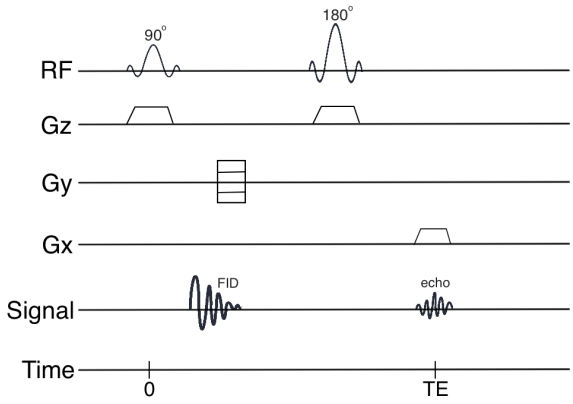

Figure 9: Simple SE-sequence using a 90 degree pulse followed by a 180 degree pulse. The image is made online with Sketchpad 5.1 (Sketch.IO, Inc).

2.2 MRS

In MRS, single voxel techniques are often used to obtain spectra from a small VOI. The most common method of achieving this is by sending three slice-selective RF excitation pulses that will only excite one volume of tissue as illustrated in figure 10.

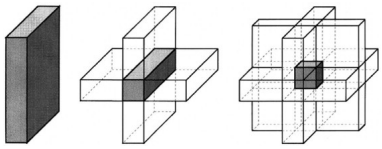

Figure 10: Three orthogonal gradients are turned to intersect at the desired volume of tissue [18].

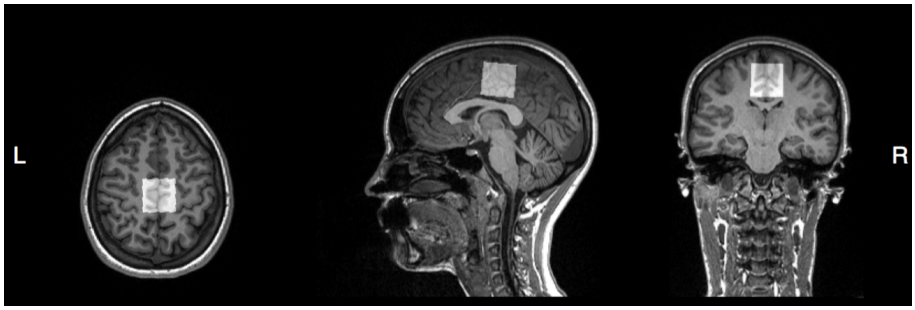

Figure 11: T1-weighted image showing a voxel in front of the left cortex from data in this thesis.

Point resolved spectroscopy (PRESS) and stimulated excitation method (STEAM) are two such techniques commonly used in MRS. PRESS uses one 90 degrees pulse and two 180 degrees pulses to excite the entire net magnetisation from one voxel to produce the echo signal. STEAM applies three 90 degrees pulses to excite about one-half of the net magnetisation to produce the echo signal [6]. This results in PRESS having a 50% larger echo signal, a larger SNR and TE compared to STEAM [6]. The TE for PRESS is usually 30-35 msec but can be larger if a metabolite of interest has a longer T2, while the TE for STEAM is around 7 msec, which can be beneficial for observing resonances with a shorter T2.

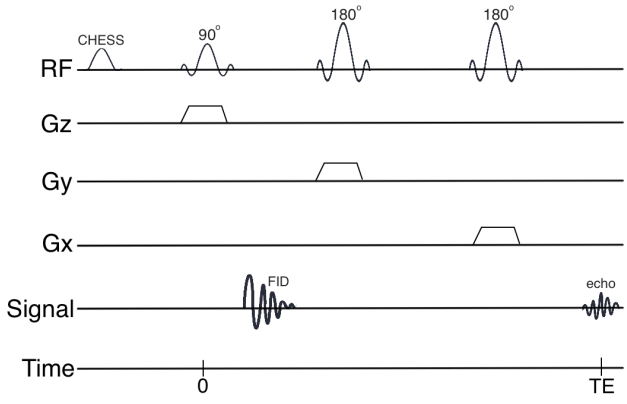

Figure 12: Simple PRESS pulse sequence. CHESS pulse is added for suppressing water. The image is made online with Sketchpad 5.1 (Sketch.IO, Inc).

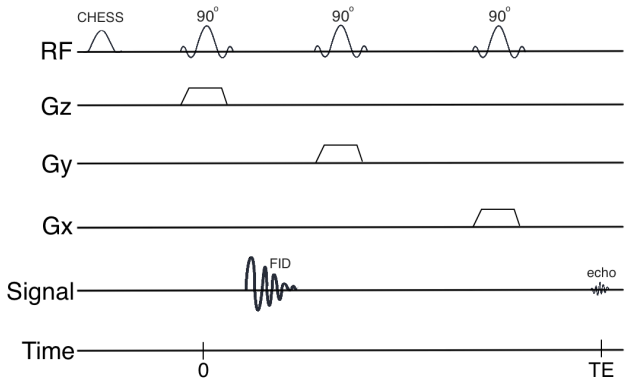

Figure 13: Simple STEAM pulse sequence. CHESS pulse is added for suppressing water. The image is made online with Sketchpad 5.1 (Sketch.IO, Inc).

To be able to detect any signals from metabolites in a sample, water suppression is required. Chemical shift selective (CHESS) pulse is the most common water suppression sequence and uses a frequency-selective RF pulse to suppress water by centring the pulse around the water resonant frequency. From one single CHESS pulse, a suppression factor of 100 or more is possible, making it a useful approach for decreasing the water signal of a sample [6]. Variable power and optimized relaxation delays (VAPOR) is another sequence used for suppression of water. Studies suggest that VAPOR is more robust than CHESS in producing a spectral baseline without as many residuals, side loops and is more effective in suppressing the water signal [81] [82].

When examining a voxel near the scalp, signals from metabolites may also be undetectable due to the high concentration of fat at 1.3 ppm. Outer volume suppression (OVS) technique is a common way of eliminating fat signals. Instead of removing certain frequencies, OVS suppresses selective pulses in a specific area to eliminate unwanted tissue in the VOI.

The metabolites that are of interest in this assignment are overlapping other metabolites with much higher concentrations, making them difficult to detect using conventional MRS sequences. Spectral editing techniques like MEGA-PRESS and HERMES will therefore be used in this project.

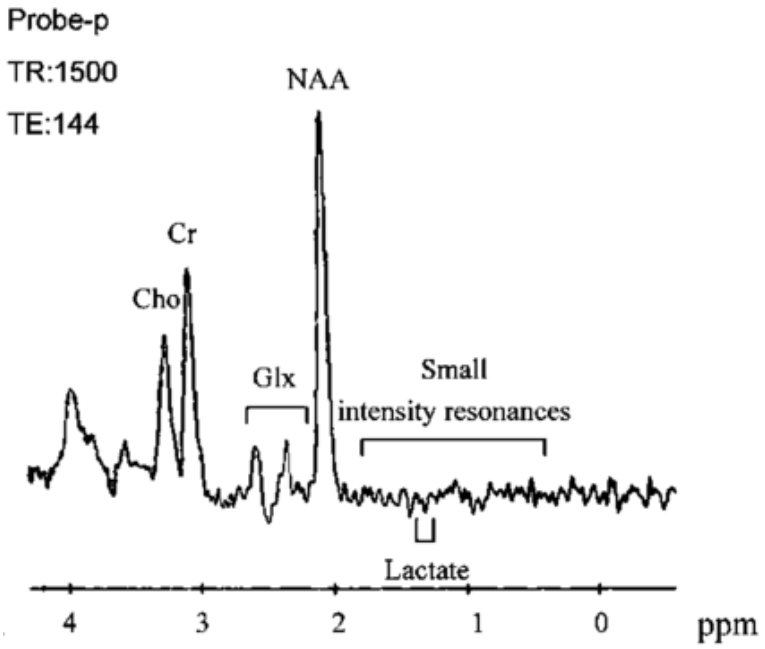

Figure 14: PRESS spectre measured with a TR of 150 ms and a TE of 144 ms [41]. The image is made online with Sketchpad 5.1 (Sketch.IO, Inc).

2.2.1 MEGA-PRESS

MEGA-PRESS is an editing sequence taking advantage of the J-coupling effects, making it possible to detect metabolites in the millimolar range with overlapping frequencies. Applying RF-pulses to one signal from a coupled spin metabolite can affect the coupled partners appearance in the spectrum without affecting frequencies from the other metabolites overlapping GABA and GSH. This permits GABA or GSH signals to be isolated from signals with overlying frequencies but with greater concentrations like Creatine (Cr) and water [39]. MEGA-PRESS is similar to PRESS except it ads two RF-pulses, or editing pulses, to the sequence. Figure 15 illustrates how a simplified MEGA-PRESS sequence may look like.

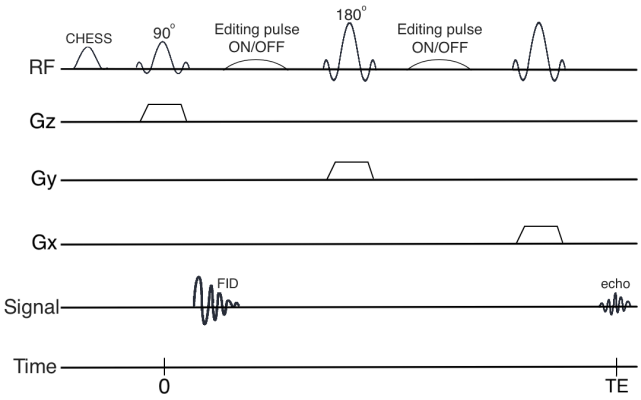

Figure 15: Simple MEGA-PRESS pulse sequence. The image is made online with Sketchpad 5.1 (Sketch.IO, Inc).

This method requires two datasets: One where the RF-pulse is applied to a coupled signal, usually referred to as 'ON', and the other where the RF-pulse is applied at a frequency outside the metabolite region, usually referred to as 'OFF'. The 'OFF' editing pulse is often set at 7.5 ppm were it does not suppress any signals in the spectre. The RF-pulse applied to GABA spin is at 1.9 ppm to modulate the shape of the coupled spin at 3 ppm, while the RF-pulse applied to GSH spin is at 4.56 ppm to interfere with the coupled spin at 2.95 ppm. When the RF pulse is 'ON', the metabolite of interest is affected while the Cr, water and other stronger metabolites stay unchanged. When the 'OFF' spectre is subtracted from the 'ON' spectre it is possible to see GABA or GSH without as many overlapping frequencies [39].

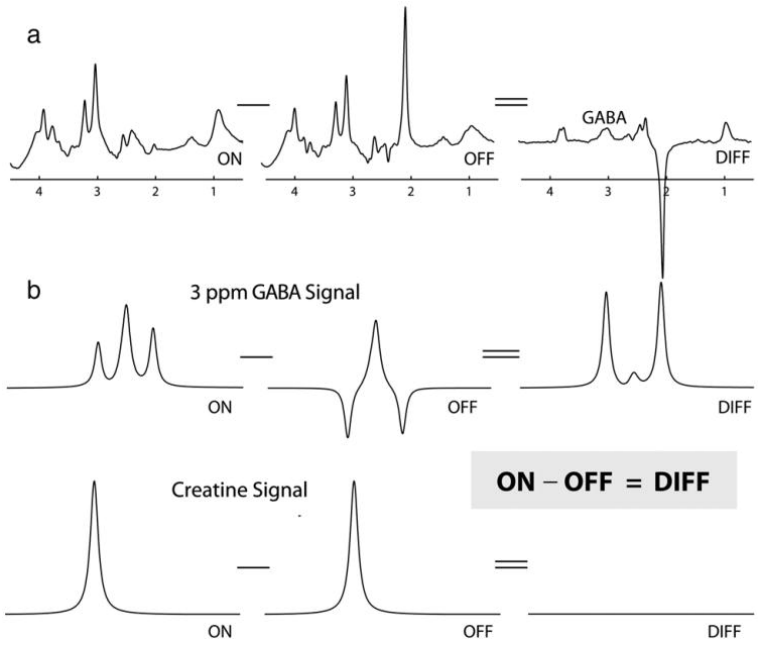

Figure 16: Schematic diagram of MEGA-PRESS editing for GABA. (a) Editing pulses applied at 1.9 ppm modulate the shape of the GABA signals at 3 ppm (b). Subtracting scans acquired without these pulses (labeled OFF) from scans acquired with the editing pulses (ON) removes overlying creatine signals from the edited spectrum, revealing the GABA signal in the difference spectrum (labeled DIFF). (b) shows the effect of editing pulses on signals at 3 ppm only [77].

When a selective RF pulse is used on a metabolite, only the T2 relaxation is what effects the intensity of the signal as a function of TE [48]. Research shows that the optimal TE value for GABA is 68ms [49] and for GSH is 131ms [51]. Smaller or higher TE values result in a loss of signal.

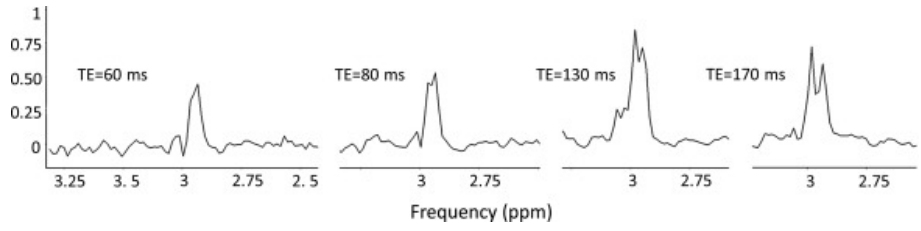

Figure 17: GSH signal using MEGA-PRESS with different TE values [53].

The sequence used for MEGA-PRESS differs from one scanner to the next depending on field

strength, operating system and model of scanner. These differences influence variations in timing and bandwidth of the editing RF-pulses [39].

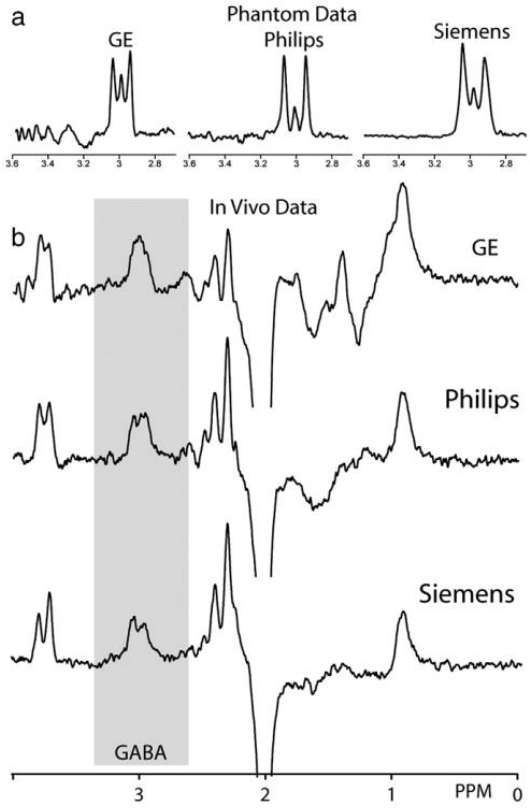

Figure 18: MEGA-PRESS spectre of GABA from three different vendors: GE, Philips and Siemens. (a) Phantom data with 10 mM of GABA. (b) *In vivo* edited spectra. For this experiment tge TE eas set to 68 ms, TR 2 s. The editing pulses was applied at 1.9 ppm (ON) and 7.46 ppm (OFF) [42].

2.2.2 HERMES

HERMES is a spectral editing method that acquires more than two edited signals from molecules simultaneously, unlike MEGA-PRESS that detects one molecule at a time [40]. This is accomplished using Hadamard-encoded sequences of editing pulses, which can edit several molecules at the time, and Hadamard reconstructions of the received spectra, which can divide spectra for individual molecules.

GABA and GSH have overlapping signals around 3ppm, each with resolved signals at 1.9 and

4.56 ppm. In MEGA-PRESS, GABA and GSH are separated from each other and other overlying frequencies by using selective RF pulses to 1.9 and 4.56 individually in the 'ON' state with different TE values. HERMES, however, runS four combinations of editing pulses at the same time with one TE value of 80 ms which provides both spin systems at once. This is done by applying various combinations of the 'ON' and 'OFF' pulses: (ON, ON), (ON, OFF), (OFF, ON) and (OFF, OFF), where ON has the value of +1 and OFF as -1. The editing design of HERMES can be expressed as a Hadamard encoding matrix H, as shown in figure 19. The ON scans are summed and the OFF scans are subtracted individually with respect to GABA and GSH in order to reconstruct the edited spectrum from other molecules [40].

	Editing pulses		Encoding Matrix		Signals	
Experiment	GABA	GSH	H		GABA	GSH
A	ON	ON	1	1	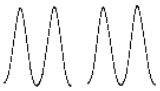	
B	ON	OFF	1	-1		
C	OFF	ON	-1	1		
D	OFF	OFF	-1	-1		

Figure 19: Four-step HERMES scheme for two molecules. The image is made online with Sketchpad 5.1 (Sketch.IO, Inc).

When HERMES and MEGA-PRESS use water as reference, the water signal is set to 0 Hz. The editing pulses are set to -18 Hz for GSH modulations, since the coupled spin 4.56 ppm is equivalent to -18 Hz and very close to water, and 356 Hz for GABA modulations, which is the equivalent to 1.9 ppm. A typical HERMES sequence could have the following pattern as displayed in table 1.

Table 1: Typical HERMES sequence.

Experiment	Edit pulse frequency 1 (Hz)	Edit pulse frequency 2 (Hz)
A	-18	-356
B	-356	-356
C	-18	-18
D	-1000	-1000

Figure 20 is taken by the GE scanner with the editing pulses in table 1. The pictures illustrate what the spectrum looks like when the editing pulse is set at A, B, C or D. Figure 20 (a) portrays experiment A when both signals from the area -18 Hz and -356 Hz are suppressed. Signals surrounding -18 Hz and -356 Hz, like the water and NAA signal, will then also be suppressed. Meanwhile in figure 20 (b) only signals around -356 Hz are suppressed, making the baseline more diagonal upwards to the left due to the significant water signal in the sample. In figure 20 (c) only the signals around -18 Hz are being modulated, and in (d) the editing pulse is too far away from the metabolites of interest to affect any of them, so the GABA, GSH, water and NAA signal stay unmodulated. To be able to get a good difference spectrum of GABA and GSH, as shown in figure 16, one needs to run the raw data from the MR-scanner in a spectral processing toolkit for quantitative analysis. Then it will be possible to obtain spectrums showing GABA or GSH signals.

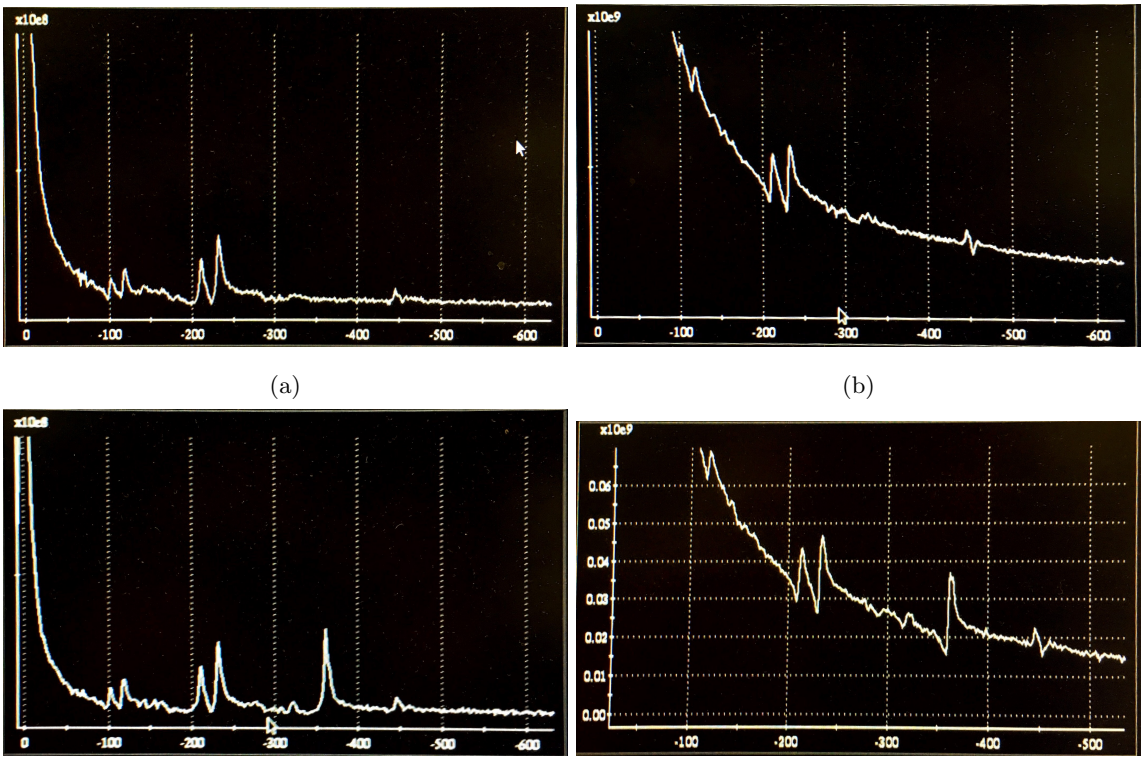

Figure 20: MRS spectrum in the frequency domain. (a) Spectrum with suppressed signals at -18 and -356 Hz modulating both GABA and GSH signals. (b) Editing pulses suppress signals at -356 Hz to modulate only the GABA signal. (c) Only signals at -18 Hz are being suppressed. (d) No signals in the spectrum showed in the window are being modulated due to the editing pulse being set at 1000 Hz. These images are taken from the GE scanner at Haukeland University Hospital.

2.2.3 Universal Sequence

Sequencies often vary depending on research sites and vendors which can lead to changes in the structure of the received signal. The universal sequence is similar to MEGA-PRESS and HERMES except it uses different excitation pulse and timings as shown in figure 21. Standardising RF pulse shapes, durations, amplitudes and timings is the goal of the universal sequence and is nessesary for multivendor studies [55].

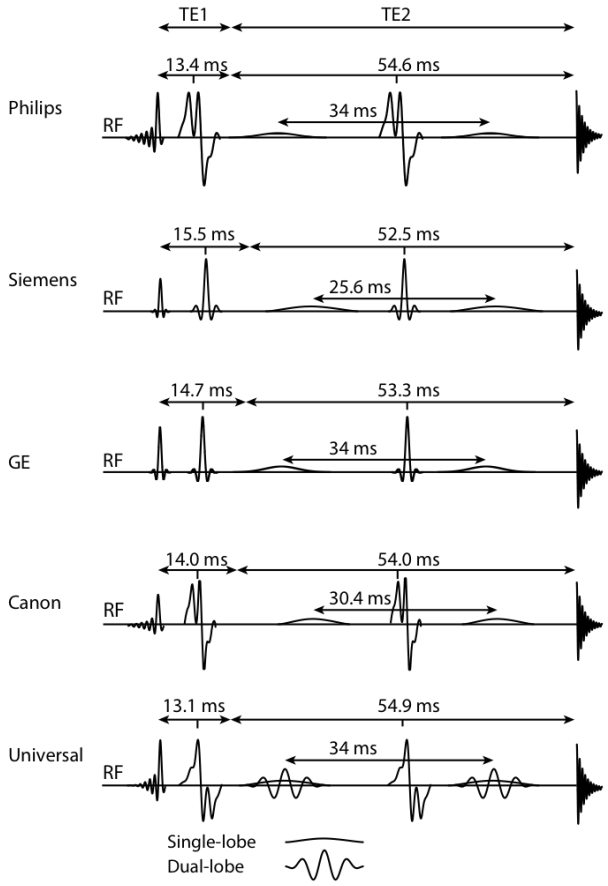

Figure 21: Pulse sequences diagrams representing RF pulse shapes and timings for the vendor-native Philips Siemens, GE and Canon sequences, and the universal MEGA-PRESS sequence at TE = 68 ms. The dual-lobe editing pulse shown on the universal sequence is for the universal HERMES sequence [55].

The universal sequence can be used at varying TEs, altering the refocusing and editing pulse timings and is therefore functional for both HERMES and MEGA-PRESS sequences [55]. The universal sequence is the first sequence made to improve inter-vendor similarities during MEGA-PRESS and HERMES operations in the hope of developing an optimal sequence for testing the reproducibility of GABA and GSH across different vendors to minimise variation.

2.2.4 Spectral Processing

Spectral processing is necessary for transforming the measured FID signals to a spectre [78]. The first process is correcting the FID signal for phase variations due to eddy currents generated by the gradients. Then a low-pass filter is applied to remove the remaining water signal, i.e. to reduce noise from the spectre. The last step is padding zeroes on the right side of the signal to increase the total number of data points which will improve the digital resolution of the spectra [78].

The time domain data are then Fourier transformed into the frequency domain to be able to perform more advanced operations. When the data is transformed to the frequency domain some metabolite peaks may be inverted, or their line shapes may be distorted, acquiring a phase correction, either manual or automatic [78].

After phase correction, the baseline tends to be distorted or tilted as seen in figure 22, lower row. The user can fix this by selecting spectral points as baselines and letting the computer create a smooth curve through these points, establishing a flat baseline which makes it much easier to determine metabolite peak areas later [78]. These peak areas in the frequency domain corresponds to the signal size/strength in the time domain. The reason one chooses to be in the frequency domain is that it is impossible to perform manual baseline corrections in the time domain, thus resulting in errors when calculating the area under the curve for a given metabolite [78].

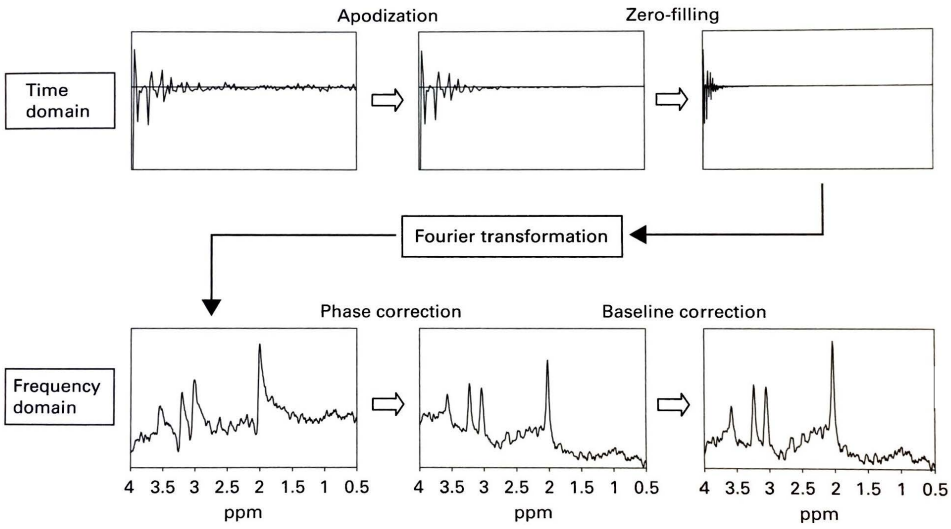

Figure 22: Overview of the major processing steps for spectral analysis [79]. Several preprocessing steps are performed in the time domain starting with an apodization (low-pass filtering) to remove water signal and zero-filling. After zero-filling the signal is Fourier transformed to the frequency domain where phase correction and baseline corrections are performed.

Determining the peak areas of the metabolites is the final step in spectral processing. The metabolites of interest can be quantified in terms of metabolite ratios or metabolite concentrations [78]. The metabolite ratio, often denoted the scaling factor ($\beta(i,t)$), represents the MR signal relative to an internal variable. These ratios are calculated by dividing the area of the metabolite peak(s) of interest by the area of a reference peak, such as Cr or water, from the spectrum. It is then required to use computer algorithms which rely on fitting ideal or experimental model spectra to *in vivo* spectra. Since the content of water in brain tissue is assumed constant across the brain and participants, and known to be approximately 55M, the measured water is a good internal reference for determining β. Many potential errors are also avoided using an internal reference like water since both water and metabolite signals are obtained from the same volume, acqusition and pulse sequence [78].

The value of β can still be challenging to control since it depends on parameters like voxel size and position, gradient crushers, phase cycles, RF coil tuning and matching, and the gain of the RF receiver chain [78]. Additionally, the water signal is approximately 40 000 times taller than GABA and GSH so small variations in the measurement of water can cause great changes in their measured

concentration ratio [56]. Beta can therefore change from one patient to the next and also between vendors.

Other problems associated with spectral analysis are linked to overlapping signals from various metabolites having low SNR and distorted baselines. It can be hard to obtain estimates of the concentrations of metabolites like GABA and GSH that have 5-10 times lower concentration than some of its overlapping signals. Most analysis programs therefore include a fitting error. When the fit error is greater than 20% it indicates that the measured peak area is unreliable, and if it is greater than 50% the measurements are meaningless. The program used in this project for spectral analysis is called Gannet 3.0 [75] which includes fit error estimates. This will be discussed further in chapter 3.9.

2.3 Brain Metabolites

2.3.1 GABA

GABA is the primary inhibitory neurotransmitter in the adult mammalian brain and is a successor of glutamate (Glu), the main excitatory neurotransmitter [17]. The difference between these two is that excitatory neurotransmitter increases the probability of electrical signals being sent from one neuron to the other, while the inhibitory neurotransmitter decreases the probability of neuronal firing. The relationship of GABA and Glu is likely to be involved in neuropsychiatric disorders such as anxiety, obsessive-compulsive disorders, substance addiction, depression, schizophrenia, primary insomnia and autism spectrum disorder [20][21][22][23][24][25], as well as in neurological diseases such as Parkinson's disease, Amyotrophic lateral sclerosis and diabetic neuropathy [26][27][28]. To understand the role of inhibitory neurotransmitters in a healthy brain has therefore interested scientists as this is also closely linked to understanding brain function and physiology.

The concentration of GABA is about 1 mM in healthy adults [56]. The frequencies at which the GABA molecule resonates are 1.89 ppm, 2.28 ppm and 3.01 ppm [19], where the peak at 3.01 ppm is used for quantification in MRS. Molecules with higher concentration, such as Cr, overlap all three peaks, making it essential to use special editing techniques to distinguish the overlapping peaks.

Unfortunately, the GABA concentration received from MEGA-PRESS and HERMES is not able to subtract the overlapping frequencies from macro molecules [35]. The measured GABA concentration ratio is therefore usually referred to as GABA+.

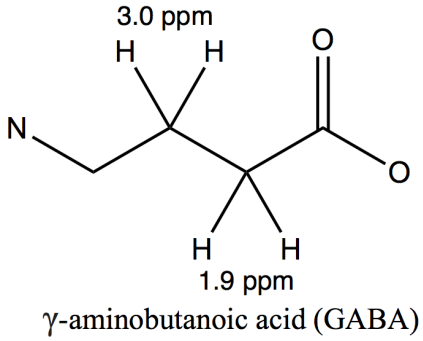

Figure 23: Structure of a GABA molecule made with ChemDraw 18 (PerkinElmer, USA).

2.3.2 GSH

GSH, L-glutamyl-L-cysteinyl-glycine, is a tripeptide that consists of the three amino acids: Cysteine, Glutamic acid and Glycine as illustrated in figure 25 [36]. It exists as both reduced glutathione (GSH) and oxidized glutathione (GSSG). GSH's main function is to protect the cells against oxidative stress. Free radicals like anion (O_2^-), hydrogen peroxide (H_2O_2) and hydroxyl radicals (OH^-) can cause DNA strand break, lipid peroxidation, and protein modification [36]. The reduced glutathione removes free radicals by donating an electron from its amino acid Cysteine to the free radical. Glutathione is then transformed to its oxidized form GSSG when two GSH bind together at the sulphur atoms [37] as shown in figure 24. Low concentrations of antioxidants like GSH is therefore connected with neurodegenerative diseases due to oxidative stress like Schizophrenia, Bipolar disorders, Alzheimer's disease and Parkinson disease [29][30][33][32][31][36].

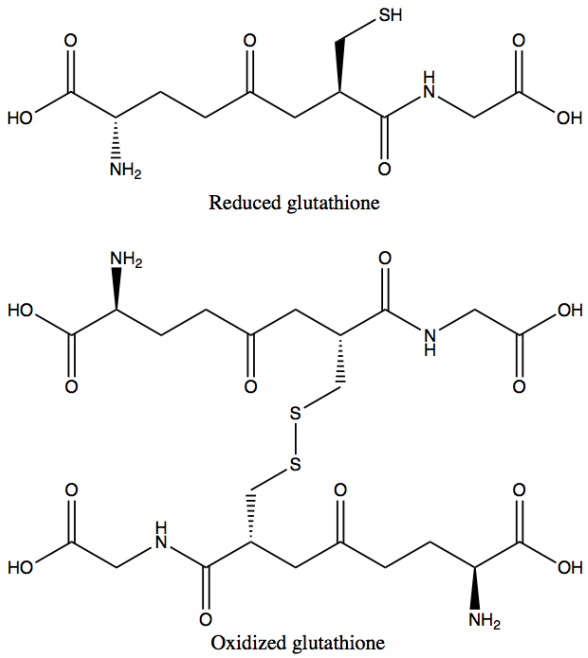

Figure 24: Reduced and oxidized glutathione made with ChemDraw 18 (PerkinElmer, USA).

GSH resonate at 2.93 ppm, 2.97 ppm and 4.56 ppm as depicted in the figure below [19]. The frequencies around 3 ppm overlap with both Cr and GABA, which has a resonance frequency at 3.03 ppm and 3.01 ppm. The GSH resonance frequency at 4.56 ppm lies very close to water with frequency at 4.68 ppm. One way of reducing errors is by using a longe TE so that the water signal becomes weaker and the baseline decreases in height [51]. This can result in an improved spectrum, making it easier to find the GSH concentration with less uncertainty.

The concentration of glutathione in healthy adults range from 1 mM to 3 mM [36] while Cr is about 8 mM. Since it overlaps with Cr, which has a much bigger concentration than GSH, errors in GSH quantification can be expected.

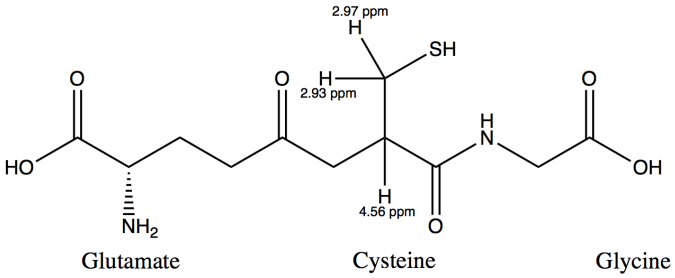

Figure 25: Structure of a GSH molecule made with ChemDraw 18 (PerkinElmer, USA).

2.4 Aims

This thesis aims to evaluate the measured values of GABA+ and GSH by using the editing methods for vendor-native sequences and universal sequences for HERMES and MEGA-PRESS. Since different settings in sequences directly impact the results, there is an overall aim to implement a universal sequence in the clinic, where the result does not change depending on the scanner and rather facilitate comparison across scanners and sites. However, there is always a danger that a common implementation is less reliable or accurate than an implementation optimized for a specific vendor. Hence the importance of the current thesis.

Technical evaluations of fit error, relative amplitude from the baseline of the spectra, SNR, spectral linewidth and the variability between subjects was studied to evaluate if the measurements of GSH and GABA+ were robust.

3 Materials and methods

3.1 MRI and MRS Acqusitions

The imaging and spectral acquisitions were performed on Siemens MAGNETOM Prisma (Siemens Healthcare, Erlangen, Germany) and GE Healthcare (General Electric, Milwaukee, United States of America) using a 20 channel head coil for Prisma and 32 channel head coil for GE scanning healthy participants ageing 28.1 $\pm$ 11.7 The machines are located at the Department of Radiology at the Haukeland University Hospital.

All acquisitions were in accordance with ethical guidelines. Data were acquired as part of an ongoing neurocognitive study in healthy participants conducted by members of the Bergen fMRI group.

3.1.1 GE Data Collection

After the subject's position is known from a fast spin echo scan (scout), a more detailed anatomical image sequence is acquired using a Spoiled Gradient Recalled Acquisition in Steady State (SPGR) pulse sequence. Images from this sequence are then used for positioning the MRS voxel. Before measuring GABA+ and GSH, the scanner undergoes a quick automated prescan to adjust the transmitter gain, receiver gain, centre frequency adjustments, coil tuning/matching and shimming [78][80].

After the prescan the desired GABA+ edited MEGA-PRESS is recorded, with parameters as shown in table 2. The TE value chosen for GABA was 68.0 ms, as this is the optimal TE to receive the greatest signal for GABA. A more detailed description of the MEGA-PRESS sequence is found in section 2.2.1.

Table 2: GABA+ edited MEGA-PRESS protocol parameters. TE=Echo time, TR=Repetition time, FOV=Field of view and VF=Voxel fraction.

Parameter	Value
TE	68.0 ms
TR	2000.0 ms
FOV	24.0 cm
VF	30/30/30 mm
Edit pulse frequency 1	1.90 ppm
Edit pulse frequency 2	1.90 ppm
Edit 'OFF' pulse frequency	7.50

The next sequence recorded was the GSH edited MEGA-PRESS sequence with parameters as outlined in table 3. GSH has a maximum signal when TE is 131.0 ms, as described in section 2.2.1, and this TE value was thus used for MEGA-PRESS.

Table 3: GSH edited MEGA-PRESS protocol parameters. TE=Echo time, TR=Repetition time, FOV=Field of view and VF=Voxel fraction.

Parameter	Value
TE	131.0 ms
TR	2000.0 ms
FOV	24.0 cm
VF	30/30/30 mm
Edit pulse frequency 1	4.56 ppm
Edit pulse frequency 2	4.56 ppm
Edit 'OFF' pulse frequency	7.50

HERMES was the last sequence recorded, and this measured both GABA+ and GSH, as described in section 2.2.2. To be able to do this, a TE value between the optimal TE values for GABA and GSH was chosen to get sufficient signals from both metabolites. The parameters used for HERMES are shown in table 4.

Table 4: HERMES protocol parameters. TE=Echo time, TR=Repetition time, FOV=Field of view and VF=Voxel fraction.

Parameter	Value
TE	80.0 ms
TR	2000.0 ms
FOV	24.0 cm
VF	30/30/30 mm
Edit pulse frequency 1	1.90 ppm
Edit pulse frequency 2	4.56 ppm
Edit 'OFF' frequency	7.50

In summary, in this thesis, four different sequences were used:

- Vendor-native HERMES sequence
- Vendor-native MEGA-PRESS sequence
- Universal HERMES sequence
- Universal MEGA-PRESS sequence

The vendor-native sequences are sequences optimised for a specific scanner. The sequences were chosen through research agreements between projects and equipment suppliers and through international collaboration with the environment in Baltimore (Postdoctoral Fellow Muhammed Saleh, Professor Richard Edden (The Johns Hopkins University School of Medicine, Baltimore, USA)). Some characteristics of the vendor-native sequence for GE are listed below, were TE1 is the time between the initial 90-degree pulse and the first editing pulse while TE2 is the time from the editing pulse to the echo as seen in figure 21:

- 90 and 180-degree pulses are symmetric
- Editing pulses are sinc-Gaussian
- Editing pulses are positioned TE/2 apart
- TE1 is 14.7 ms

- TE2 is 53.3ms for MEGA-PRESS and 65.3 for HERMES

The universal sequence is made to fit all scanner and some of its characteristics are listed below:

- 90 and 180-degree pulses are asymmetric
- Editing pulses are Hanning-filtered Gaussian
- Editing pulses are positioned TE/2 apart
- TE1 is 13.1 ms
- TE2 is 54.9ms for MEGA-PRESS and 66.9 for HERMES

The two sequences have some similarities, but the most notable difference is the slice-selective pulses. When Postdoctoral Fellow Muhammad Saleh and his colleagues chose the slice-selective pulses for the universal sequence, they wanted the pulse to be as close to an ideal rectangular profile as possible, following an iterative approach. The outcome was the product of a centre-symmetric Gaussian and an asymmetric sinc [55]. The pulse used in the vendor-native sequence looks less like a rectangle compared to the universal sequence. It has therefore a much larger transition band and will excite less inside and more outside the voxel than the universal frequency.

One thing to keep in mind is that GE does not use PRESS in its editing sequence like Siemens, but a pulse sequence called Proton Brain Exam (PROBE-P). PROBE-P is quite similar to PRESS, but it has a built-in sequence that starts recording without suppressing water in 8-16 recordings. It then uses a CHESS pulse to suppress water before running the editing pulses. The water signal from the unsuppressed water recording is later used as a reference in the analysis.

Figure 26: GE 3T MR 750 Discovery system (General Electric, Milwaukee, United States of America) at the Department of Radiology, Haukeland University Hospital.

3.1.2 Siemens Data Collection

The protocol for Siemens is similar to GE as Siemens also start with a localizer scan, followed by a more detailed image sequence and a quick prescan. Unlike GE, Siemens starts with the GABA+ and GSH edited HERMES sequence, with parameters as in table 4. The last step was running the GABA+ edited MEGA-PRESS sequence portrayed in table 2.

The vendor-native characteristics used for Siemens are listed below:

- 90 and 180-degree pulses are symmetric
- Editing pulses are Hanning-filtered Gaussian
- Editing pulses are positioned less than TE/2 apart
- TE1 is 15.5 ms
- TE2 is 52.5 ms for MEGA-PRESS and 64.5 ms for HERMES

One can see that the biggest difference form the vendor-native sequence used on GE is the longer TE1 value and that the editing pulses are positioned less than TE/2, which is reported by Postdoctoral Fellow Muhammad Saleh and his colleagues of not beeing optimal for detecting GABA+ and GSH [55].

The characteristics of the universal sequence used on Siemens is the same as those used on GE listed in section 3.1.1. There are, on the other hand, still some differences between the scanning

sequences and protocols used for GE and Siemens in both the vendor-native and universal sequence. One of the differences is that Siemens uses PRESS. Since PRESS does not have a build in water suppression sequence, it first makes a recording without water suppression, and then it runs a separate recording with water suppression before running the editing pulses for GABA+ and GSH. A significant difference in Siemens and GE is that the water suppression sequence used for Siemens is not CHESS but VAPOR. VAPOR is used for its ability to suppress water without affecting as much of the other signals in the voxel fraction. It may therefore provide higher concentration ratios, especially of smaller metabolites close to water or metabolites with coupled spins near water, like GSH [81].

Another difference is that vendors often implement different crusher gradients which dampen unwanted signals, and the number of phase cycling which reduces artefacts by running pulses a number of times, each time with a different phase, to cancel out undesired signals [83]. This was unfortunately not looked at in this thesis but could be investigated and standardised in future studies.

Figure 27: Siemens MAGNETOM 3T Prisma (Siemens Healthcare, Erlangen, Germany) at the Department of Radiology, Haukeland University Hospital.

3.2 Study Participants

MRS data from 47 volunteer participants were included in this thesis to compare measurements from GE and Siemens 3T. The participants were mostly physics students from the local university. The MRS data of 11 participants were not included for further analysis because of technical problems at time of acquisition. Total acqusition time in the MR scanner was approximately 30 minutes. Voxels were manually placed either the lateral prefrontal region in the brain when the vendor-native sequence were used and in the occipital cortices region of the brain when the universal regions were used. The reason for this is that data included here were included from two ongoing studies. All data collection was performed in accordance with ethical guidelines. And written informed concent was obtained from all the participants. The data collected were then anonymised revealing only the participant's age and gender. The age difference in the four groups is shown in table 5.

Table 5: Study participants per scanner.

Scanner	Nb. of participants	Mean(Yrs) ± Std(Yrs)	Male	Female
$GE_{vendor\text{-}native}$	9	35.1 ± 21.3	7	2
$Siemens_{vendor\text{-}native}$	8	25.1 ± 2.6	5	3
$GE_{universal}$	10	27 ± 5.8	7	3
$Siemens_{universal}$	9	25 ± 5.5	6	3
Sum	36	28.1 ± 11.7	25	11

Table 6 summarises the number of participants per scanner and sequence type. It was not possible to do measurements on both scanners with the vendor native and universal sequences for HERMES and MEGA-PRESS for all subjects due to limited scanner access. HERMES was the only sequence performed on both vendors with the vendor-native and universal model. MEGA-PRESS was performed for GABA on the GE using both the vendor native and the universal version, and it was run on Siemens using the universal model.

Table 6: Number of acquired data included in the analysis per scanner and sequence type.

GE Vendor-native	Nb. of participants	SIEMENS Vendor-Native	Nb. of participants
$HERMES_{GABA}$	9	$HERMES_{GABA}$	8
$HERMES_{GSH}$	9	$HERMES_{GSH}$	8
$MEGA\text{-}PRESS_{GABA}$	6	$MEGA\text{-}PRESS_{GABA}$	0
$MEGA\text{-}PRESS_{GSH}$	9	$MEGA\text{-}PRESS_{GSH}$	0
GE Universal	Nb. of participants	SIEMENS Universal	Nb. of participants
$HERMES_{GABA}$	10	$HERMES_{GABA}$	9
$HERMES_{GSH}$	10	$HERMES_{GSH}$	9
$MEGA\text{-}PRESS_{GABA}$	10	$MEGA\text{-}PRESS_{GABA}$	9
$MEGA\text{-}PRESS_{GSH}$	0	$MEGA\text{-}PRESS_{GSH}$	0

3.3 Spectral Processing

3.3.1 MRS Quantification and Spectral Analysis

The software package Gannet 3.0 (Edden et al., 2014) was used for spectral and quantitative analyses of raw data received during each MRS acquisition. Gannet consists of codes operating in MatWorks R2017b (Mathematical computing software, Massachusetts, USA) and is created to overcome experimental instability and to subtract the accurate amount of Cr signal that overlaps with GABA and GSH. The raw data is stored in specific file formats, which for Siemens MRI scanners are known as "Twix files" and for GE MRI scanners are known as "P-files". Some additional changes were performed in the gannet script GannetPreInitialise whether the Twix or P-file were from a HERMES or MEGA-PRESS acquisition.

GannetLoad Output:

The first step is loading the raw file data to Matlab by using the GannetLoad command. Figure 28 is one of the GannetLoad outputs from data used in this thesis and illustrates three plots and a panel of information about GSH or GABA+, depending on which metabolite were chosen to be analysed. The plot in the top left corner has two spectres, which both represent the difference spectrum after subtracting the 'OFF' spectrum from the 'ON' spectrum. The spectre on the top is before frequency

and phase correction, and the spectre below is after frequency and phase correction. The plot in the top right corner shows the frequency of the signal that is most abundant in the sample, which in this case is the water signal, plotted against time. The four red circles in this plot have been rejected due to the fitting parameters used for frequency correction being located more than three standard deviations from the mean. Rejection is performed for both the 'ON' and 'OFF' scans so that there is an even number of 'OFF' and 'ON's for subtraction. The bottom left plot shows the frequency of Cr in ppm over time. The PRE in the upper half of the spectre should vary with the water plot in the top right of the image. The lower half of the spectrum, POST, presents a more uniform plot and is the result of frequency and phase correction. The panel describes the file name, the total number of acquisitions, the volume of the voxel, the alignment method used, how many of the acquisitions were rejected and the code version used.

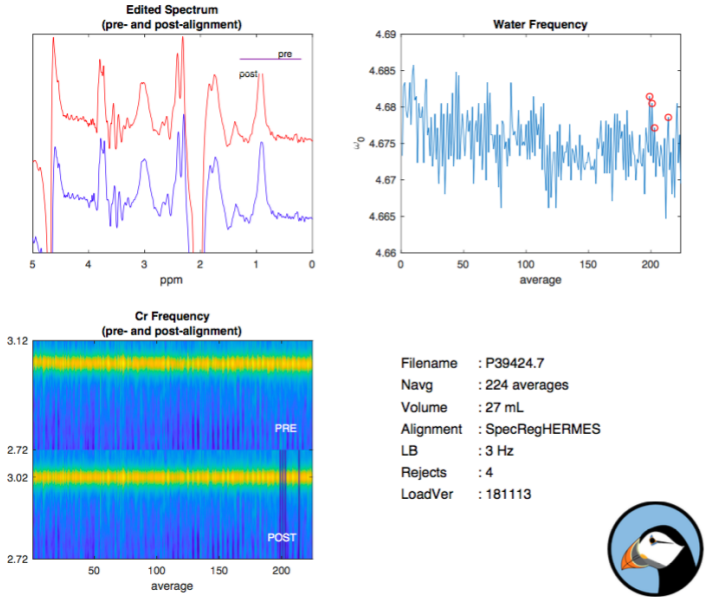

Figure 28: GannetLoad output. Top left figure shows the spectra before and after phase correction. Top right plot illustrates the water frequency warying with time. Bottom left plot shows the pre and post phase correction of Cr over time. The panel hilights the file name, number of acqusitions, volum of the voxel, the alignement methode used, the exponential line broadening applied to data in Hz, and how many outliners were rejected, and the code version used for GannetLoad.

GannetFit Output:

In this step, the spectrum is fitted against an ideal model. Figure 29 is the GannetFit output from the same participants as in figure 28. The plot in the top left corner shows the edited spectrum of the GABA+ and Glx signal. The blue spectre is the GABA+-edited spectre while the red is the model of best fit, where a Gaussian model is used. The black spectre underneath is the residual between the red and blue spectra. The plot in the bottom shows the reference signals to which GABA+ and GSH are quantified, where the water signal is modelled as a mixed Gaussian-Lorentzian. Again, the red shows the modelling, blue shows the data and black shows the residuals. The panel on the right contains information about the file name, the integral area of GABA+, Glx, water and Cr, the full-width-half-maximum linewidth (FWHM) of water and Cr, the fit error of the models and the GABA+ concentration relative to the unsupressed water signal, and one can find the concentration ratio of GABA+ relative to the Cr signal in the 'OFF' specra, and is expressed in institutional units. The Glx spectre is the result of glutamate and glutamine resonance contributions and will not be analyzed in this thesis.

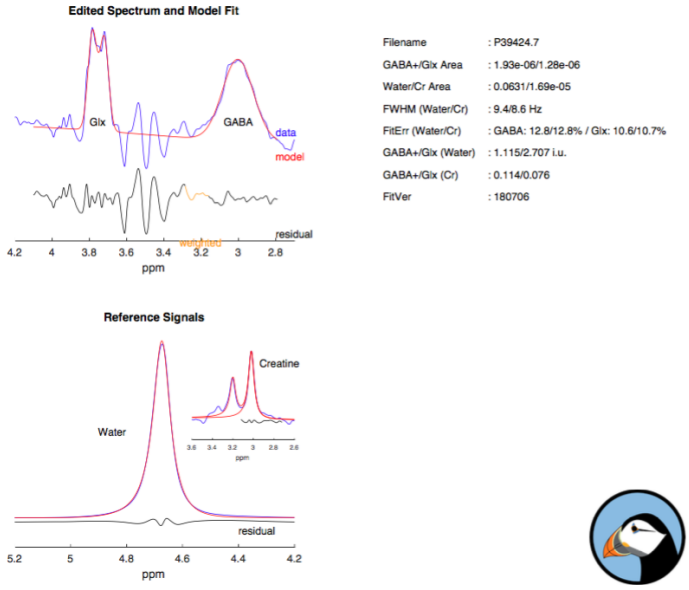

Figure 29: GannetFit Output. The plot top left shows the GABA+ and Glx resonance spectre in blue with the model of fit in red. The black line underneath is the subtracted residuals from model fit. The plot in the bottom right illustrates the water and Cr signal, while the panel lists the filename, GABA+, Glx, water and Cr area, the FWHM of water and Cr, the fit error GABA+ and Glx with water and Cr as reference, the GABA+ and Glx ratio with water and Cr as reference and at last the fit GannetFit code version.

GannetCoRegister Output:

GannetCoRegister describes the voxel location and geometrical parameters. This code makes use of SPM12 (NITRC, London, UK), which is a software package that calculates the spatial position of every pixel of the T1-weighted image and places the MRS voxel in this image [43]. Figure 30 is the outcome of GannetCoRegister and shows the voxel in the patient.

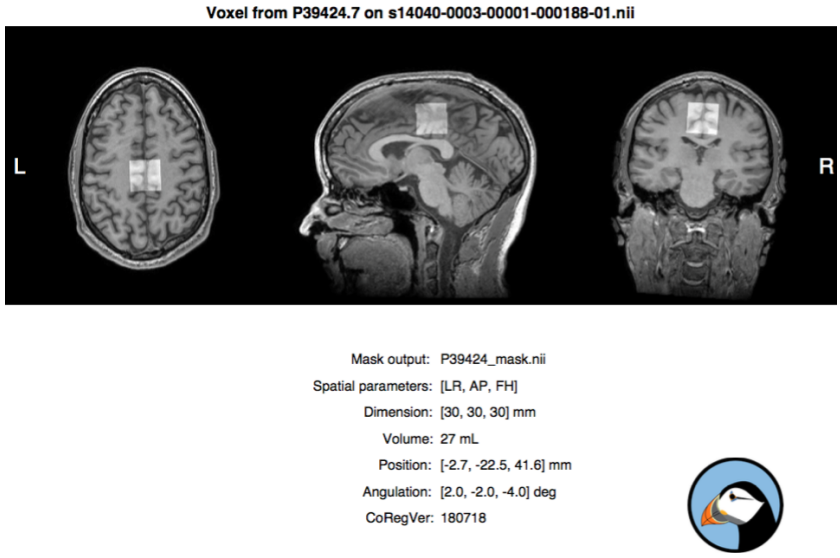

Figure 30: GannetCoRegister Output. The figure presents the positioned voxel in the participant. The panel describes the mask output, the spatial parameters, the volume fractions, volum, position of the voxel, the angulation in degrees and the code version for GannetCoRegister.

GannetSegment Output:

GannetSegment shows the concentration of gray matter, white matter and CSF in the form of 4 images as seen in figure 31. The concentrations are also described and in a panel under the images. The panel also contains the CSF-corrected GABA+ and Glx ratio. GannetSegment does this by calling an SPM segmentation of the T1-weighted image and registers the voxel mask generated by GannetcoRegister [43].

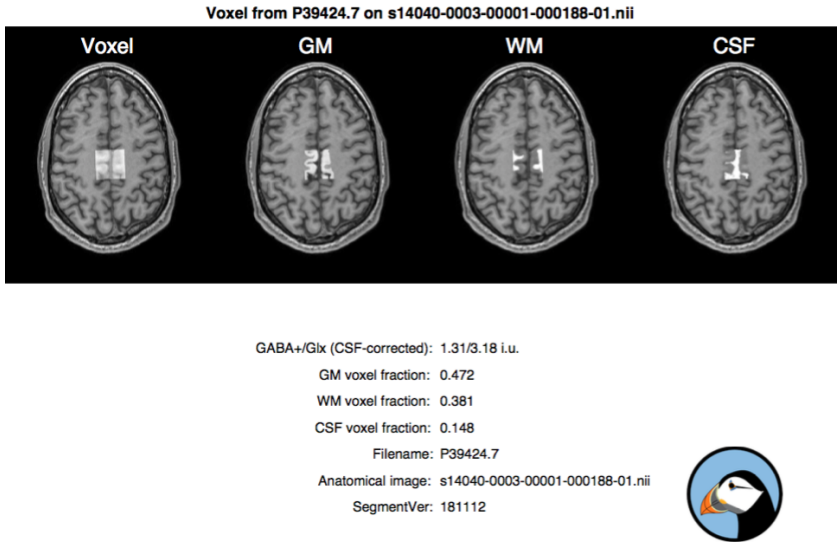

Figure 31: GannetSegment Output. The figure presents one photo of the voxel and the content of Gray matter, white matter and CSF in the voxel. The panel provides CSF-corrected GABA+ and Glx ratio with water as a reference. Then it lists the GM, WM and CSF voxel fraction, the filename, the name of the anatomical T1-weighted image file and the code version of GannetSegment.

GannetQuantify Output:

Gannet Quantify is the last step in the quantitative analysis package which Gannet offers. In this step, the panel to the right in figure 32 presents an estimated value of GABA+, or GSH, considering the relaxation of water signals in grey matter, white matter and CSF and how the concentration of GABA+, or GSH, differ in gray and white matter [44]. The alpha is the concentration of white matter devided by the concentration of white matter. Water is used as a reference for these calculations provided by Gannet, and is therefore chosen as the reference in this project.

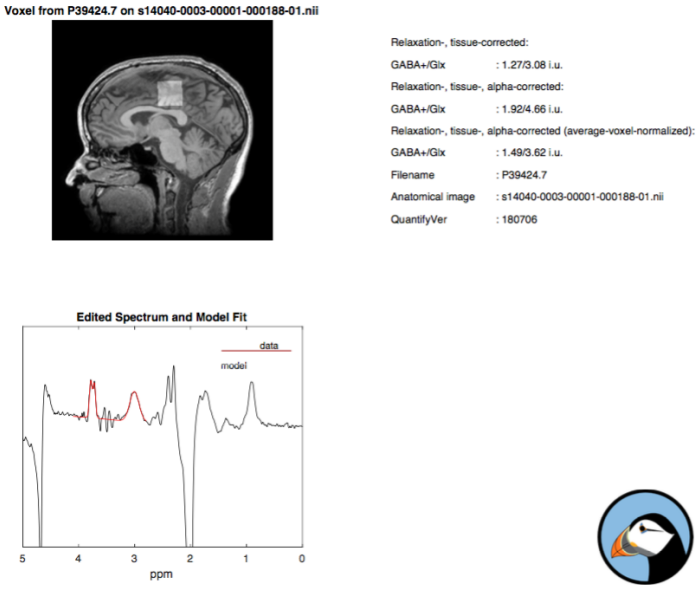

Figure 32: GannetQuantify Output. The figure in the top left corner shows the voxel placed in one of the T1-weighted images. The plot in the bottom left presents the edited spectrum of GABA+ and Glx and the model fit. The panel provides first with the relaxation and tissue corrected ratio of GABA+ and Glx, then the relaxation, tissue and alpha-corrected ratio, then lastly the relaxation, tissue, alpha-corrected and average-voxel-normalised ratio of GABA+ and Glx with water as a reference.

3.3.2 Spectral Processing Steps

The pre-processing steps in this project are listed below and start in the time domain:

- Correcting FID signals for phase variations due to eddy currents
- Apply low pass filter to remove remaining water signal
- Applying an apodization filter to improve spectral resolution [65]
- Zero-padding to improve resolution

The last steps are in the frequency domain:

- Phase correction after the time domain data are Fourier transformed

- Baseline correction

After the pre-scan, the data were visually inspected by the radiographers for artefacts in the spectre. These artefacts could be distorted baseline, high unwanted lipid signals, wide peaks or if the signal is small in size (low SNR) reflecting patient motion. Some of the quality parameters that are considered are explained more thoroughly in the next section.

3.3.3 Quality Parameters

Fit Error

The fit error describes how well the modelled spectra fit the acquired spectra. If the fit is of good quality, the fit error is low and the given metabolite ratio is reliable. Typical fit errors in similar *in vivo* studies of GABA ranges from 5–6% [58], were fit errors below 12% is considered being of good quality [57].

SNR

SNR is defined as the height of the largest metabolite peak divided by the root-mean-square amplitude of the noise in a signal [66]. When the SNR is calculated in Gannet, the height of GABA+ or GSH is divided by the standard deviation of the noise signal between 10 and 12 ppm in the DIFF spectrum.

SNR is proportional to voxel size and to the square root of the number of acquisitions. The voxels in single voxel spectroscopy are bigger than those used in regular MRI to compensate for only having one voxel and to shorten the number of acquisitions [72]. The voxel size used in this project is 3x3x3cm.

Since the SNR could not be obtained from the computer used in the beginnig of this assignment, the amplitude ratio relative to the baseline was measured in addition to the SNR. Due to considerable baseline differences between 3.3 ppm and 3.5 ppm across participants and scanner, these two points were averaged and subtracted from the height of GABA+ or GSH. More suitable regions for finding the amplitude exist, such as 10-12 ppm used in Gannet, but due to limitations in data, the computer only had access of data from 4.2-2.8 ppm. These measurements are therefore meant to implement the results from the concentration ratio and fit error to get a visual representation of GABA+ and GSH measurements, but validation might be required to establish validity.

Spectral Linewidth

Linewidth is usually defined in the frequency domain as the full-width half-maximum (FWHM), and indicates how well the resolution of a spectrum is. Good shimming is required for producing narrower linewidth which results in less overlapping of signals and better resolution [66]. Gannet provides the measured FWHM from GABA+ and GSH.

3.4 Statistical Analysis

All statistical analyses and boxplots presented in this thesis were made in R Commander (version 2.5-1), while the histograms were made in C++ to better illustrate the sampled data. Spectras received from Gannet were overlapped in Gimp (GNU Image Manipulation Program, 2.8.22-1). All estimates of the amplitudes of the individual spectra also were performed in Gannet. The amplitudes were found by measuring the same distance from the x-axis to the individual baselines and the same distance from the x-axis to the GABA+ and GSH peaks.

Coefficient of variations (CV) were calculated to examine the variance among the measured data and were used to determine the variation relative to the mean value of a sample, CVs were calculated in Excel by dividing the standard deviation by the mean value and multiplying by 100%. Inter-individual CVs observed for edited GABA measurements in literature are reported to be 6–24% [59] [60] [61] [62] [63] [64]. Hence CVs in this thesis were considered to be of good quality if they were within this range.

Two different t-tests were used in this project. A paired t-test was used when mean values from two tests on the same sample of individuals were compared, and an independent t-test was used when the means from two samples with unequal variance were compared. When there was one sample of individuals, Excel was used to calculate the p-value for the paired t-test. The p-value predicts the probability of whether the mean values of two distributions are different. An alpha is then chosen as threshold for significant findings. A common level for educational research is 0.05 and is therefore chosen for this project. If the p-value is below 0.05 there is a significant difference in the mean values. The p-value for two different subject groups were calculated by using an online t-test calculator for two independent means [46].

To determine if there was a relationship between different groups, a correlation coefficient (r) was calculated. To find out if r is sufficient, a critical value table for Person's correlation coefficient was used. The table requires to know the alpha level, which is chosen to be 0.05, the degree of freedom

(df) and the calculated r. The df is equal to 1 less than the number of subjects if the subjects are the same in both tests, or 2 less then the sample size if the subjects are different for the two tests. A relationship between the two groups exist if the calculated r is bigger then the critical r found in the table. The null hypothesis is then rejected and one can accept the alternative hypothesis saying there is a statistically significant relationship. If the calculated r is below the critical r, one fails to reject the null hypothesis saying one cannot be 95% certain that a relationship exists within two sample sizes [47].

4 Results

4.1 Comparison of HERMES and MEGA-PRESS

4.1.1 Vendor-Native Sequences on GE

GABA+ and GSH Concentration Ratio

There is a significant overlap in the estimated GABA+ concentration ratios found by using the vendor-native version of HERMES and MEGA-PRESS as seen in table 7, with MEGA-PRESS having a slightly higher mean value than HERMES. Since the p-value is above α, the values from HERMES and MEGA-PRESS are not statistically different. However, the correlation coefficient is very low, implying that there is not a significant correlation.

Figure 33 (a) illustrates the GABA+ concentration ratio between each subject and shows how the data samples from HERMES presents fluctuating values. Between-session CVs from GABA+ reveals that HERMES has a CV above what is reported in other studies which were below 24% [59] [60] [61] [62] [63] [64]. This might imply that the data recieved from HERMES does not provide the most robust results.

Concentration ratios of GSH were found by implementing HERMES and MEGA-PRESS, but data from MEGA-PRESS will not be considered due to errors either in the raw data or the spectral processing. The CV of the ratio was 70%, the fit errors high, and when the spectra were visually analysed the spectra did not correctly represent GSH. There is evidence that the vendor-native HERMES sequence was more beneficial for measuring GSH, although the CV is still higher than related studies.

Table 7: GE: Concentration ratio of GABA+/H20 and GSH/H2O, relaxation-, tissue-, and alpha-corrected (average-voxel-normalized), from the ventor-native sequences. r = correlation coefficient.

GROUP	Mean ± Std (CV)	p-value	r
$\text{HERMES}_{\text{GABA+}}$	2.2 ± 0.8 (36%)		
$\text{MEGA-PRESS}_{\text{GABA+}}$	2.5 ± 0.4 (16%)	0.3	-0.1
$\text{HERMES}_{\text{GSH}}$	0.8 ± 0.2 (25%)		

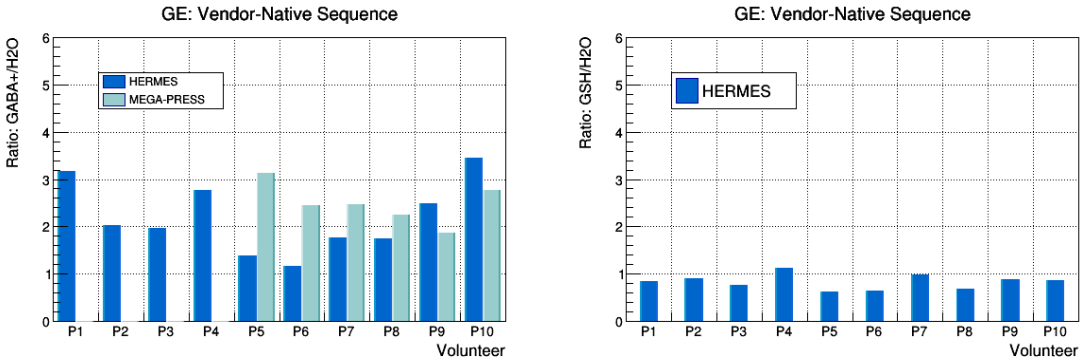

(a) (b)

Figure 33: Ratio of GABA+/H2O and GSH/H2O, relaxation-, tissue-, and alpha-corrected (average-voxel-normalised) from the GE scanner at Haukeland University Hospital. The GABA+ and GSH concentration ratio for each participant is plotted in C++. (a) GABA+ ratio found by implementing the vendor-native HERMES sequence on 10 participants and the vendor-native MEGA-PRESS sequence on 6 participants. (b) GSH ratio from vendor-native HERMES sequence.

Fit Error

The fit errors, which estimates the error between the real spectre and the fit of the Gaussian model, are outlined in table 8. From this table, one can see that the vendor-native HERMES sequence receives the highest fit error from GABA+ and the lowest fit error from GSH. This test could indicate that HERMES might be more suited for measuring GSH, while MEGA-PRESS might be more suited for measuring GABA+. Overall, the relationship of HERMES and MEGA-PRESS is significant, considering the p-value from GABA+ is above α, indicating similar distributions of the fitt error values, and the high correlation coefficient.

Figure 43 presents the fit error for each participant. This figure illustrates that there are some fluctuating. However, the fit error does not exceed 12%, which indicates that the concentration ratio of GABA+ and GSH should be reliable, as mentioned in section 3.3.3.

Table 8: GE: Fit Error of GABA+ and GSH from the vendor-native sequencies. r = correlation coefficient.

GROUP	Mean ± Std (CV)	p-value	r
$\text{HERMES}_{\text{GABA+}}$	9.7 ± 0.6 (6%)		
$\text{MEGA-PRESS}_{\text{GABA+}}$	6.9 ± 2.5 (36%)	0.06	-0.6
$\text{HERMES}_{\text{GSH}}$	8.6 ± 2.8 (33%)		

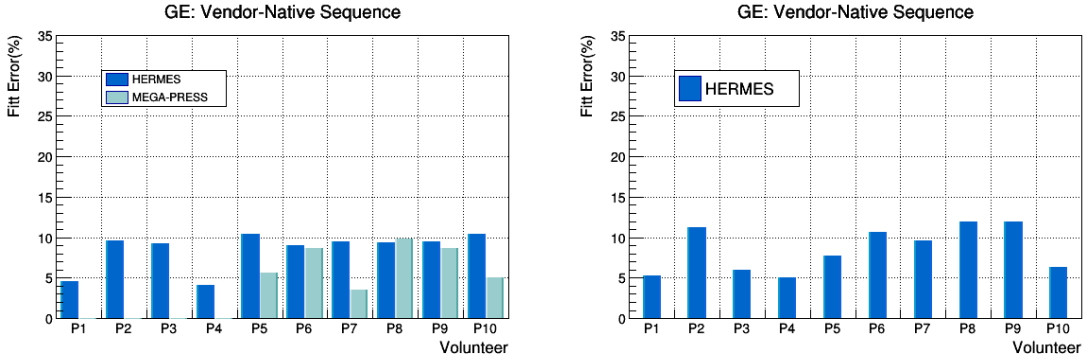

(a) (b)

Figure 34: Histogram showing the fit error GABA+ and GSH for each particitant from the GE scanner. (a) Vendor-native GABA+ edited HERMES and MEGA-PRESS sequence for 10 and 6 participants respectfully, (b) vendor-native GSH edited HERMES sequence on 10 participants.

Spectral Overlap of Edited Spectrum and Model Fit

GABA+ and GSH spectra from all participants of the lateral prefrontal region of the brain are overlapped in figure 35. The GABA+ peaks are detected at 3 ppm for all participants. Measurements of GABA+ revealed that MEGA-PRESS contribute to a higher amplitude in the signals and improved the overlap between participants. The low CV from MEGA-PRESS compared to HERMES confirms that MEGA-PRESS has the best reproducability, table 9. Peaks from HERMES, seen in figure 35 (a), are further apart and the respective signals are not as noticeable from the noise.

The HERMES and MEGA-PRESS mean values from these measurements are significantly different ($p - value(amp_{GABA+}) < \alpha$), but there were found a statistical relationship between the two sequence types($r(amp_{GABA+}) = 0.7$). This result indicates that MEGA-PRESS receives the highest

amplitude of the two sequences.

The GSH spectra can be seen at approximately 2.9 ppm for all participants and show significantly lower variation in signal strength between patients compared to GABA+ measured with HERMES. Figure 35 (c) illustrate some baseline variations between participants, but the respective amplitudes does not seem to be affected to a large extent ($CV(amp_{GSH}) = 14\%$).

Table 9: GE: Height of peak relative to baseline of GABA+ and GSH from vendor-native sequences. r = correlation coefficient.

GROUP	Mean ± Std (CV)	p-value	r
$\text{HERMES}_{\text{GABA+}}$	7.1 ± 2.1 (30%)		
$\text{MEGA-PRESS}_{\text{GABA+}}$	14.5 ± 1.4 (10%)	< 0.00001	0.7
$\text{HERMES}_{\text{GSH}}$	6.0 ± 0.9 (14%)		

Table 30 lists the SNR and FWHM of GABA+ and GSH. These findings validates that the SNR of GABA+ is higher when measured with MEGA-PRESS compared to HERMES. The high CV from MEGA-PRESS might be caused by the fluctuating baseline between participants and due to one of the signals being substantially taller than the rest. The analysis of SNR and FWHM did not confirm any correlation between the two sequences. The FWHM is considerably thinner for MEGA-PRESS compared to HERMES, which could indicate that MEGA-PRESS is more suited for measuring GABA+.

Table 30 shows that the CVs of FWHM is superior to the CVs of the SNR. This could be a result of baseline differences due to the water reference varying to a small extent between participants. As mentioned in section 3.3.3 the noise is measured from 10 to 12 ppm. This region might not be as sensitive to the changes in water concentration compared to GABA+ and GSH, which could result in higher SNR values depending on the effect of the water suppresion.

Table 10: GE: SNR and FWHM of GABA+ and GSH with vendor-native sequences

GROUP	SNR			FWHM		
	$Mean \pm std$ (CV%)	p-value	r	$Mean \pm std$ (CV%)	p-value	r
$HERMES_{GABA+}$	9.0 ± 2.0 (22%)			26.6 ± 4.1 (15%)		
$MEGA\text{-}PRESS_{GABA+}$	15.6 ± 2.1 (50%)	0.002	0.2	19.9 ± 1.6 (8%)	0.02	0.3
$HERMES_{GSH}$	9.9 ± 2.6 (30%)			10.4 ± 1.1 (10%)		

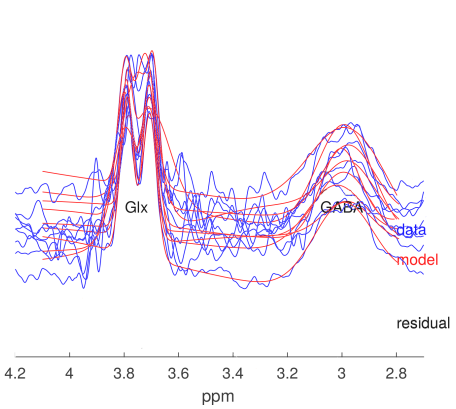

(a) GABA+: HERMES

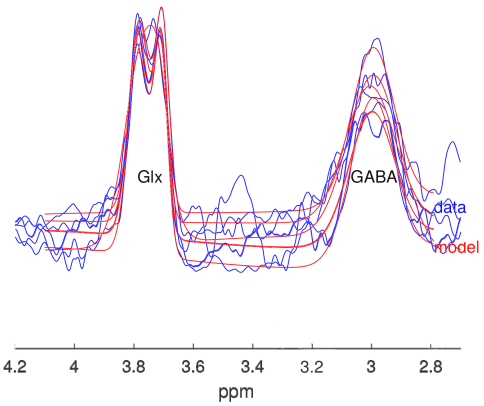

(b) GABA+: MEGA-PRESS

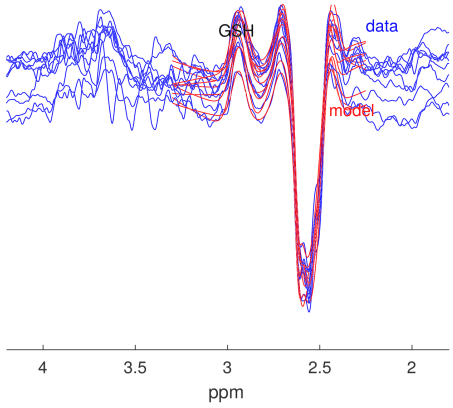

(c) GSH: HERMES

Figure 35: Spectral overlap of spectra from GABA+ and GSH. (a) GABA+ found by the vendor-native HERMES sequence. (b) GABA+ found by implementing the vendor-native MEGA-PRESS sequence. (c) GSH found by the vendor-native HERMES sequence.

4.1.2 Vendor-Native Sequences on Siemens

GABA+ and GSH Concentration Ratio

For the Siemens scanner, there was no water reference for MEGA-PRESS, so it was only possible to quantify the data from HERMES. The mean, standard deviation and CVs of GABA+ and GSH are outlined in table 11 and the acquired data from each participant are presented in figure 36. CVs of both GABA+ and GSH are very high. These fluctuating values are illustrated in figure 36.

Table 11: Siemens: Concentration ratio of GABA+/H20 and GSH/H2O, relaxation-, tissue-, and alpha-corrected (average-voxel-normalized), from the ventor-native sequences. r = correlation coefficient.

GROUP	Mean ± Std (CV)
$\text{HERMES}_{\text{GABA+}}$	2.2 ± 1.1 (50%)
$\text{HERMES}_{\text{GSH}}$	1.3 ± 0.6 (46%)

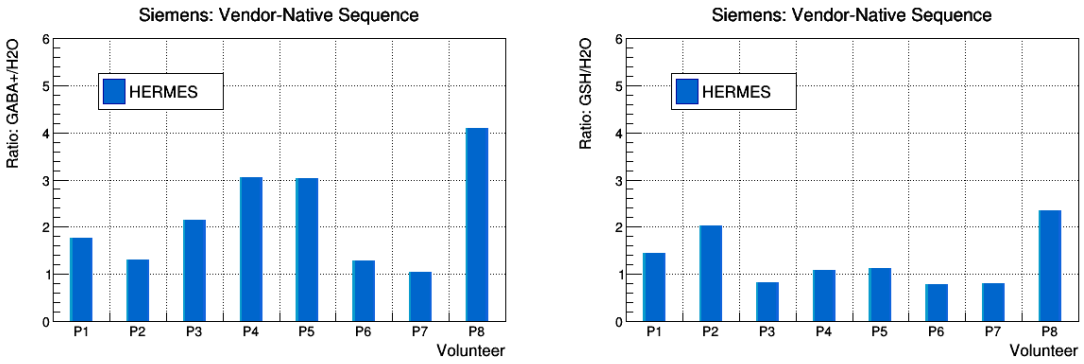

(a) (b)

Figure 36: Ratio of GABA+ and GSH, relaxation-, tissue-, and alpha-corrected (average-voxel-normalized), from the Siemens scanner at Haukeland University Hospital. (a) Vendor-native GABA+ edited HERMES sequence, (b) vendor-native GSH edited HERMES sequence.

Fit Error

Fitting errors of GABA+ and GSH from the HERMES sequence is presented in table 12 and figure 37. GSH exhibits the best fit quality between the participants compared to the fit quality of GABA+

with the same participants.

Table 12: Siemens: Fit Error of GABA+ and GSH from the vendor-native sequencies. r = correlation coefficient.

GROUP	Mean ± Std (CV)
$HERMES_{GABA+}$	11.7 ± 4.6 (39%)
$HERMES_{GSH}$	9.2 ± 2.1 (23%)

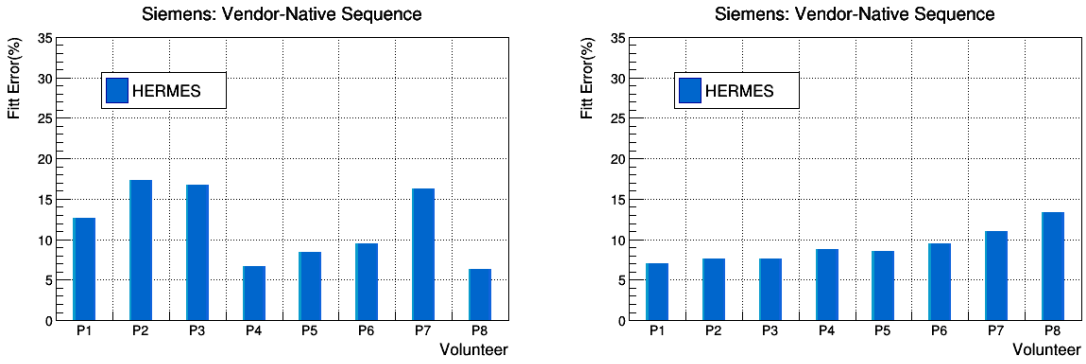

(a) (b)

Figure 37: Histogram showing the fit error of GABA+ and GSH from the Siemens scanner. The bars represent the fit error values from each participant in the scanner. (a) Vendor-native GABA+ edited HERMES sequence, (b) vendor-native GSH edited HERMES sequence.

Spectral Overlap of Edited Spectrum and Model Fit

GABA+ and GSH spectra from all participants of the lateral prefrontal region of the brain are overlapped in figure 44. GABA+ has the highest amplitude of the two with almost twice the mean and CV. Figure 13 (a) clearly shows that two of the peaks from GABA+ are significantly taller than the rest. This could indicate that if there were more participants there might be a trend of lower GABA+ values than the current mean value of GABA+.

Table 13: Siemens: Height of Peak relative to Baseline of GABA+ and GSH from vendor-native sequences. r = correlation coefficient.

GROUP	Mean ± Std (CV)
$\text{HERMES}_{\text{GABA+}}$	14.3 ± 3.5 (24%)
$\text{HERMES}_{\text{GSH}}$	5.9 ± 2.8 (47%)

The SNR of GABA+, table 14, was found to be remarkably short, which could be the result of the high baseline around 4 ppm as seen in figure 38, while the FWHM has a large variation among participants. This could be a result of the varying amplitude of GABA+ and GSH as illustrated in figure 38.

Table 14: Siemens: SNR and FWHM of GABA+ and GSH with vendor-native sequences. r = correlation coefficient.

GROUP	SNR	FWHM
	$Mean \pm std$ (CV%)	$Mean \pm std$ (CV%)
$\text{HERMES}_{\text{GABA+}}$	7.3 ± 2.5 (34%)	20.3 ± 5.3 (26%)
$\text{HERMES}_{\text{GSH}}$	8.3 ± 2.0 (24%)	12.1 ± 4.8 (40%)

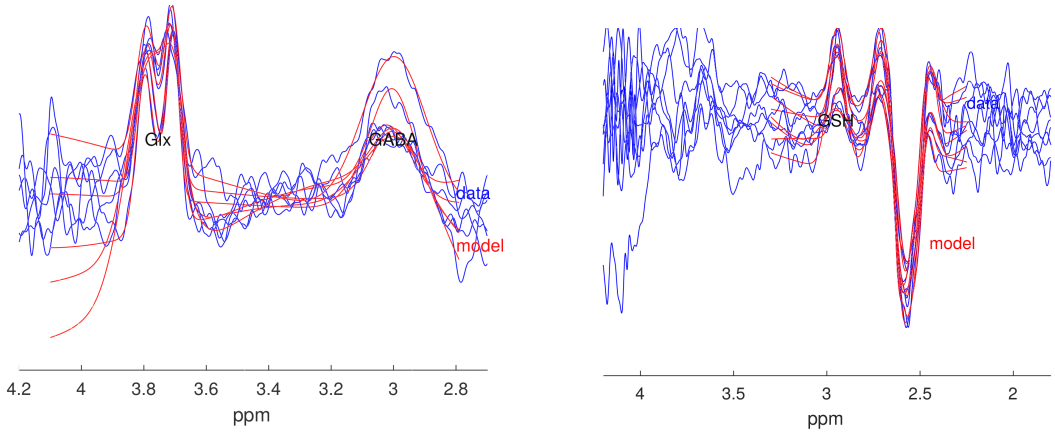

(a) GABA+: HERMES

(b) GSH: HERMES

Figure 38: Overlayed spectra of GABA+ and GSH from GE. (a) GABA+ found by using the universal HERMES sequence, (c) GSH measured by the universal HERMES sequence.

4.1.3 Universal Sequences on GE

GABA+ and GSH Concentration Ratio

The concentration ratio of GABA+ received from HERMES and MEGA-PRESS do overlap ($p - value(ratio_{GABA+}) = 0.2$), however the correlation is not significant ($r(ratio_{GABA+}) = -0.1$). Since the CV of GABA+ is above 40% for MEGA-PRESS, there seems to be an error in the measurements, which could be one reason why these sequences do not correlate. Unfortunately, there was no analysis with a universal MEGA-PRESS sequence for GSH due to time limitations (i.e. subject time in the scanner).

Table 15: GE: Concentration ratio of GABA+/H20 and GSH/H2O, relaxation-, tissue-, and alpha-corrected (average-voxel-normalized), from the universal sequences. r = correlation coefficient.

GROUP	Mean ± Std (CV)	p-value	r
$HERMES_{GABA+}$	1.4 ± 0.4 (29%)		
$MEGA\text{-}PRESS_{GABA+}$	1.9 ± 0.8 (42%)	0.2	-0.1
$HERMES_{GSH}$	0.7 ± 0.2 (29%)		

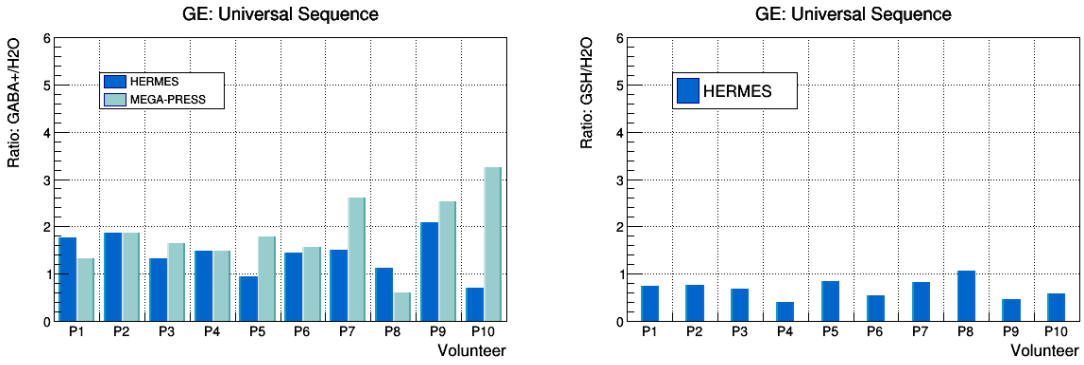

(a) (b)

Figure 39: Histograms of the concentration ratios from each participant using the universal sequences on the GE scanner. (a) Universal GABA+ edited sequence (b) universal GSH edited sequence.

Fit Error

Percentage fit errors of GABA+ and GSH measured with universal HERMES sequences are in agreement with previous studies, however the fit error of GABA+ from MEGA-PRESS is too high, table 16. The results from the fit error analysis indicates a moderate correlation although it is not significant ($p - value(FitError_{GABA+}) = 0.5, r(FitError_{GABA+}) = 0.4$). Figure 40 (a) shows the fit errors from all participants measured with HERMES and MEGA-PRESS, and it clearly shows that the modelled fit of participant 3, 8 and 9 are unreliable for MEGA-PRESS.

Table 16: GE: Fit Error of GABA+ and GSH from universal sequences. r = correlation coefficient.

GROUP	Mean ± Std (CV)	p-value	r
$HERMES_{GABA+}$	11 ± 2.9 (26%)		
$MEGA\text{-}PRESS_{GABA+}$	12.7 ± 8.4 (66%)	0.5	0.4
$HERMES_{GSH}$	7.4 ± 3.1 (41%)		

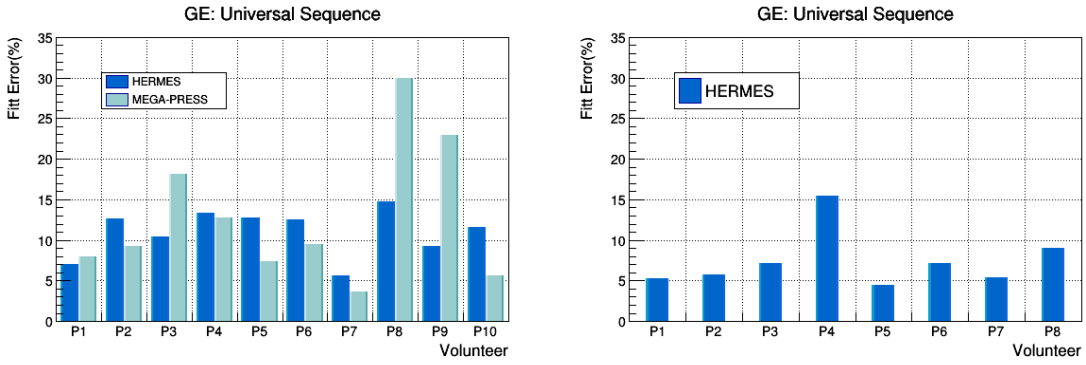

(a) (b)

Figure 40: Histogram providing the fit error values of GABA+ and GSH for each particitant from the GE scanner. (a) Universal GABA+ edited HERMES and MEGA-PRESS sequence, (b) universal GSH edited HERMES sequence.

Spectral Overlap of Edited Spectrum and Model Fit

GABA+ and GSH spectra from all participants of the optical cortical region of the brain can be seen in figure 41. Visual inspections of the overlapped GABA+ signals from MEGA-PRESS, figure 41 (b), display large variations in the position of the peaks and baseline.There are some overlap in the amplitude of GABA+ from HERMES and MEGA-PRESS, but no significant correlation as seen in table17. CVs listed in table 17 indicates that GSH followed by GABA+ using HERMES offers the most robust results.

Table 17: GE: Height of Peak relative to baseline of GABA+ and GSH from universal sequences. r = correlation coefficient.

GROUP	Mean ± Std (CV)	p-value	r
$HERMES_{GABA+}$	9.6 ± 1.4 (15%)		
$MEGA\text{-}PRESS_{GABA+}$	10.7 ± 2,4 (21%)	0.26	0.005
$HERMES_{GSH}$	6.8 ± 0.8 (11%)		

The reported values from the universal GABA+ edited MEGA-PRESS sequence has a higher SNR than the universal HERMES sequence, but a far worst reproducibility as presented in table 30. Furthermore, the FWHM of the GABA+ edited MEGA-PRESS sequence is poor, mainly due

to one of the peaks having an exceedingly smaller FWHM than the rest, as seen in figure 41 (b). There is not found a significant relationship between HERMES and MEGA-PRESS, but the results indicate than HERMES has a clear advantage over MEGA-PRESS in terms of producing spectra with minor variations among participants.

Table 18: GE: SNR and FWHM of GABA+ and GSH from universal sequences. r = correlation coefficient.

GROUP	SNR			FWHM		
	$Mean \pm std$ (CV%)	p-value	r	$Mean \pm std$ (CV%)	p-value	r
$HERMES_{GABA+}$	20.3 ± 4.1 (20%)			25.7 ± 5.1 (20%)		
$MEGA\text{-}PRESS_{GABA+}$	22.1 ± 15.1 (68%)	0.7	-0.2	19.4 ± 5.2 (26%)	0.1	0.2
$HERMES_{GSH}$	16.0 ± 3.9 (24%)			10.4 ± 1.4 (13%)		

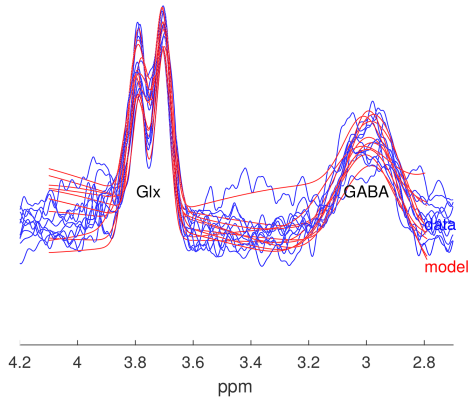

(a) GABA+: HERMES

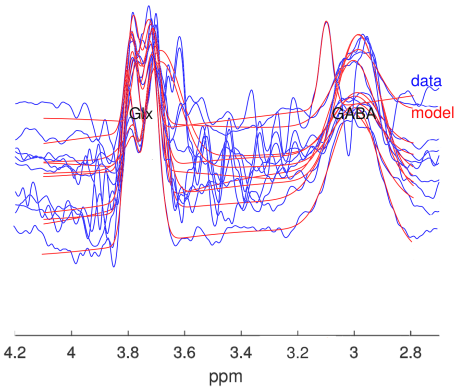

(b) GABA+: MEGA-PRESS

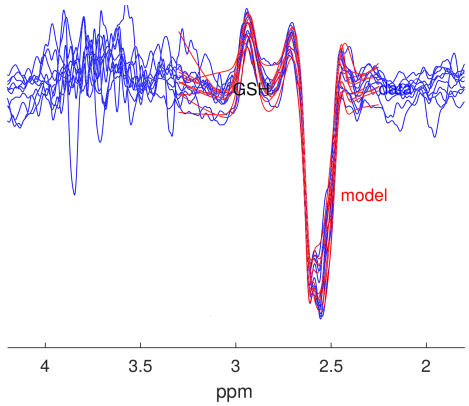

(c) GSH: HERMES

Figure 41: Overlayed spectra of GABA+ and GSH from GE. (a) GABA+ found by using the universal HERMES sequence. (b) The universal MEGA-PRESS sequence is used for finding GABA+. (c) GSH found by the universal HERMES sequence.

4.1.4 Universal Sequences on Siemens

GABA+ and GSH Concentration Ratio

The mean values of GABA+ measured with the universal HERMES and MEGA-PRESS sequence are significantly different ($p - value(ratio_{GABA+}) = 0.004$), however there is a strong correlation between the two sequences ($r(ratio_{GABA+}) = 0.8$). The concentration ratios of GABA+ tends to be slightly higher from MEGA-PRESS compared to HERMES, as shown in figure 42, which could result in the low p-value in table 19. Not only do the universal MEGA-PRESS sequence provide higher

consentration ratios, it also provides a low variation among subjects ($CV(ratio_{MP,GABA+} = 12\%$). These results suggest that the universal MEGA-PRESS sequence could be better suited for Siemens than HERMES when measuring GABA+.

Since there were no measurements of GSH with the universal MEGA-PRESS sequence on Siemens, it is not possible to determine if MEGA-PRESS could be optimal for both GABA+ as well as GSH. The analysis does nonetheless suggest that HERMES has a good agreement between participants suggesting that the sequence is well suited for GSH measurements.

Table 19: Siemens: Concentration ratio of GABA+/H20 and GSH/H2O, relaxation-, tissue-, and alpha-corrected (average-voxel-normalized), from the universal sequences. r = correlation coefficient.

GROUP	Mean ± Std (CV)	p-value	r
$HERMES_{GABA}$	2.8 ± 0.6 (21%)		
$MEGA\text{-}PRESS_{GABA}$	3.4 ± 0.4 (12%)	0.004	0.8
$HERMES_{GSH}$	1.3 ± 0.2 (15%)		

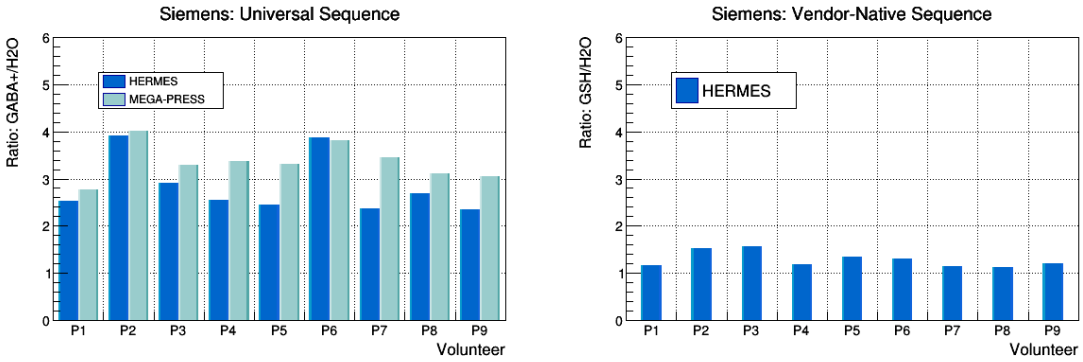

(a) (b)

Figure 42: Concentration ratios of GABA+ and GSH from each participant using the Siemens scanner. (a) universal GABA+ edited sequences (b) universal GSH edited sequences.

Fit Error

Fit errors of GABA+ from the universal sequences are generally low with a moderate correlation to each other as seen in table 20. The mean value and CVs of GABA+ and GSH are small, indicating a good and consistent fit among all the participant's spectra. GABA+ measured with MEGA-PRESS

shows the best fit with the least variation, which is also illustrated in figure 43.

Table 20: Siemens: Fit Error of GABA+ and GSH from universal sequences. r = correlation coefficient.

GROUP	Mean ± Std (CV)	p-value	r
$\text{HERMES}_{\text{GABA}}$	6.0 ± 1.1 (18%)		
$\text{MEGA-PRESS}_{\text{GABA}}$	4.2 ± 0.7 (17%)	0.004	0.5
$\text{HERMES}_{\text{GSH}}$	8.3 ± 1.6 (19%)		

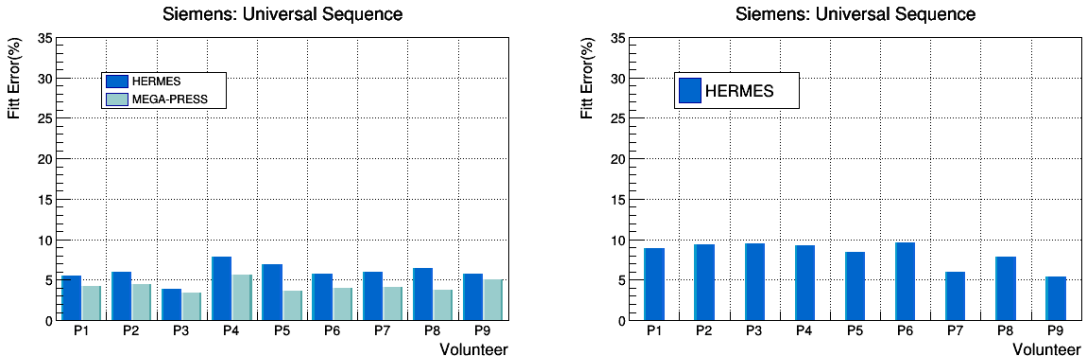

(a) (b)

Figure 43: Histogram showing the fit error GABA+ and GSH for each particitant from the Siemens scanner. (a) Universal GABA+ edited HERMES and MEGA-PRESS sequence, (b) vendor-native GSH edited HERMES sequence.

Spectral Overlap of Edited Spectrum and Model Fit

Figure 44 shows the GABA+ and GSH spectra from all participants of the occipital cortices region of the brain. Visual inspections indicate that GABA+ measured with HERMES has the lowest variation between subjects while MEGA-PRESS has the greatest measured amplitude. This is supported by direct measurements on each figure presented in table 21. The difference in the mean distributions of GABA+ measured with HERMES and MEGA-PRESS is significant ($p - value(Amp_{GABA+} = 0.05)$, and there is evidence of a significant relationship ($r(Amp_{GABA+} = 0.9)$. These results indicate that there is a relationship between HERMES and MEGA-PRESS, with MEGA-PRESS receiving a higher signal. There seem to be some baseline differences in the spectra

of GABA+ and GSH, however the amplitude and position of the peaks over the x-axis are similar. This is indicated by the low CVs in table 21.

Table 21: Siemens: Height of Peak relative to Baseline of GABA+ and GSH from universal sequences. r = correlation coefficient.

GROUP	Mean ± Std (CV)	p-value	r
$\text{HERMES}_{\text{GABA}}$	11.1 ± 0,3 (3%)		
$\text{MEGA-PRESS}_{\text{GABA}}$	14.8 ± 1.1 (8%)	0.05	0.9
$\text{HERMES}_{\text{GSH}}$	6.0 ± 0,5 (9%)		

The SRN and FWHM of GABA+ edited HERMES and MEGA-PRESS had the best reproducibility in this thesis, 30. The analysis provides evidence of a significant correlation between the two sequences in SNR, where MEGA-PRESS has the highest SNR. In addition to MEGA-PRESS receiving the highest SNR, it also receives the narrowest FWHM. The GABA+ edited MEGA-PRESS sequence shows a clear advantage uposed to HERMES in therms of meassuring GABA+ with Siemens.

Table 22: Siemens: SNR and FWHM of GABA+ and GSH from universal sequences

GROUP	SNR			FWHM		
	$Mean \pm std$ (CV%)	p-value	r	$Mean \pm std$ (CV%)	p-value	r
$\text{HERMES}_{\text{GABA+}}$	11.1 ± 1.8 (16%)			22.9 ± 2.1 (9%)		
$\text{MEGA-PRESS}_{\text{GABA+}}$	18.7 ± 3.2 (17%)	> 0.0001	0.6	19.7 ± 1.0 (5%)	0.003	0.2
$\text{HERMES}_{\text{GSH}}$	12.7 ± 2.7 (20%)			12.4 ± 5.7 (46%)		

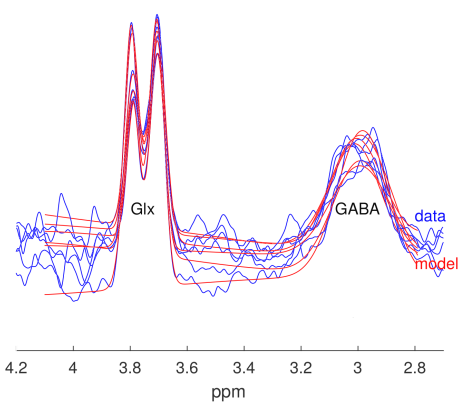

(a) GABA+: HERMES

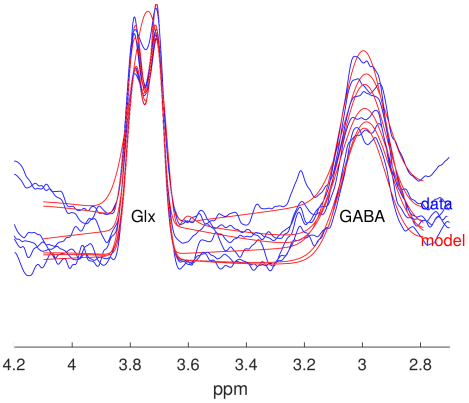

(b) GABA+: MEGA-PRESS

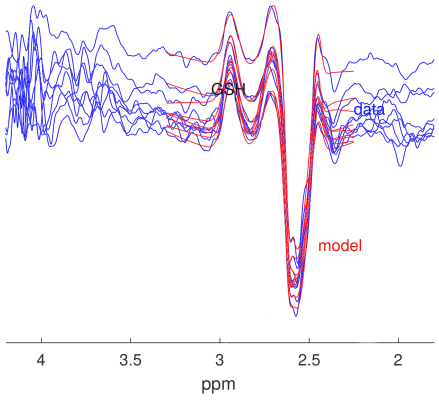

(c) GSH+: HERMES

Figure 44: Spectral overlap from the Siemens scanner using the universal sequence for (a) HERMES and (b) MEGA-PRESS for GABA+ and (c) HERMES for GSH.

4.2 Comparison Across Vendors: GE and Siemens

4.2.1 GE and Siemens with Vendor-Native Sequences

GABA+ and GSH concentration ratio

The participants examined on GE are unfortunately not the same as those who were examined by Siemens. For this reason a two sampled t-test is applied instead of a paired t-test. Since HERMES was only executed for Siemens, it will only be possible to compare the data from HERMES between the vendors.

GABA+ and GSH concentration ratios from GE and Siemens are displayed in table 23. The concentration ratio of GABA+ from GE and Siemens have the same mean value, where GE has the greatest degree of agreement between the participants with its CV of 36%. Since the p-value is above α, the null hypothesis is accepted, which indicates no proof against GE and Siemens receiving different values of GABA+. The measured correlation coefficient however is below the critical correlation coefficient, meaning there is no significant relationship between the two scanners.

GSH values between GE and Siemens were significantly different ($p-value(ratio_{GABA+} = 0.03)$ as shown in table 23, while the correlation were proven to be strong ($r(ratio_{GABA+} = 0.8)$.

The relationship across scanners when measuring GSH shows a significant correlation, table 23. The CVs between the measurements from GE and Siemens are then again not in line with previous studies with lower CVs (CV<24%), which is essential to interpret the results correctly. This might indicate that the results are not that significant and would need further investigation.

Table 23: GE and Siemens: Concentration ratio of GABA+/H20 and GSH/H2O, relaxation-, tissue-, and alpha-corrected (average-voxel-normalized), from the vendor-native sequences. r = correlation coefficient.

GROUP	Mean ± Std (CV)	p-value	r
GE_{GABA}	2.2 ± 0.8 (36%)		
$Siemens_{GABA}$	2.2 ± 1.1 (50%)	~ 1	0.02
GE_{GSH}	0.8 ± 0.2 (25%)		
$Siemens_{GSH}$	1.3 ± 0.6 (46%)	0.03	0.8

Fit Error

Both GABA+ and GSH has some similarity in mean values of fit errors ($p-value(Fiterror_{GABA+} = 0.08$, $p-value(Fiterror_{GSH} = 0.6)$ and correlation of fit errors between vendors ($r(Fiterror_{GABA+} = 0.8$, $r(FiterrorGSH = 0.9)$, as shown in table 24, indicating that there is a trend of Siemens having higher fit errors than GE. The fit error from both vendors are witin the recomended range compared to related studys (fit error $< 12\%$) revealing a good quality fit of the model.

Table 24: GE and Siemens: Fit Error of GABA+ and GSH from the vendor-native HERMES sequence. r = correlation coefficient.

GROUP	Mean ± Std (CV)	p-value	r
GE_{GABA}	9.7 ± 0.6 (6%)		
$Siemens_{GABA}$	11.7 ± 4.6 (39%)	0.08	0.8
GE_{GSH}	8.6 ± 2.8 (33%)		
$Siemens_{GSH}$	9.2 ± 2.1 (23%)	0.6	0.9

Spectral Overlap of Edited Spectrum and Model Fit

The results from GABA+ measurements of the spectra between vendors show no significant correlation ($r(Amp_{GABA+} = 0.3)$ and reveals that the measured data are significantly different ($p - value(Amp_{GABA+} = 0.006)$, table 25.

The spectra of GSH from GE and Siemens were not significantly different ($p-value(Amp_{GSH} = 0.9$), however the measured correlation coefficient is below the critical correlation for the given sample size indicating that there is no significant relationship between GSH amplitude measurements with GE and Siemens.

Table 25: GE and Siemens: Height of peak relative to baseline of GABA+ and GSH with vendor-native HERMES sequences. r = correlation coefficient.

GROUP	Mean ± Std (CV)	p-value	r
GE_{GABA+}	7.1 ± 2.1 (30%)		
$Siemens_{GABA+}$	14.3 ± 3.5 (24%)	0.006	0.3
GE_{GSH}	6.0 ± 0.9 (14%)		
$Siemens_{GSH}$	5.9 ± 2.8 (47%)	0.9	0.3

Table 26 provides a list of the SNR and FWHM from vendor-native GABA+ and GSH edited HERMES sequences from GE and Siemens. The analisys confirmed no significant correlation considering GE and Siemens.

Table 26: GE and Siemens: SNR and FWHM of GABA+ and GSH with vendor-native HERMES sequences. r = correlation coefficient.

SCANNER	SNR			FWHM		
	$Mean \pm std$ (CV%)	p-value	r	$Mean \pm std$ (CV%)	p-value	r
GE_{GABA}	9.0 ± 2.0 (22%)			26.6 ± 4.1 (15%)		
$Siemens_{GABA+}$	7.3 ± 2.5 (34%)	0.2	0.03	20.3 ± 5.3 (26%)	0.03	-0.3
GE_{GSH}	9.9 ± 2.6 (30%)			10.4 ± 1.1 (10%)		
$Siemens_{GSH}$	8.3 ± 2.0 (24%)	0.3	0.2	12.1 ± 4.8 (40%)	0.4	0.2

Figure 45 presents the overlapped spectra form vendor-native sequences used for GE and Siemens. Visual analysis from viewing the spectra suggest a poor relationship across subjects and vendors.

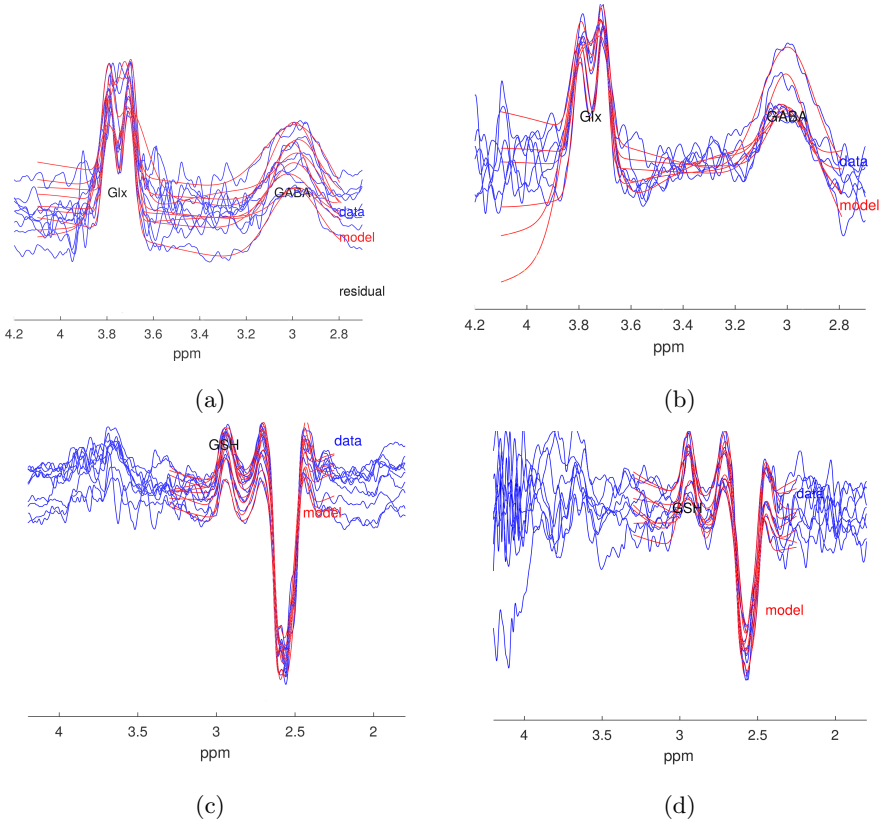

Figure 45: Spectral overlap from GE and Siemens using the vendor-native sequences for (a) HERMES and (b) MEGA-PRESS for GABA+ and (c) HERMES for GSH.

4.2.2 GE and Siemens with Universal Sequences

GABA+ and GSH concentration ratio

Six of the participants from GE and Siemens were tested on both scanners. The distributions of the means of GABA+ from GE and Siemens is significantly different with a strong correlation ($p - value(ratio_{GABA+}) = 0.005, r(ratio_{GABA+}) = 0.9$), table 27. This analysis reveals that even though the received values between GE and Siemens are different, the correlation is strong. Since the variance between the participants in the two scanners is relatively small, the gap in mean values could have something to do with the different parameters settings, for instance, by the water suppression methods used by GE and Siemens.

The universal MEGA-PRESS sequence used to measure GABA+ showed no correlation between vendors revealing values that were significantly different. The CV of GABA+ is three times higher for GE than Siemens, which suggest that the universal MEGA-PRESS sequence is, for the time being, not as optimal for GE compared to Siemens.

The results reveal no correlation between GSH values of the sampled data from GE and Siemens. Values were significantly different ($p - value(Ratio_{GSH} = 0.001$) and show no significant correlation when compared to the critical correlation for the chosen α.

Table 27: GE and Siemens: Concentration ratio of GABA+/H20 and GSH/H2O, relaxation-, tissue-, and alpha-corrected (average-voxel-normalized), from the universal sequences. r = correlation coefficient.

GROUP	Mean ± Std (CV)	p-value	r
$GE_{HERMES,GABA}$	1.4 ± 0.5 (29%)		
$Siemens_{HERMES,GABA}$	2.8 ± 0.5 (21%)	0.005	0.9
$GE_{MEGA\text{-}PRESS,GABA+}$	2.0 ± 0.6 (32%)		
$Siemens_{MEGA\text{-}PRESS,GABA+}$	3.3 ± 0.3 (10%)	0.003	0.1
$GE_{HERMES,GSH}$	0.7 ± 0.2 (29%)		
$Siemens_{HERMES,GSH}$	1.3 ± 0.2 (15%)	0.001	-0.3

Fit Error

The fit error of GABA+ was within an acceptable range (fit error < 12%) when measured with HERMES, as seen in table 28. The relationship between GE and Siemens is significant ($p -$

$value(FitError_{HERMES,GABA+}) = 0.0004, r(FitError_{HERMES,GABA+}) \sim 1)$, which provides evidence to suggest that GE receives higher fit errors when using the universal sequence compared to Siemens.

Values received from MEGA-PRESS has a higher fit error from GE, revealing a p-value below α, and a significant correlation between the two vendors. The high correlation between GE and Siemens confirms that Siemens has a substantially better fit than GE. Since some of the values from GE has a fit of above 20%, as seen in figure 40, the results from GE using MEGA-PRESS are more uncertain than HERMES.

Prosentage fit errors from GE and Siemens measuring GSH is not significantly different with a strong correlation ($p-value(FitError_{HERMES,GSH}) = 0.3$, $r(FitError_{HERMES,GSH}) = 0.9$). The variation in fit error values from GE is however substantially higher, which indicate that Siemens had a superior fit compared to GE using the universal sequences.

Table 28: GE and Siemens: Fit Error of GABA+ and GSH from universal sequences. r = correlation coefficient.

GROUP	Mean ± Std (CV)	p-value	r
$GE_{HERMES,GABA}$	11.8 ± 1.5 (13%)		
$Siemens_{HERMES,GABA}$	5.9 ± 1.7 (29%)	0.0004	~ 1
$GE_{MEGA\text{-}PRESS,GABA+}$	12.2 ± 6.2 (51%)		
$Siemens_{MEGA\text{-}PRESS,GABA+}$	4.3 ± 0.8 (18%)	0.01	0.7
$GE_{HERMES,GSH}$	7.8 ± 3.6 (46%)		
$Siemens_{HERMES,GSH}$	6.2 ± 0.9 (15%)	0.3	0.9

Spectral Overlap of Edited Spectrum and Model Fit

The two spectra of GABA+ from HERMES, seen in figure 46 (a) and (b), appear similar in peak position and amplitude with little variation between subjects. Their measured amplitudes are outlined in table 29 and show no significant difference in amplitude across scanners and a strong correlation.

Visual inspections of GABA+ from MEGA-PRESS on GE, figure 46 (c), display large variations in peak, baseline, amplitude. One of the GABA+ peaks has shifted to 3.1 ppm possessing a much smaller area under the curve compared to the others. Amplitudes from GE and Siemens from the MEGA-PRESS sequences are considered to be significantly different with no correlation, as shown

in table 29.

GSH measurements from GE and Siemens have a p-value above α, confirming that their mean values are not statistically different. Unfortunately, no correlation was found in the analysis of GSH ($r(Amp_{HERMES,GSH}) = 0.1$), indicating that there might not exist a relationship between the received values.

Table 29: Height of Peak relative to Baseline of GABA+ and GSH. r = correlation coefficient.

GROUP	Mean ± Std (CV)	p-value	r
$GE_{HERMES,GABA+}$	9.6 ± 1.4 (15%)		
$Siemens_{HERME,GABA+}$	11.2 ± 2.4 (21%)	0.2	0.8
$GE_{MEGA\text{-}PRESS,GABA+}$	10.7 ± 2.4 (21%)		
$Siemens_{MEGA\text{-}PRESS,GABA+}$	15.1 ± 2.1 (14%)	0.01	0.01
$GE_{HERMES,GSH}$	6.8 ± 0.8 (11%)		
$Siemens_{HERMES,GSH}$	6.0 ± 0.5 (9%)	0.09	0.1

The analysis of SNR reveale a significant overlap and correlation between universal GABA+ and GSH edited HERMES sequences, as listed in table 30. Data from the FWHM confirms a moderate correlation between the GSH edited HERMES sequence.

No significant correlation between GE and Siemens were found from the GABA+ edited MEGA-PRESS sequence. These results indicate that spectra acquired from the universal MEGA-PRESS sequence may not be suitable for GE.

Table 30: GE and Siemens: SNR and FWHM of GABA+ and GSH with universal sequences. r = correlation coefficient.

SCANNER	SNR			FWHM		
	$Mean \pm std$ (CV%)	p-value	r	$Mean \pm std$ (CV%)	p-value	r
$GE_{H,GABA}$	14.4 ± 4.3 (30%)			25.7 ± 5.1 (20%)		
$Siemens_{H,GABA+}$	11.2 ± 1.7 (16%)	0.1	0.6	22.9 ± 2.1 (9%)	0.2	-0.2
$GE_{MP,GABA+}$	21.4 ± 4.36 (20%)			19.0 ± 5.9 (31%)		
$Siemens_{MP,GABA+}$	18.7 ± 3.5 (19%)	0.08	0.2	19.9 ± 0.9 (4%)	0.7	0.3
$GE_{H,GSH}$	15.0 ± 3.9 (26%)			10.4 ± 1.6 (15%)		
$Siemens_{H,GSH}$	13.1 ± 2.6 (19%)	0.3	-0.6	12.6 ± 6.1 (48%)	0.4	0.5

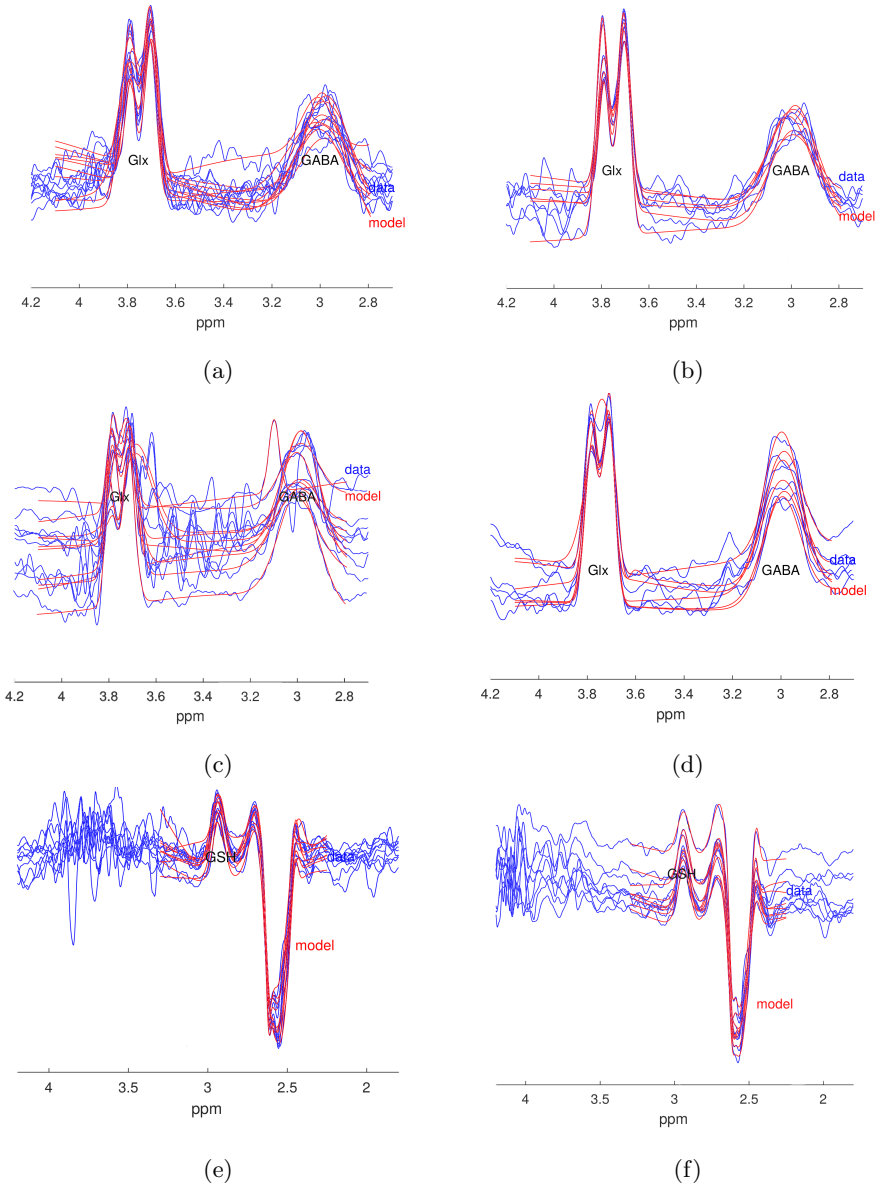

Figure 46: Spectral overlap from GE and Siemens using the universal sequences for (a) HERMES and (b) MEGA-PRESS for GABA+ and (c) HERMES for GSH.

4.2.3 GE and Siemens with Vendor-Native Sequences and Universal Sequences

GABA+ and GSH concentration ratio

From table 31 it is possible to see that the universal HERMES sequences tend to have smaller CVs than the vendor-native HERMES sequence. The mean values found by the vendor-native HERMES sequences are more similar between GE and Siemens, but when CVs are as high as 40-50% this similarity seems to be more of a coincidence than a result of similarity between vendors.

Table 31: GE and Siemens: Concentration ratio of GABA+/H20 and GSH/H2O, relaxation-, tissue-, and alpha-corrected (average-voxel-normalized), from the vendor-native and universal sequences. r = correlation coefficient.

SCANNER	Vendor-Native Sequence		Universal Sequence	
	$Mean \pm std$	CV%	$Mean \pm std$	CV%
$GE_{HERMES,GABA}$	2.2 ± 0.8	36%	1.4 ± 0.4	29%
$Siemens_{HERMES,GABA}$	2.2 ± 1.1	50%	2.8 ± 0.6	21%
$GE_{MEGA\text{-}PRESS,GABA}$	2.5 ± 0.4	16%	2.0 ± 0.6	32%
$Siemens_{MEGA\text{-}PRESS,GABA}$	-	-	3.3 ± 0.3	10%
$GE_{HERMES,GSH}$	0.8 ± 0.2	25%	0.7 ± 0.2	29%
$Siemens_{HERMES,GSH}$	1.3 ± 0.6	46%	1.3 ± 0.2	15%

Figure 47 (a) and (b) shows all the data points and how they vary between vendor and HERMES sequence type. The wiskers presented in the figure represent the maximum value + 1.5*IQR (Interquartile range) and minimum values - 1.5*IQR. Outliners (small circles) lie further than 1.5*IQR and are the remaining 0.7% of the data. The length of the box equals the IQR, while the line going through the box is the median. The bottom line of the box shows the middel value of the smallest number and the median, while the top line of the box shows the number between the highest value and the median. The red dots represent the data samples from the individual participantes. The boxplots indicate that the universal HERMES sequence has the best reproducibility, but it is clear that the values are further apart.

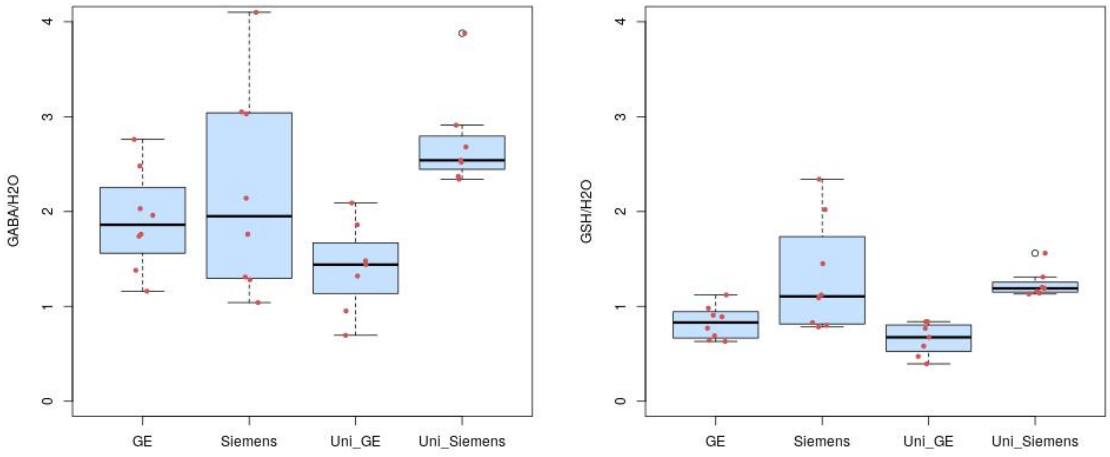

(a) (b)

Figure 47: Boxplot of vendor native and universal HERMES editing methods on GE and Siemens. The black horisontal line in the boxplot indicate were the median is while the red dots represent the data samples from the individual participantes. (a) Concentration ratio of GABA+/H20, relaxation-, tissue-, and alpha-corrected (average-voxel-normalized), (b) Concentration ratio of GSH/H2O, relaxation-, tissue-, and alpha-corrected (average-voxel-normalized). GE = vendor-native HERMES sequence on GE, Siemens = vendor-native HERMES sequence on Siemens, Uni_GE = universal HERMES sequence on GE and Uni_Siemens = universel HERMES sequence on Siemens

Siemens using the universal MEGA-PRESS sequence provides the best reproducibility of data from the subjects as seen in table 31 while the universal MEGA-PRESS sequence on GE did not produce reliable results in this thesis as discussed in section 4.1.4 and 4.2.2. Figure 48 shows the data received from the vendor-native MEGA-PRESS sequence on GE and universal MEGA-PRESS sequence on GE and Siemens, with Siemens showing the least variability.

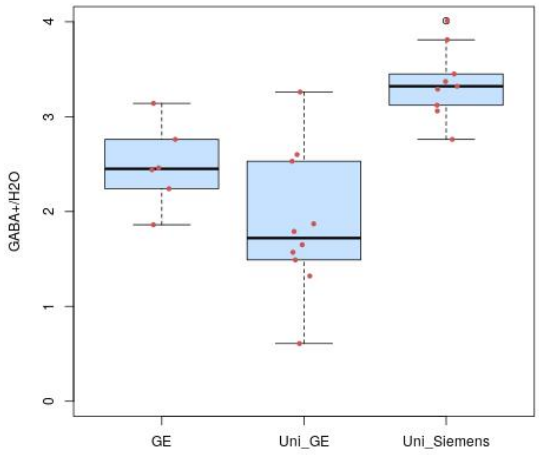

Figure 48: Boxplot of vendor native and universal GABA+ edited MEGA-PRESS sequences on GE and Siemens.The black horisontal line in the boxplot indicate were the median is while the red dots represent the data samples from the individual participantes. GE = vendor-native MEGA-PRESS sequence on GE, Uni_GE = universal MEGA-PRESS sequence on GE and Uni_Siemens = universel MEGA-PRESS sequence on Siemens.

Fit Error

There seems to be a trend of receiving lower fit error values from the universal sequency, with the exception of GABA+ measurements on GE. CVs of the sampled data from Siemens improve when the universal sequence is applied, while worsening when applied on GE. This can also be seen in the form of boxplots in figure 49 and 50. This results might hint that the universal sequence is best suited for Siemens for improving the repeatability within a group of subjects.

Table 32: GE and Siemens: Fit error of GABA+ and GSH from the vendor-native and universal sequences

SCANNER	Vendor-Native Sequence		Univerrsal Sequnece	
	$Mean \pm std$	CV%	$Mean \pm std$	CV%
$GE_{HERMES,GABA}$	9.7 ± 0.6	6%	11.8 ± 1.5	13%
$Siemens_{HERMES,GABA}$	11.7 ± 4.6	39%	5.9 ± 1.7	29%
$GE_{MEGA\text{-}PRESS,GABA}$	6.9 ± 2.5	36%	12.7 ± 2.9	66%
$Siemens_{MEGA\text{-}PRESS,GABA}$	-	-	4.2 ± 0.7	17%
$GE_{HERMES,GSH}$	8.6 ± 2.8	33%	7.8 ± 3.6	46%
$Siemens_{HERMES,GSH}$	9.2 ± 2.1	23%	6.2 ± 0.9	15%

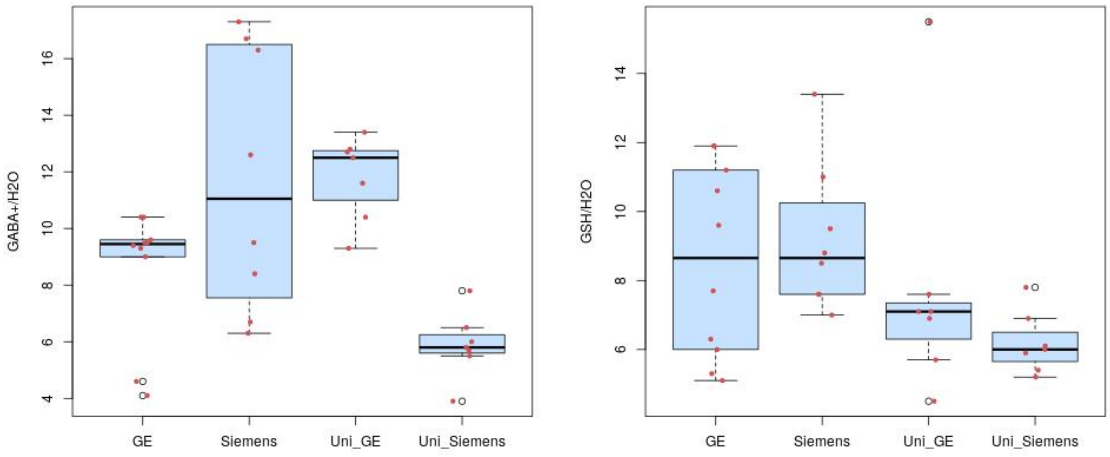

(a) (b)

Figure 49: Boxplot of vendor native and universal HERMES editing methods on GE and Siemens. The black horisontal line in the boxplot indicate were the median is while the red dots represent the data samples from the individual participantes. (a) Concentration ratio of GABA+/H20, relaxation-, tissue-, and alpha-corrected (average-voxel-normalized), (b) Concentration ratio of GSH/H2O, relaxation-, tissue-, and alpha-corrected (average-voxel-normalized). GE = vendor-native HERMES sequence on GE, Siemens = vendor-native HERMES sequence on Siemens, Uni_GE = universal HERMES sequence on GE and Uni_Siemens = universel HERMES sequence on Siemens.

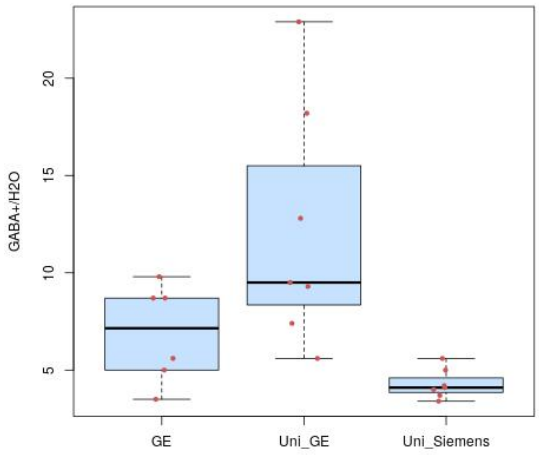

Figure 50: Boxplot of vendor native and universal GABA+ edited MEGA-PRESS sequences on GE and Siemens. GE = vendor-native MEGA-PRESS sequence on GE, Uni_GE = universal MEGA-PRESS sequence on GE and Uni_Siemens = universel MEGA-PRESS sequence on Siemens.

Spectral Overlap of Edited Spectrum and Model Fit

Table 33 presents measured values of the individual spectra in figure 51 illustrating the overlappet HERMES spectra and 52 illustrating the overlapped MEGA-PRESS spectra. The results in table 33 show a trend of lower CVs when the universal sequence is implemented with the exception of GABA+ measured with the universal MEGA-PRESS sequence.

Table 33: GE and Siemens: Height of peak relative to baseline of GABA+ and GSH from the vender-native and universal sequences

SCANNER	Vendor-Native Sequence		Univerrsal Sequnece	
	$Mean \pm std$	CV%	$Mean \pm std$	CV%
$GE_{HERMES,GABA}$	7.1 ± 2.1	(30%)	9.6 ± 1.4	(15%)
$Siemens_{HERMES,GABA}$	14.3 ± 3.5	(24%)	11.2 ± 2.4	(21%)
$GE_{MEGA\text{-}PRESS,GABA}$	10.1 ± 1.0	(10%)	10.7 ± 2.4	(22%)
$Siemens_{MEGA\text{-}PRESS,GABA}$	-	-	14.8 ± 1.1	(8%)
$GE_{HERMES,GSH}$	6.0 ± 0.9	(14%)	6.8 ± 0.8	(11%)
$Siemens_{HERMES,GSH}$	5.9 ± 2.8	(47%)	6.0 ± 0.5	(9%)

The results of the SNR from the universal sequence are substantially better than the vendor-native sequence, as presented in table 34. The SNR is increased in size and the CVs are lower, with the exeption of the universal GABA+ edited HERMES sequence. From the results in table 33 and 34, it would seem like implementing the universal HERMES sequence on GE and Siemens improves the reproducibility of the spectre.

Table 34: GE and Siemens: SNR of GABA+ and GSH from the vender-native and universal sequences

SCANNER	Vendor-Native Sequence		Univerrsal Sequnece	
	$Mean \pm std$	CV%	$Mean \pm std$	CV%
$GE_{HERMES,GABA}$	9.0 ± 2.0	(22%)	14.4 ± 4.3	(30%)
$Siemens_{HERMES,GABA}$	8.3 ± 2.0	(24%)	11.2 ± 1.7	(16%)
$GE_{MEGA\text{-}PRESS,GABA}$	15.6 ± 2.1	(50%)	21.4 ± 4.36	(20%)
$Siemens_{MEGA\text{-}PRESS,GABA}$	-	-	18.7 ± 3.5	(19%)
$GE_{HERMES,GSH}$	9.9 ± 2.6	(30%)	15.0 ± 3.9	(26%)
$Siemens_{HERMES,GSH}$	8.3 ± 2.0	(24%)	13.1 ± 2.6	(19%)

Table 35 summarises FWHM form the vendor-native and universal sequences from GE and Siemens. The analysis from the FWHM shows a trend of higher CVs for the universal sequences, indicating that the vendor-native sequences has slightly superior results.

Table 35: GE and Siemens: FWHM of GABA+ and GSH from the vender-native and universal sequences

SCANNER	Vendor-Native Sequence		Univerrsal Sequnece	
	$Mean \pm std$	CV%	$Mean \pm std$	CV%
$GE_{HERMES,GABA}$	26.6 ± 4.1	(15%)	25.7 ± 5.1	(20%)
$Siemens_{HERMES,GABA}$	20.3 ± 5.3	(26%)	22.9 ± 2.1	(9%)
$GE_{MEGA\text{-}PRESS,GABA}$	19.9 ± 1.6	(8%)	19.0 ± 5.9	(31%)
$Siemens_{MEGA\text{-}PRESS,GABA}$	-	-	19.9 ± 0.9	(4%)
$GE_{HERMES,GSH}$	10.4 ± 1.1	(10%)	10.4 ± 1.6	(15%)
$Siemens_{HERMES,GSH}$	12.1 ± 4.8	(40%)	12.6 ± 6.1	(48%)

From visual inspections of figure 51, it would seem as though the baseline differences decrease when using the universal sequences. This could result in the trend of lower SNR seen in table 35.

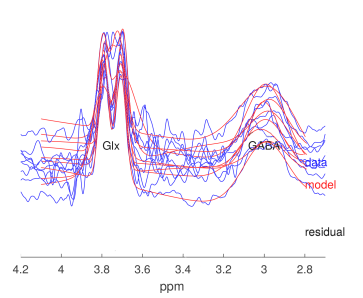

(a) GE: vender-native$_{\text{GABA+}}$

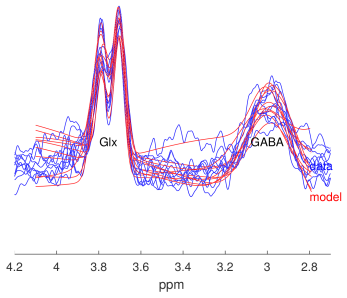

(b) GE: universal$_{\text{GABA+}}$

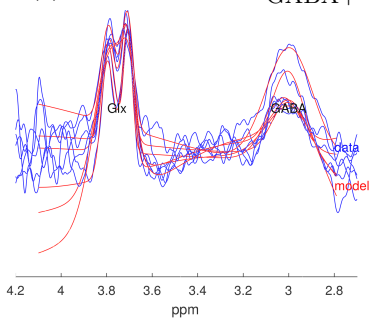

(c) Siemens: vender-native$_{\text{GABA+}}$

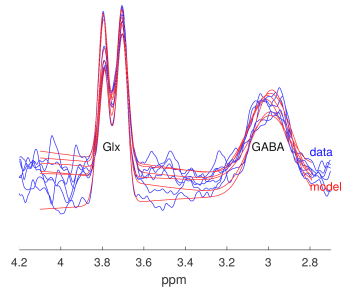

(d) Siemens: universal$_{\text{GABA+}}$

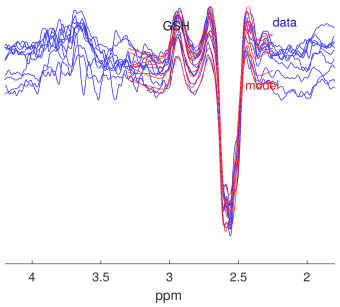

(e) GE: vender-native$_{\text{GSH}}$

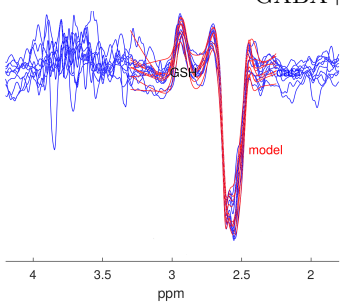

(f) GE: universal$_{\text{GSH}}$

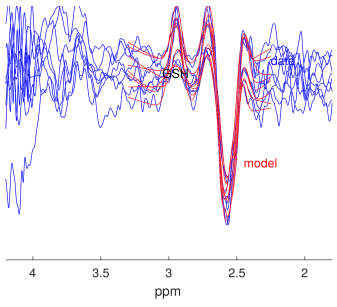

(g) Siemens: vender-native$_{\text{GSH}}$

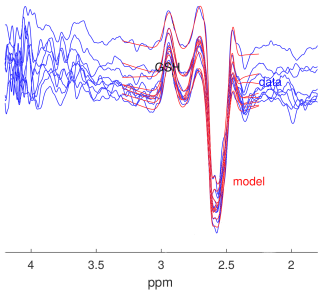

(h) Siemens: universal$_{\text{GSH}}$

Figure 51: Spectral overlap from GE and Siemens using the vendor-native and universal HERMES sequences.

Figure 52 illustrate the differences in GABA+ spectra using the vendor-native and universal sequences on GE and the universal sequence on Siemens. This figure clearly indicates that the universal MEGA-PRESS sequence was not suited for GE.

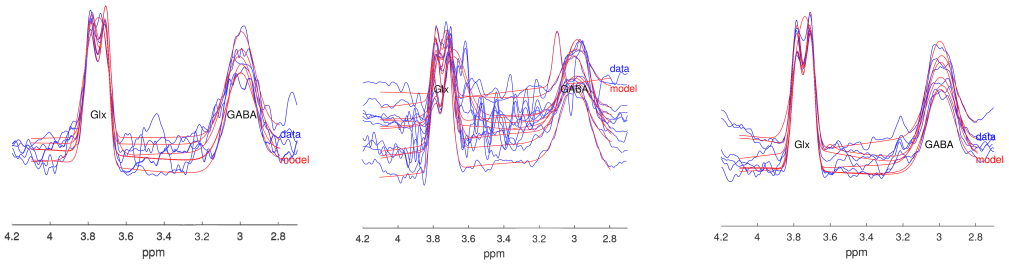

(a) GE: vender-native$_{\text{GABA+}}$ (b) GE: universal$_{\text{GABA+}}$ (c) Siemens: universal$_{\text{GABA+}}$

Figure 52: Spectral overlap from GE and Siemens using the vendor-native and universal MEGA-PRESS sequences.

5 Discussion and Outlook

The goal of this thesis was to examin how well vendor-native and universal sequences for HERMES and MEGA-PRESS detect GABA+ and GSH *in vivo* and to see if it is possible to get comparable results between GE and Siemens systems at Haukeland University Hospital. Technical evaluations of fit error, relative amplitude from the baseline of the spectra, SNR, FWHM and the variability between subjects were studied to evaluate if the measurements were of good quality. The discussion section starts by evaluating the results and then examine some methodological considerations.

5.1 Comparison of HERMES and MEGA-PRESS

5.1.1 Vendor-Native Sequences on GE

Quantitative estimates of GABA+ measured by HERMES and MEGA-PRESS overlap partly in this part of the study ($p - value(ratio_{GABA+}) = 0.3$), however there does not seem to be a correlation between the sequences ($r(ratio_{GABA+}) = -0.1$). Figure 33 (a) illustrates the overlap, but if there were a correlation between HERMES and MEGA-PRESS one would expect a decline in one sequence if there were decline in the other for the respective participant. What one finds instead are fluctuating HERMES values ($CV(ratio_{H,GABA+}) = 36\%$) around more or less constant MEGA-PRESS values ($CV(ratio_{MP,GABA+}) = 16\%$). From table 8 it is seen that GABA+ measured with MEGA-PRESS also tends to have the lowest fit error ($mean(FitError_{MP,GABA+}) = 6.9, mean(FitError_{H,GABA+}) = 9.7$) and table 30 indicates the spectra has the greatest SNR of the two sequences ($mean(SNR_{MP,GABA+}) = 15.6, mean(SNR_{H,GABA+}) = 9.0$). This could be caused by the spectrum having a maximum signal at TE=68 ms where it thereby declines with longer TE values [49] as mentioned in chapter 2.2.1. This analysis therefore indicates that the GABA+ edited MEGA-PRESS technique is best suited for the GE system.

The MEGA-PRESS editing technique for GSH is not considered in this assignment due to fluctuating concentration ratio, large fit errors and errors in GSH spectra. GSH editing with the HERMES technique had a much better outcome. The CV of the concentration ratio between subjects ($CV(ratio_{GSH}) = 25\%$) is almost the same as CVs in literature, and the fit error ($mean(FitError_{GSH}) = 8.6$) is within recommended boundaries, (FitError$< 12\%$). The GSH spectra overlap nicely as seen in figure 35 (b), with some baseline variations. These variations could be the result of individual differences in water references. However, as the water signal from individual participants was not analysed explicitly in this thesis, this can not be verified. Based on these

findings, the vendor-native HERMES sequence is adequate for measuring GSH, but more work is needed to further minimise the variance in concentration ratios across participants.

5.1.2 Vendor-Native Sequences on Siemens

There were no measurements for either GABA+ or GSH by vendor-native MEGA-PRESS sequences, so the focus in this section was on the vendor-native HERMES sequence. The results show that simultaneous measurements of GABA+ and GSH had a poor reproducibility of the concentration ratios with a CV of 50% for GABA+ and 46% for GSH, table 11, which is the largest in this project. This could be the result of the separation between the editing pulses, which is less than TE/2 and therefore not optimal as mentioned in section 3.1.2.

The fit error from the spectrum of GABA+, table 12, is amongst the higher fit error values ($mean(FitError_{GABA+}) = 11.7$) with fluctuating results between participants ($CV(FitError_{GABA+})$ = 39%). This can result in spectrum not having the same foundation when the concentration ratio is measured, and could be one reason why the concentration ratio of GABA+ has a CV of 50%. From figure 44 one can undoubtedly see two peaks high above the other peaks in the overlapped GABA+ spectra, which could indicate that if there were more participants there might be a trend of lower GABA+ values than the current mean value of GABA+. The figure also illustrates variations in the baseline around 4 ppm, which may explain why the SNR of GABA+ is lower than the measured amplitude($mean(SNR_{GABA+}) = 7.3, mean(Amp_{GABA+}) = 14.3$). If the water suppression were not sufficient one could expect a lower SNR due to the increased baseline were the noise is measured (10-12 ppm). However, since the water signal was not explicitly examined in this thesis, it is not possible to say that the poor SNR of GABA+ is due to the water suppression.

The FWHM for both GABA+ and GSH had a poor reproducibility ($CV(FWHM_{GABA+}) = 26\%, CV(FWHM_{GSH}) = 40\%$), which could be the result of fluctuating SNR. As mentioned in section 3.3.3, one method of improving the SNR is by increasing the acquisition time, which might be beneficial when using the vender-native sequence on Siemens. From these findings, it is clear that Siemens using the vendor-native HERMES sequence did not produce reliable results of the concentration ratio from GABA+ or GSH.

5.1.3 Universal Sequences on GE

The results of this analysis found no significant correlation in ratio, fit error, amplitude, SNR or FWHM between the universal GABA+ edited HERMES and MEGA-PRESS sequence. There were

however a significant overlap in their mean distributions of concentration ratio confirmed by the high p-value of 0.2. The missing correlation could be caused by the fluctuating values received from MEGA-PRESS. Table 15 indicates the GABA+ concentration ratio from MEGA-PRESS has a poor reproducibility ($CV(ratio_{MP,GABA+}) = 42\%$), and table 16 clearly shows a fit error above what is considered reliable ($mean(FitError_{MP,GABA+}) = 12.7, CV(FitError_{MP,GABA+}) = 66\%$), with come fit error s above 20%, figure 40.

Visual inspections of figure 41 (b) confirms that spectra from MEGA-PRESS has fluctuating SNR, FWHM and baselines, demonstrating a bad overlap of the GABA+ spectra. HERMES has conciderably better results from the fit error and spectral overlap, but the reproducibility of the concentration ratio ($CV(ratio_{H,GABA+}) = 29\%$) is still above what is found in similar studies ($CV < 24\%$). Based on these results can conclude that the universal HERMES sequence is more adequate at measuring GABA+ compared to the universal MEGA-PRESS sequence, but that HERMES also needs further optimalisation to improve reproducibility.

Estimates of GSH with the universal HERMES sequence had the same CV from the concentration ratio as GABA+. However, GSH had a lower fit error ($mean(FitError_{GSH}) = 7.4$) and lower CVs from the spectral amplitude measurements ($CV(Amp_{GSH}) = 15\%$), SNR ($CV(SNR_{GSH}) = 24\%$) and FWHM ($CV(FWHM_{GSH}) = 13\%$). These results suggest that the universal GSH edited HERMES sequence is sufficient at measuring GSH although more work remains to minimise the high CV of the concentration ratios.

5.1.4 Universal Sequences on Siemens

Quantitative measurements of GABA+ measured by the universal MEGA-PRESS and HERMES sequences on Siemens confirms a significant correlation in the concentration ratio ($r(ratio_{GABA+}) = 0.8$) even though HERMES has reduced GABA+ concentration levels which effects the p-value ($p - value(ratio_{GABA+}) = 0.004$). The reproducibility of the sequences are within acceptable range ($CV(ratio_{H,GABA+}) = 21\%, CV(ratio_{MP,GABA+}) = 12\%$) indicating that the results are reliable. The fit error from the GABA+ spectra from the two sequences are the low ($mean(FitError_{H,GABA+}) = 6$, $mean(FitError_{MP,GABA+}) = 4.2$), showing a moderate correlation ($r(FitError_{GABA+}) = 0.5$). Table 21 and 30 also present a signifficant correlation for HERMES and MEGA-PRESS between the measured amplitude and SNR.

The amplitudes of GABA+ from MEGA-PRESS are considerably higher than the amplitudes of GABA+ from HERMES, implying that although the two editing methods are measuring the

same concentration, MEGA-PRESS measures a higher value, which is also expected due to optimal TE used for MEGA-PRESS. From these results, both sequences are well suited for measuring the concentration ratio of GABA+, but the universal MEGA-PRESS sequence comes out as the sequence with the best reproducibility, lowest fit error and greatest SNR.

CV from the concentration ratio of GSH is also low ($CV(ratio_{H,GSH}) = 15\%$), showing there is a good reproducibility, and the fit error ($mean(FitError_{H,GSH}) = 8.3$) is within the recommended range. The overlapped spectra in figure 44 (c) have some variations in the baseline but the amplitude and SNR show little fluctuation ($CV(Amp_{H,GSH}) = 9\%, CV(SNR_{H,GSH}) = 20\%$). The reproducibility of GSH in general showed promising results with the exception of the FWHM of GSH measured with HERMES, which proves to be high. This outcome suggests that the edited HERMES sequence can represent GSH sufficiently. Unfortunately, there were no measurements of GSH using the universal MEGA-PRESS sequences. Otherwise, it would be interesting to see if the data correlated as well as for GABA+.

5.2 Comparison Across Vendors: GE and Siemens

5.2.1 GE and Siemens with Vendor-Native Sequences

The vendor-native HERMES sequence used on GE and Siemens for measuring the concentration ratio of GABA+ has a significant overlap ($p - value(ratio_{GABA+}) \sim 1$), but no correlation ($r(ratio_{GABA+}) = 0.02$) suggesting that there is no relationship between the vendors for vendor-native implementations. The low correlation coefficient could be the outcome of high CVs from the concentration ratios, which are all above 24% as shown in table 32. The difference in GE and Siemens could also be caused by two of the subjects in Siemens having uncommonly large SNR. The relationship between the vendors might have been proven to be greater if the number of participants were larger.

The difference in mean values of GSH using HERMES on GE and Siemens is, on the other hand, statistically significant ($p-value(ratio_{GABA+}) = 0.03$), having a strong relationship ($r(ratio_{GABA+}) = 0.8$). The CV, however, reveals a large variation in GSH concentration ratios from Siemens ($CV(ratio_{GSH}) = 46\%$), as well as no significant correlation in amplitude, SNR and FWHM between vendors. These findings make it hard to correctly interpret the strong correlation in concentration ratios. It could therefore seem like the correlation between concentration ratios were more based on chance. More research should therefore be done to optimize the vendor-native HERMES sequence

on Siemens and use a larger number of subjects with the goal of reducing the CV.

5.2.2 GE and Siemens with Universal Sequences

The correlation between GABA+ concentration ratios from GE and Siemens with the universal HERMES sequence is significant ($r(ratio_{H,GABA+}) = 0.9$). Furthermore the correlation between fit error ($r(FitError_{H,GABA+}) \sim 1$), amplitude ($r(Amp_{H,GABA+}) = 0.8$) and SNR was also significant ($r(SNR_{H,GABA+}) = 0.6$), with overlapping values for the amplitude and SNR ($p - value(AmpH, GABA+) = 0.2, p - value(SNRH, GABA+) = 0.1$). One setback is the difference in the mean values of the concentration ratios ($p - value(ratio_{H,GABA+}) = 0.005$), which could be caused by the different water suppression methods used by GE and Siemens. If the two vendors receive different water reference the calculated GABA+/H2O from GE would be different compared to the calculated GABA+/H2O from Siemens. If the water suppression were standardized across vendors this could perhaps correct the difference in concentration ratios.

Another challenge is the high CV from GE. Table 27 shows that CV from GABA+ ($CV(ratio(GE)_{H,GABA+}) = 29\%$) are higher compared to similar studies where CVs vary between 6-24%, as mentioned in section 3.3.3. Siemens, on the other hand, has a lower variability across subjects ($CV(ratio(Siemens)_{H,GABA+}) = 21\%, CV(ratio(Siemens)_{MP,GABA+}) = 10\%$) and can, therefore, be considered as having more valid results. Siemens also provides with the lowest fit errors that range between 4.3-6.2%, which is good compared to fit errors found in literature that range between 5-6%, as mentioned in 3.3.3. Between the two scanners, Siemens shows most promising results with the universal HERMES sequence.

The similarities between GABA+ in GE and Siemens with the universal MEGA-PRESS sequence is less promising. The correlation is not sufficient ($r(ratio_{MP,GABA+}) = 0.1$) and the mean values significantly differ ($p - value(ratio_{MP,GABA+}) = 0.003$). One of the reasons for this low correlation could be that some of the spectra from GE were of poor quality as mentioned in section 4.1.3. More work is, therefore, needed to optimize the universal MEGA-PRESS sequence for GE to obtain spectra with less variability.

Quantitative measurements of GSH show a significant difference in mean values ($p - value(ratio_{H,GSH}) = 0.001$), showing a trend of higher concentration ratio on Siemens. There is a weak negative correlation between the concentration ratios between the vendors, but it is not significant ($r(ratio_{H,GSH}) = -0.3$). There is, however, a significant correlation in the fit error and SNR, and a moderate correlaton in the FWHM. However, the high CV obtaind from the GE scanner in

concentration ratio ($CV(ratio(GE)_{H,GSH}) = 29\%$), fit error ($CV(FitError(GE)_{H,GSH}) = 46\%$) and the high CV of the FWHM from Siemens ($CV(FWHM(Siemens)_{H,GSH}) = 46\%$) confirms the these results are unreliable. These findings reveal that there might be a correlation in GSH measurements, although this is difficult given the high uncertainties in the measurements.

5.2.3 GE and Siemens with Vendor-Native Sequences and Universal Sequences

When comparing the results from the vendor-native and universal sequences it is important to keep in mind that the sample groups were small, and the sample group measured with the vendor-native sequence are not the same as those measured with the universal sequence. The most important finding when comparing the vendor-native sequence to the universal sequence is the trend of lower CVs observed for the universal HERMES sequence, as shown in table 31. This illustrates that the universal HERMES sequence might improve the reproducibility of GABA+ and GSH measurements, which is an essential step towards quantifications. The universal-sequences did, however, receive higher CVs from the FWHM compared to the vendor-native sequences, presented in table 35, suggesting that the FWHM could be optimised further. The reproducibility of measurements from Siemens was most beneficial for the universal HERMES sequences, receiving reliable concentration ratios, fit errors, amplitude measurements and SNR, as seen in table 31, 32, 33, 34, respectfully. The results of this analysis therefore confirms that the universal sequences are better suited for Siemens compared to the vendor-native sequence.

GE received less favorable results from the universal sequences, especially the universal MEGA-PRESS sequence. The universal sequences tended towards higher CVs in the concentration ratio, fit error and FWHM, seen in table 31, 32 and 35 respectfully, but there were a slight improvement in the measured amplitude and SNR, table 34. Returning to the question in the beginning of the study, it is now possible to state that the universal sequence needs further work on GE before it can produce results with the same reproducibility as the vendor-native sequences.

5.3 Methodological Considerations

5.3.1 Inclusion/Exclusion Criteria

The participants included in this thesis are mostly of males. This is due to the fact that there are more male students physics at UiB than females at the moment, so recruiting them was easier. It could have been prefered to have full gender balance, and this is likely to be achieved if inclusion is

continued. Some studies suggest that there might be a difference in the concentration of GABA and GSH between males and females [64] [67], so to have chosen a more equal gender balance would have been better for testing the reproducibility in the different scans across participants. Other studies have concluded that there is no difference between genders, so the results on the matter are mixed [68].

The number of participants in this thesis is limited. When the sample size increases the t-distribution gets thinner, while if the sampling size is small, like in this case, the t-distribution gets wider. If the t-distribution is wider the probability of getting extreme values in the sample becomes larger. This results in less information and statistical power to detect an effect. With a smaller sample size it might be possible to observe trends in the data not occurring by chance, but without significant proof due to the limited number of participants. In this thesis, the sample size was large enough to achieve statistically significant results, but the CVs were in general greater than CVs from related studies suggesting a need for increased sample size. The mean value could then become more stable so that the differences or similarities across groups would be more thrustworthy.

5.3.2 The VOI

The lateral prefrontal and occipital cortices region of the brain were chosen as VOIs for this project. The reason there are two different regions being examined is coincidental and caused by grouping data from different subprojects. Choosing the exact VOI for every participant is dificult to do manually, but optimising this could result in less within-subject and between-subject variations since the concentration of GABA and GSH changes in different regions of the brain [70] [69] [71].

The voxel size used in this thesis is 27ml, which is of recommended proportions when it comes to MEGA-PRESS and HERMES. A smaller voxel might be easier to place and give less partial volume effects [38], but at the expense of the acquisition time which would have to be longer to obtain the same SNR. A longer acquisition time provides a better SNR as mentioned in section 3.3.3, but if the patient starts to move the final spectrum will have a worse SNR. For now, it has therefore been prefered to have a bigger voxel.

5.3.3 MRS Limitations

The MEGA-PRESS and HERMES scans are relatively long (8-10 min). Editing techniques rely on subtraction methods and are even more sensitive to motion than PRESS, so staying perfectly still for several minutes is difficult. Head movements during the scan change the region were the voxel

was intended to be, which could result in a spectrum with more lipid or air than intended [38]. This change in position could then ruin the spectra.

As mentioned earlier, the voxels were not placed in the same region, which could affect the GABA and GSH level. Another limitation is that there is not yet a MEGA-PRESS or HERMES application for calculating the geometry of a participants brain to place the voxel at the same spot, reducing the within-subject and between-subject variations. In the future, localisation sequences like PRESS which rely on manual placement of a voxel might be replaced by sequences that have automatic placement of a voxel to increase reproducibility in a study [73].

Another limitation concerning MEGA-PRESS and HERMES is that the bandwidth is narrow, which increases the chemical shift displacement error (CSDE). The chemical shift displacement errors are inversely proportional to the bandwidth and occur since metabolite in a VOI has a chemical shift. The frequency difference in the spectra combined with a broader bandwidth like LASER and semi-LASER exhibits can provide a better-resolved spectrum on a shorter amount of time [74]. LASER could, therefore, be a good replacement for PRESS in the HERMES and MEGA-PRESS sequence.

Receiving similar results in a study with two different vendors is limited by the fact that the systems are not identical. Vendors use various amplifiers to generate amplified radio frequencies, the shimming protocols are different, and the water suppression methods, crusher gradients and the number of phase cycling to dampen or remove signals are still not standardized in the universal sequence. Vendors are not necessarily interested in standardizing across vendors as this may require revealing some restricted information of their systems.

5.4 Conclusion

The results of this thesis indicate that the vendor-native MEGA-PRESS sequence on GE provided robust measurements of GABA+, and that the universal HERMES and MEGA-PRESS sequences on Siemens provided robust measurements of GABA+ and GSH, with little variation between participants. Measurements from GE using the universal sequence and Siemens using the vendor-native sequence produced spectra with poor reproducibility.

Results from the analysis confirm that MEGA-PRESS tends to measure a higher concentration ratio, which could be due to MEGA-PRESS choosing optimal TE values. HERMES might therefore benefit from choosing a longer acqusition time to increase SNR. The correlation of HERMES and MEGA-PRESS was only sufficient when the universal editing sequences were used on Siemens. Oth-

erwise, there was no significant relationship between HERMES and MEGA-PRESS across vendors, although it was possible to measure overlapping values at a group level.

In this thesis, there were only found a significant correlation between GE and Siemens from the vendor-native GSH edited HERMES sequence, and the universal GABA+ edited HERMES sequence. The correlation in GSH concentration ratio from GE and Siemens using the vendor-native sequence were put to question considering Siemens presented high CVs and since there were no correlation in measurements of the amplitude, SNR and FWHM. The relationship found between GE and Siemens when measuring GABA+ with the universal HERMES sequence was more robust considering the higher reproducibility between subjects and the significant correlation found in concentration ratio, fit error, amplitude and SNR.

The great gap in mean values from GE and Siemens using the universal HERMES sequence might be due to other differences in the two scanners, such as the water suppression methods used; CHESS and VAPOR. To minimise differences in vendors in the future one should try to standardise further aspects of the universal sequence, for instance, the water suppression method, gradient crushers, the RF phase cycling scheme and implement a localisation tool like sLASER that does not rely on manual placement of the voxels. This could enhance the reproducibility, spectral quality and agreement within vendors in the future.

In conclusion, although some optimisations are still needed, across vender implementation to standardise quantification of GABA+ and GSH is considered to be feasible.

References

[1] George Samuel Hurst John Oliver Stoner Jack D. Graybeal Steven Chu , 2019. *Spectroscopy.* Encyclopaedia Britannica. [ONLINE] Available at: https://www.britannica.com/science/spectroscopy. [Accessed 2 May 2019].

[2] Proctor WG, Yu FC. *The dependence of a nuclear magnetic resonance frequency upon chemical compound.* Phys Rev 1950; 77:717.

[3] Daniel J Bell, A.Prof Frank Gaillard (2019) *1.5 T vs 3.0 T.* Radiopedia [ONLINE] Available at: https://radiopaedia.org/articles/15-t-vs-30-t. [Accessed 2 May 2019].

[4] Jansen, J. F., Backes, W. H., Nicolay, K., & Kooi, M. E. (2006). *1 H MR Spectroscopy of the Brain: Absolute Quantification of Metabolites 1.* 1 Department of Radiology, Maastricht University Hospital, P. Debyelaan 25, 6202 AZ Maastricht, the Neth- erlands; and Biomedical NMR, Department of Biomedical Engineering, Eindhoven University of Technology, Eind- hoven, the Netherlands.

[5] Store Norske Leksikon (2019). *Kjernemagnetisk resonans (NMR)* Available at: https://snl.no/kjernemagnetisk_resonans_(NMR) [Accessed 2 May 2019].

[6] Mark A. Brown, Richard C. Semelka (2003) *MRI: Basic Principles and Applications* Third Edition. Pages1-37, 181-195. John Wiley & Sons.

[7] Atle Bjørnerud (2008). *The Physics of Magnetic Resonance Imaging.* Pages 7-17, 34-43. Oslo University Press.

[8] Questions and Answers in MRI. 2018. *Origin of the MR Signal.* [ONLINE] Available at: http://mriquestions.com/origin-of-mr-signal.html. [Accessed 15 November 2018].

[9] XRayPhysics - Interactive Radiology Physics. 2014. *MRI Physics: Pulse Sequences* [ONLINE] Available at: http://xrayphysics.com/sequences.html [Accessed 17 November 2018].

[10] Barker, P. B. (2010). *Clinical MR spectroscopy: techniques and applications.* Cambridge: Cambridge University Press.

[11] Questions and Answers in MRI. 2018. *Flip (or Tip) Angle* AD Elster, ELSTER LLC. [ONLINE] Available at: http://mriquestions.com/what-is-flip-angle.html. [Accessed 17 November 2018].

[12] Questions and Answers in MRI. 2018. *Origin of the MR Signal* AD Elster, ELSTER LLC. [ONLINE] Available at: http://mriquestions.com/origin-of-mr-signal.html.[Accessed 17 November 2018].

[13] Dr. Ian Hunt, Department of Chemistry at the University of Calgary *Chemical Shift* [ONLINE] Available at: http://www.chem.ucalgary.ca/courses/350/Carey5th/Ch13/ch13-nmr-2.html [Accessed 15 May 2019].

[14] de Graaf, Robin. (2007). *In vivo NMR spectroscopy : principles and techniques.* Chichester: John Wiley & Sons.

[15] Khan Academy. (2014). Diamagnetic anisotropy. [Online Video]. 23 July 2014. Available from: https://nb.khanacademy.org/science/organic-chemistry/spectroscopy-jay/proton-nmr/v/diamagnetic-anisotropy. [Accessed: 14 May 2019].

[16] Khan Academy. (2014). Spin-spin splitting (coupling). [Online Video]. 23 July 2014. Available from: https:https://nb.khanacademy.org/science/organic-chemistry/spectroscopy-jay/proton-nmr/v/spin-spin-splitting-coupling. [Accessed: 14 May 2019].

[17] Kwang W.Jeon. (2002) *International Review of Cytology: A Survey of Cell Biology.* Academic Press.

[18] Hongxia Lei, Lijing Xin, Rolf Gruetter, Vladimír Mlynárik. (2014) *The principle of volume determination using three slice* [digitized photograph]. Available at: https://www.sciencedirect.com/science/article/pii/B9780124016880000021#f0010 [12.02.19].

[19] Govindaraju, V., Young, K., Maudsley, A.A., 2000. *Proton NMR chemical shifts and coupling constants for brain metabolites.* NMR Biomed. 13 (3), 129–153.

[20] Goddard AW, Mason GF, Almai A, Rothman DL, Behar KL, Petroff OA, et al. *Reductions in occipital cortex GABA levels in panic disorder detected with 1H-magnetic resonance spectroscopy.* Archives of general psychiatry. 2001;58(6):556-61.

[21] Simpson HB, Shungu DC, Bender J, Jr., Mao X, Xu X, Slifstein M, et al. *Investigation of cortical glutamate-glutamine and gamma-aminobutyric acid in obsessive-compulsive disorder by proton magnetic resonance spectroscopy.* Neuropsychopharmacology : official publication of the American College of Neuropsychopharmacology. 2012;37(12):2684-92.

[22] Epperson CN, O'Malley S, Czarkowski KA, Gueorguieva R, Jatlow P, Sanacora G, et al. *Sex, GABA, and nicotine: the impact of smoking on cortical GABA levels across the menstrual cycle as measured with proton magnetic resonance spectroscopy.* Biological psychiatry. 2005;57(1):44-8.

[23] Bhagwagar Z, Wylezinska M, Jezzard P, Evans J, Ashworth F, Sule A, et al. *Reduction in occipital cortex gamma-aminobutyric acid concentrations in medication-free recovered unipolar depressed and bipolar subjects.* Biological psychiatry. 2007;61(6):806-12.

[24] Yoon JH, Maddock RJ, Rokem A, Silver MA, Minzenberg MJ, Ragland JD, et al. *GABA concentration is reduced in visual cortex in schizophrenia and correlates with orientation-specific surround suppression.* The Journal of neuroscience : the official journal of the Society for Neuroscience. 2010;30(10):3777-81.

[25] Morgan PT, Pace-Schott EF, Mason GF, Forselius E, Fasula M, Valentine GW, et al. *Cortical GABA levels in primary insomnia.* Sleep. 2012;35(6):807-14.

[26] Emir UE, Tuite PJ, Oz G. *Elevated pontine and putamenal GABA levels in mild- moderate Parkinson disease detected by 7 tesla proton MRS.* PLoS One. 2012;7(1):e30918.

[27] Foerster BR, Callaghan BC, Petrou M, Edden RA, Chenevert TL, Feldman EL. *Decreased motor cortex gamma-aminobutyric acid in amyotrophic lateral sclerosis.* Neurology. 2012;78(20):1596-600.

[28] Foerster BR, Pomper MG, Callaghan BC, Petrou M, Edden RA, Mohamed MA, et al. *An imbalance between excitatory and inhibitory neurotransmitters in amyotrophic lateral sclerosis revealed by use of 3-T proton magnetic resonance spectroscopy.* JAMA Neurol. 2013;70(8):1009-16.

[29] Matsuzawa D, Obata T, Shirayama Y, Nonaka H, Kanazawa Y, Yoshitome E, et al. *Negative correlation between brain glutathione level and negative symptoms in schizophrenia: a 3T 1H-MRS study.* PLoS One. 2008;3(4):e1944.

[30] Lavoie S, Murray MM, Deppen P, Knyazeva MG, Berk M, Boulat O, et al. *Glutathione precursor, N-acetyl-cysteine, improves mismatch negativity in schizophrenia patients.* Neuropsychopharmacology : official publication of the American College of Neuropsychopharmacology. 2008;33(9):2187-99.

[31] Mandal PK, Tripathi M, Sugunan S. *Brain oxidative stress: detection and mapping of anti-oxidant marker 'Glutathione' in different brain regions of healthy male/female, MCI and Alzheimer patients using non-invasive magnetic resonance spectroscopy.* Biochem Biophys Res Commun. 2012;417(1):43-8.

[32] Srinivasan R, Ratiney H, Hammond-Rosenbluth KE, Pelletier D, Nelson SJ. *MR spectroscopic imaging of glutathione in the white and gray matter at 7 T with an application to multiple sclerosis.* Magn Reson Imaging. 2010;28(2):163-70.

[33] Kulak A, Cuenod M, Do KQ. *Behavioral phenotyping of glutathione-deficient mice: relevance to schizophrenia and bipolar disorder.* Behav Brain Res. 2012;226(2):563-70.

[34] Sofic E, Lange KW, Jellinger K, Riederer P. *Reduced and oxidized glutathione in the substantia nigra of patients with Parkinson's disease.* Neuroscience letters. 1992;142(2):128- 30.

[35] Harris AD, Puts NA, Barker PB, Edden RA. *Spectral-editing measurements of GABA in the human brain with and without macromolecule suppression.* Magn Reson Med. 2015 Dec;74(6):1523-9. doi: 10.1002/mrm.25549. Epub 2014 Dec 17. PubMed PMID: 25521836; PubMed Central PMCID: PMC4470877.

[36] Ralf Dringen. (1999) *Metabolism and Functions of Glutathione in Brain* Physiologisch-chemisches Institut der Universita Èt, Hoppe-Seyler-Str. 4, D-72076 Tu Èbingen, Germany

[37] Cooper Aj, Kristal BS. (1997) *Multiple Roles of Glutathione in the Central Nervous System.* Biol Chem.

[38] Maiken Kirkegaard Brix. (2018) *Establishing reliable MR spectroscopy techniques for measuring GABA and Glutathione in the human brain.* Thesis for the Degree of Philosophiae Doctor (PhD). University of Bergen, Norway.

[39] Paul G. Mullins, David J. McGonigle, Ruth L. O'Gorman, Nicolaas A.J. Puts, Rishma Vidyasagarh, C. John Evans, Richard A.E. Edden. (2015) *Current practice in the use of MEGA-PRESS spectroscopy for the detection of GABA.* NIH Public Access Author Manuscript Neuroimage. Author manuscript; available in PMC 2015 February 01. Available at: https://www.ncbi.nlm.nih.gov/pmc/articles/PMC3825742/pdf/nihms433653.pdf [Accessed: 04.12.18]

[40] Kimberly L. Chan, Nicolaas A. J. Puts, Michael Schär, Peter B. Barker, and Richard A. E. Edden. (2016) *HERMES: Hadamard Encoding and Reconstruction of MEGA-Edited Spectroscopy.* US National Library of Medicine National Institutes of Healt. Published in final edited form as: Magn Reson Med. 2016 Jul; 76(1): 11–19. Available at:https://www.ncbi.nlm.nih.gov/pmc/articles/PMC5385137/[Accessed: 20.02.19]

[41] Daoud, Gruchy, Constans, Saumureau, Bayou, Amy, Védrine, Vu, Rötig, Laumonnier, Vourc'h, Andres, Leporrier, Briault. (2008) *Proton MRS single voxel (9.8 cm 3) PRESS spectra measured with multiple TEs.* [digitized photograph]. Available at:[https://www.researchgate.net/figure/Proton-MRS-single-voxel-98-cm-3-PRESS-spectra-measured-with-multiple-TEs-a-35-ms-b_fig3_23476220][30.03.19].

[42] Paul G. Mullins, David J. McGonigle, Ruth L. O'Gorman, Nicolaas A.J. Puts, Rishma Vidyasagarh, C. John Evans, Richard A.E. Edden. (2015) *Schematic diagram of MEGA-PRESS editing for GABA.* [digitized photograph]. Available at: https://www.ncbi.nlm.nih.gov/pmc/articles/PMC3825742/figure/F1/ [30.03.19]

[43] GABA Analysis Toolkit. 2015. GannetCoRegister and GannetSegment. [ONLINE] Available at: http://gabamrs.blogspot.com/2015/01/gannetcoregister-and-gannetsegment.html. [Accessed 16 April 2019].

[44] Gannet. 2016. Tissue-Corrected GABA Values in Gannet. [ONLINE] Available at: http://www.gabamrs.com/blog/2016/3/2/tissue-corrected-gaba-values-in-gannet. [Accessed 16 April 2019].

[45] In Young Choi, Sang Pil Lee, Hellmut Merkle, Jun Shen (2006) *In vivo detection of gray and white matter differences in GABA concentration in the human brain* NeuroImage, Elsevier.

[46] Devore JL, Berk KN *Modern Mathematical Statistics with Applications, Second Edition* Pages 461-462, 499-501, Springer Science +Buisiness Media,LLC 2012.

[47] UNeag School of Education – University of Connecticut. 2009. Statistical Significance. Del Siegle, Ph.D. [ONLINE] Available at: *https* : *//researchbasics.education.uconn.edu/statistical*$_s$*ignificance/*. [Accessed 22 May 2019].

[48] Shulman, Rothman (2004). *Brain Energetics and Neuronal Acticity.* Yale University School of Medicine. New Haven, Conneticut, USA.

[49] Edden, Puts, Barker (2012). *Macromolecule-suppressed GABA-edited magnetic resonance spectroscopy at 3T.* NIH Public Access. Magn Reson Med. 2012 September ; 68(3): 657–661. doi:10.1002/mrm.24391.

[50] GyroMagician, (2013), *Free Induction Decay (FID) nuclear magnetic resonance signal seen from a well shimmed sample with labels* [ONLINE]. Available at: *https* : *//commons.wikimedia.org/wiki/File* : *Nmr_fid_good_shim_EN.svg* [Accessed 3 February 2019].

[51] L. An, Y. Zhang, M. Thomasson, L. Latour, H. Baker, J. Shen, S. Warach (2009) *Measurement of Glutathione in Normal participants and StrokePatients at 3 T Using J-Difference Spectroscopy with MinimizedSubtraction Errors* NIH Public Access. J Magn Reson Imaging. 2009 August ; 30(2): 263–270. doi:10.1002/jmri.21832.

[52] Faezeh. Nezhad, A. Anton, M. Parkes, B. Deakin, R. Williams (2017). *Quantification of Glutathione in the Human Brain byMR Spectroscopy at 3 Tesla: Comparison of PRESSand MEGA-PRESS.* Magnetic resonance in medicine, 78(4), 1257–1266. doi:10.1002/mrm.26532.

[53] Faezeh. Nezhad, A. Anton, M. Parkes, B. Deakin, R. Williams (2017). *GSH signal from the GSH/Ace phantom using the MEGA-PRESS pulse sequence at different TE values.* Magnetic resonance in medicine, 78(4), 1257–1266. doi:10.1002/mrm.26532. [digitized photograph] Available at:[https://www.ncbi.nlm.nih.gov/pmc/articles/PMC5469715/figure/mrm26532-fig-0003/] [04.04.19].

[54] Muhammad G. Saleh, Daniel Rimbault, Mark Mikkelsen, Georg Oeltzschner, Anna M. Wang, Dengrong Jiang, Ali Alhamud, Jamie Near, Michael Schär, Ralph Noeske, James B. Murdoch ,Lars Ersland, Alexander R. Craven, Gerard Eric Dwyer, Eli Renate Grüner, Li Pan (2019). *Multi-vendor standardized sequence for edited magnetic resonance spectroscopy.* 2019 Elsevier Inc.

[55] Muhammad G. Saleh, Daniel Rimbault, Mark Mikkelsen, Georg Oeltzschner, Anna M. Wang, Dengrong Jiang, Ali Alhamud, Jamie Near, Michael Schär, Ralph Noeske, James B. Murdoch ,Lars Ersland, Alexander R. Craven, Gerard Eric Dwyer, Eli Renate Grüner, Li Pan (2019). *Pulse sequence diagrams.* 2019 Elsevier Inc. [digitized photograph] Available at: [https://www.sciencedirect.com/science/article/pii/S1053811919300564] [24.04.19].

[56] Puts NA, Edden RA. *In vivo magnetic resonance spectroscopy of GABA: a methodological review.* Prog Nucl Magn Reson Spectrosc. 2012 Jan;60:29-41. doi: 10.1016/j.pnmrs.2011.06.001. Epub 2011 Jun 12. PubMed PMID: 22293397; PubMed Central PMCID: PMC3383792.

[57] Edden, R.A.E.; Puts, N.A.J.; Harris, A.D.; Barker, P.B.; Evans, C.J. *Gannet: A batch-processing tool for thequantitative analysis of gamma-aminobutyric acid-edited MR spectroscopy spectra.*J. Magn. Reson. Imaging 2014,40, 1445–1452.

[58] Puts, Borowy, Harris, Evans, Mcgonigle, Tegenthoff, Schmidt-Wilcke, Edden, Richard. (2018). *GABA Levels in Left and Right Sensorimotor Cortex Correlate across Individuals.* Biomedicines. 6. 80. 10.3390/biomedicines6030080.

[59] Mikkelsen M, Barker PB, Bhattacharyya PK, et al. *Big GABA: Edited MR spectroscopy at 24 research sites.* Neuroimage. 2017;159:32–45. doi:10.1016/j.neuroimage.2017.07.021 [https://www.ncbi.nlm.nih.gov/pmc/articles/PMC5700835/#R38].

[60] Bogner W, Gruber S, Doelken M, Stadlbauer A, Ganslandt O, Boettcher U, Trattnig S, Doerfler A, Stefan H, Hammen T. *In vivo quantification of intracerebral GABA by single-voxel 1H-MRS—How reproducible are the results?* Eur J Radiol. 2010;73:526–531. doi: 10.1016/j.ejrad.2009.01.014.

[61] Evans CJ, McGonigle DJ, Edden RAE. *Diurnal stability of γ-aminobutyric acid concentration in visual and sensorimotor cortex.* J Magn Reson Imaging. 2010;31:204–209. doi: 10.1002/jmri.21996. [https://www.ncbi.nlm.nih.gov/pubmed/20027589/].

[62] Geramita M, van der Veen JW, Barnett AS, Savostyanova AA, Shen J, Weinberger DR, Marenco S. *Reproducibility of prefrontal γ-aminobutyric acid measurements with J-edited spectroscopy.* NMR Biomed. 2011;24:1089–1098. doi: 10.1002/nbm.1662. [https://www.ncbi.nlm.nih.gov/pubmed/21290458/].

[63] Mikkelsen M, Singh KD, Sumner P, Evans CJ. *Comparison of the repeatability of GABA-edited magnetic resonance spectroscopy with and without macromolecule suppression.* Magn Reson Med. 2016a;75:946–953. doi: 10.1002/mrm.25699. [https://www.ncbi.nlm.nih.gov/pubmed/25920455/].

[64] O'Gorman RL, Michels L, Edden RA, Murdoch JB, Martin E. *In vivo detection of GABA and glutamate with MEGA-PRESS: Reproducibility and gen-*

der effects. J Magn Reson Imaging. 2011;33:1262–1267. doi: 10.1002/jmri.22520. [https://www.ncbi.nlm.nih.gov/pubmed/21509888/].

[65] E. Edmund Kim, Edward F. Jackson (1999) *Molecular Imaging in Oncology: PET, MRI, and MRS* Springer-Verlag Berlin Heidelberg.

[66] Roland Kreis (2004) *Issues of spectral quality in clinical 1H-magnetic resonance spectroscopy and a gallery of artifacts* NMR Biomed. 2004;17:361–381.

[67] Mandal PK, Tripathi M, Sugunan S. *Brain oxidative stress: detection and mapping of anti-oxidant marker 'Glutathione' in different brain regions of healthy male/female, MCI and Alzheimer patients using non-invasive magnetic resonance spectroscopy.* Biochem Biophys Res Commun. 2012;417(1):43-8.

[68] E. Aufhaus, W. Weber-Fahr, M. Sack, N. Tunc-Skarka, G. Oberthuer,1 M. Hoerst, A. Meyer-Lindenberg, U. Boettcher, and G. Ende. *Absence of Changes in GABA Concentrations with Age and Gender in the Human Anterior Cingulate Cortex: A MEGA-PRESS Study with Symmetric Editing Pulse Frequencies for Macromolecule Suppression.* Magnetic Resonance in Medicine 69:317–320 (2013) [https://onlinelibrary.wiley.com/doi/pdf/10.1002/mrm.24257].

[69] Ian Greenhouse, Sean Noah, Richard J. Maddock, Richard B. Ivry (2016) *Individual differences in GABA content are reliable but are not uniform across the human cortex.* NeuroImage, Elsevier.

[70] Evans, C. J., McGonigle, D. J. and Edden, R. A. (2010), *Diurnal stability of γ-aminobutyric acid concentration in visual and sensorimotor cortex.* J. Magn. Reson. Imaging, 31: 204-209. doi:10.1002/jmri.21996

[71] ChristopherAri Shaw (2017). *Glutathione In The Nervous System*, section 6. Routledge.

[72] Paul G. Mullins, David J. McGonigle, Ruth L. O'Gorman, Nicolaas A.J. Puts, Rishma Vidyasagar, C. John Evans, Richard A.E. Edden (2014). *Current practice in the use of MEGA-chematic diagram of MEGA-PRESS editing for GABA.PRESS spectroscopy for the detection of GABA.* NeuroImage, Volume 86, 2014, Pages 43-52, ISSN 1053-8119 [https://doi.org/10.1016/j.neuroimage.2012.12.004].

[73] Dou, W., Speck, O., Benner, T. et al. Magn Reson Mater Phy (2015). *Automatic voxel positioning for MRS at 7 T* Springer Berlin Heidelberg, ISSN 1352-8661 [https://doi.org/10.1007/s10334-014-0469-9].

[74] Deelchand, D. K., Kantarci, K. and Öz, G. (2018), *Improved localization, spectral quality, and repeatability with advanced MRS methodology in the clinical setting.* Magn. Reson. Med, 79: 1241-1250.

[75] R.A. Edden, N.A. Puts, A.D. Harris, P.B. Barker, C.J. Evans *Gannet: A batch-processing tool for the quantitative analysis of gamma-aminobutyric acid–edited MR spectroscopy spectra* J. Magn. Reson. Imag., 40 (2014), pp. 1445-1452

[76] ChemDraw Prime 18 © 1998 - 2019 PerkinElmer Inc. All Rights Reserved [Software].

[77] Mullins PG, McGonigle DJ, O'Gorman RL, Puts NA, Vidyasagar R, Evans CJ, Edden RA4. *Schematic diagram of MEGA-PRESS editing for GABA.*NeuroImage, Volume 86, 2014, Pages 43-52, ISSN 1053-8119 [https://doi.org/10.1016/j.neuroimage.2012.12.004] [digitized photograph] Available at: [https://www.sciencedirect.com/science/article/pii/S1053811919300564] [24.04.19]

[78] Gillard J, Waldman A, Barker P. (2005). Clinical MR Neuroimaging. Pages 17-51, Cambridge University Press.

[79] Gillard J, Waldman A, Barker P. (2005). Clinical MR Neuroimaging, figure 2.2: Overview of the major processing steps for spectral analysis. Page 29, Cambridge University Press.

[80] Questions and Answers in MRI. 2018. *Performing an MR Scan.* [ONLINE] Available at: http://mriquestions.com/what-are-the-steps.html?fbclid=IwAR3Hutgco8Q3CjfcMBCfwN2TKkO1iF4rJn9lsEs5y5h52ZhGtFLT-xFZwBU. [Accessed 24 May 2019].

[81] Tkáč I, Gruetter R. *Methodology of H NMR Spectroscopy of the Human Brain at Very High Magnetic Fields.* Appl Magn Reson. 2005 Mar;29(1):139-157. doi: 10.1007/BF03166960. PubMed PMID: 20179773; PubMed Central PMCID: PMC2825674.

[82] Y. Li, J. M. Lupo, D. Xu , D. A. Kelley , and S. J. Nelson (2010). *Improved metabolite quantification using VAPOR water suppression* GE Healthcare, UC Discovery grant ITL-BIO04-10148.

[83] The James Keeler Group, Department of Chemistry at the University of Cambridge. 2019. *4 Coherence Selection: Phase Cycling and Gradient Pulses.* [ONLINE] Available at: http://www-keeler.ch.cam.ac.uk/lectures/phasen_a4.pdf. [Accessed 15 May 2019].